THE JURASSIC PALEOVOLCANISM IN NORTHERN CHILE

Dissertation

zur Erlangung des Grades eines Doktors
der Naturwissenschaften
dem Fachbereich Erdwissenschaften
der Eberhard - Karls - Universität zu Tübingen

vorgelegt von
Carlos Palacios - Monasterio
aus Santiago/Chile

1978

78 533

THE JURASSIC PALEOVOLCANISM IN NORTHERN CHILE

Dissertation

zur Erlangung des Grades eines Doktors
der Naturwissenschaften
dem Fachbereich Erdwissenschaften
der Eberhard - Karls - Universität zu Tübingen

vorgelegt von
Carlos Palacios - Monasterio
aus Santiago/Chile

1978

UNIV.
LEIDEN
BIBL.

Tag der mündlichen Prüfung: 1. Dezember 1978

Dekan: Prof. Dr. A. Karger
1. Berichterstatter: Prof. Dr. H. Pichler
2. Berichterstatter: Prof. Dr. W. Weiskirchner

Gedruckt mit Unterstützung des Deutschen Akademischen Austauschdienstes.

CONTENT

Page

ABSTRACT 7

1. INTRODUCTION 8

2. TECTONIC AND PALEOGEOGRAPHIC SETTING 12

3. PREVIOUS STUDIES AND AIM OF THIS WORK 15

4. WORKING METHODS 17

5. PETROGRAPHY 19

5.1. Series A 19

5.2. Series B 19

5.3. Series C 20

6. CLASSIFICATION AND NOMENCLATURE OF JURASSIC VOLCANIC ROCKS 29

6.1. Comparison with other Magmatic Regions 31

7. GEOCHEMISTRY 34

7.1. Major Element Chemistry 34

7.2. Trace Element Chemistry 49

8. PETROGENESIS OF JURASSIC VOLCANIC SERIES 60

8.1. Series A 60

8.2. Series B and C 62

9. COMPARISON WITH OTHER VOLCANIC SUITES 67

10. DEPTH OF THE JURASSIC PALEOSEISMIC ZONE AND CRUSTAL THICKNESS 71

11. REGIONAL METAMORPHISM 73

11.1. Regional Metamorphism in Jurassic Volcanic Rocks 73

11.2. Discussion 76

11.3. Changes of the Chemical Composition by Regional Metamorphism 78

12. PALEOVOLCANISM IN CENTRAL CHILE 79

12.1. Geological Setting 79

12.2. Geochemistry 82

13. CONCLUDING REMARKS 87

14. ACKNOWLEDGMENTS 89

15. REFERENCES 90

16. ANNEX: PHOTOGRAPHY OF SOME THIN-SECTIONS 97

FIGURES

Page

1. Geological map of Northern Chile 9
2. Stratigraphic cross sections in Northern Chile 11
3. Paleogeographic scheme in Jurassic Period, Northern Chile 13
4. Mineral composition of the Jurassic volcanic series 21
5. Location of samples 28
6. Q-A-P-F double-triangle plot of Jurassic lavas 30
7. Q-A-P-F double-triangle plot of recent volcanics from Izu-Marianas, Hokkaido, Kuriles-Kamtchatka and Honsyu 32
8. Q-A-P-F double-triangle plot of Cenozoic volcanics from the Central Andes 33
9. Frequency distribution of SiO_2 in the different series of the Jurassic volcanism in Northern Chile 35
10. Colour index versus SiO_2 (in wt. %) 42
11. Na_2O and K_2O versus SiO_2 (in wt. %) 43
12. K_2O - SiO_2 diagram showing characteristic trends of the Jurassic volcanic series 44
13. CaO and MgO versus SiO_2 (in wt. %) 45
14. K_2O/Na_2O ratios versus SiO_2 (in wt. %) 46
15. TiO_2 and FeO (Fe total as FeO) versus SiO_2 (in wt. %) 47
16. AFM diagram of Jurassic volcanic rocks 48
17. Rb, Ba and Sr (in ppm) versus SiO_2 (in wt. %) 53
18. K (in wt. %) versus Rb (in ppm) 54
19. Ni, Co, Cr and V (in ppm) versus SiO_2 (in wt. %) plot of Jurassic volcanic rocks 55
20. Zr, Y and Ga (in ppm) versus SiO_2 (in wt. %) 57
21. Cu, Zn and Pb (in ppm) versus SiO_2 (in wt. %) 58
22. REE abundances in the Jurassic volcanic series normalized to a chondrite average 60
23. REE abundances in the Jurassic volcanic series and in the calculated models normalized to a chondrite average 64

Page

24. Comparison of observed trace element data to concentration expected in models 65
25. Relation between the average SiO_2 content in volcanic rocks (tholeiitic and calc-alkaline series mixed) of island arcs and continental margins and crustal thickness 72
26. Metamorphic zones in Jurassic volcanic rocks of Northern Chile 75
27. Geological map of Central Chile 80
28. Profile through the Andean Belt at $34^{o}S$ 81
29. Distribution of Mesozoic lavas of Central Chile in the Q-A-P-F double-triangle diagram 83
30. K_2O and K_2O/Na_2O versus SiO_2 (in wt. %) for Mesozoic lavas of Central Chile 84
31. MgO, CaO and Na_2O versus SiO_2 (in wt. %) of the Mesozoic volcanic rocks from Central Chile 85
32. AFM diagram of Mesozoic volcanic rocks from Central Chile 86

TABLES

Page

1. Analytical procedures for the determination of trace and rare earth elements 18
2. Petrographic descriptions of Jurassic volcanic rocks 22
3. Major element abundances of Jurassic volcanic rocks 35
4. Trace element abundances of Jurassic volcanic rocks 50
5. Solid/Liquid partition coefficients used in this study 66
6. Trace element content of peridotite used in modelling 66
7. Statistical comparison of the geochemistry of theoleiitic rock-series 68
8. Statistical comparison of the geochemistry of calc-alkaline series 69
9. Statistical comparison of the geochemistry of "alkaline" suites 70
10. Typical low-grade metamorphic mineral assemblages in the Jurassic volcanic rocks of Northern Chile 74

ABSTRACT

Petrographical and geochemical data evidence that *three different series* of igneous activity occur in the Jurassic areas of Northern Chile: *Tholeiitic, calc-alkaline* and *alkaline* suites. The geochemical differences among the three associations cannot be explained by low pressure fractionation involving the present phenocrysts phases. These differences probably reflect different source materials. The observed geochemical patterns of the Jurassic *tholeiites* are consistent with a genesis by *moderates degrees (10%) of melting of peridotite*. Subsequent fractional crystallization of olivine and clinopyroxene are indicated by the trace elements abundances. Volcanic rocks of *calc-alkaline and alkaline series* require *significantly lower degrees of melting (< 7%) of garnet-free peridotite*, followed by fractional crystallization of olivine, clinopyroxene and plagioclase. The three volcanic series are interlayered in the Jurassic outcrops of Northern Chile and the sequence cannot be correlated with a spatial or temporal zonation. Thus, the Jurassic history in the southern part of the Central Andes speaks clearly for the existence of an *island-arc system*. Although the available data are very limited for the Jurassic-Cretaceous volcanic rocks of Central Chile (Southern Andes), the geochemical patterns suggest that these rocks are demonstrably similar with the Jurassic series of Northern Chile (Central Andes).

1. INTRODUCTION

The Andes of South America can be divided into four main sections: the Austral Andes (47°S - 53°S), the Southern Andes (33°S - 47°S), the Central Andes (14°S - 33°S), and the Northern Andes (6°N - 14°S). The Central Andes in their central part (Southern Perú, Northern Chile, Southwestern Bolivia, and Northwestern Argentina) are about 1,000 km wide. This fact provides a good possibility to study the nature of the magmatism related with the interaction of converging oceanic and continental lithosphere.

The thickness of the continental crust is another parameter that exhibits notably variations along the Andean chains. Seismic and gravity studies show that under the Central Andes the continental crust reaches a thickness of up to 75 km (JAMES 1971, OCOLA et al. 1971). In that area the Andes are to be separated into the following major tectonic units (from west to east):

- The *Coastal Range* is developed between 18°S and about 43°S; its disappearance in the south coincides with the intersection of the East Chilean Rise with the South American continent. The Coastal Range consists of strongly folded Paleozoic metamorphic series and Jurassic volcanic rocks which are intruded by the huge coastal batholith (mostly granodiorite).
- The *Longitudinal Central Valley*, which is filled by thick Quaternary continental sediments, separates the Coastal Range from the Andean Cordillera. This graven structure is developed over nearly the entire length of Chile between 18°S and 43°S.
- The *Western Cordillera*, between 15°S and 27°S, is characterized by some hundreds of huge composite volcanoes which in the central part of the Andes reach altitudes of 5,000 - 7,000 m. These volcanoes represent a central-type volcanic complex which was formed during Pliocene-Pleistocene-Holocene and it is constructed over the uplift block of the Miocene-Pleistocene rhyolitic Plateau.
- The *Altiplano (Puna)* with an average height of about 3,800 m separates the Western and Eastern Cordillera. This up to 200 km wide elevated depressions forms a graben-like structure which is filled by thick series of mostly clastic sediments of Upper Cretaceous to Tertiary

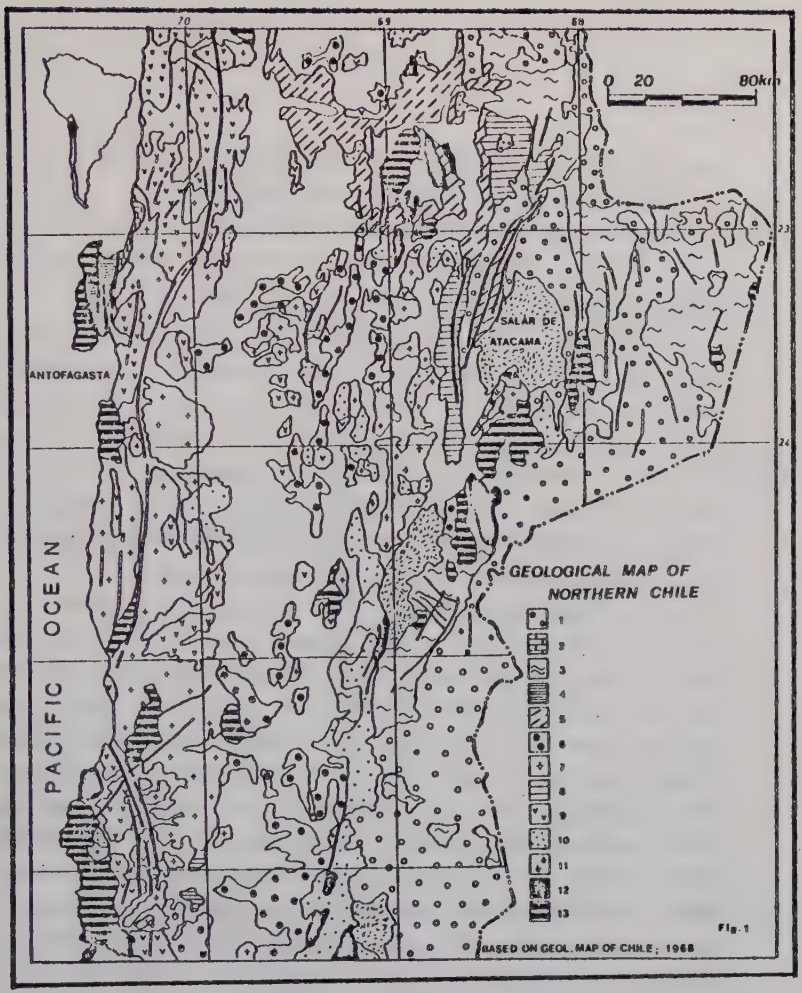

Fig.1. Geological map of Northern Chile.
1. Quaternary volcanic rocks
2. Quaternary marine sedimentary rocks
3. Tertiary volcanic rocks
4. Tertiary marine sedimentary rocks
5. Tertiary continental sedimentary rocks
6. Cretaceous volcanic rocks
7. Cretaceous granitic rocks
8. Cretaceous continental and marine sedimentary rocks
9. Jurassic volcanic rocks
10. Jurassic marine sedimentary rocks
11. Triassic volcanic and sedimentary rocks
12. Paleozoic granitic rocks
13. Paleozoic metamorphic rocks.

age. Related to the orogenic movements during the Cenozoics, strong volcanic and plutonic activity occurred.

- The *Eastern Cordillera* is composed of strongly folded Paleozoic rocks which are intruded by Miocene batholiths. Cenozoic volcanic rocks occur at the western side of the Eastern Cordillera.

The Jurassic volcanic rocks in the Central Andes occur mainly within the Coastal Range. This series corresponds to early manifestations of effusive magmatism in the Andean tectonic cycle of Northern Chile. Its outcrops occur between 16° and 26°S in the coastal region of Northern Chile (Fig. 1). The volcanic sequence is 5 to 15 km thick and mainly formed by lava flows of 5 to 20 m thickness. Porphyritic texture is common. Minor intrusions, similar in composition to the flows and volcanoclastic rocks, cut the successions.

In the *Tocopilla area* (22°S, Fig. 2), the Jurassic volcanic rocks are interbedded in Triassic-Liassic marine series (ALFARO 1974). Here, the western side (NS/30°E) of an extensive synclinal structure with a nearly NS oriented axis crops out. The eastern side of that structure crops out *in the Limon Verde area* (22°30'S, 69°10'W), conformably over marine sedimentary rocks of the Kimmeridgian (BAEZA 1976). In *the Antofagasta zone* (23°45'S), the volcanic series underlie unconformably Neocomian continental sedimentary rocks (HARRINGTON 1961). In this area, the Jurassic volcanic rocks form a great anticlinal, its western side (N10°W/45°ENE) croping out in the Antofagasta region (Fig. 2). An huge granodiorite batholith of Hauterivian age (123.5 m.y.), cut the volcanic series as it is shown in Fig. 2 (PALACIOS 1974 a). At 25°30'S, the Jurassic volcanic series overlie Middle Pliensbachian marine sedimentary rocks, the capping beds are a Neocomian continental sequence (ORTIZ et al. 1960).

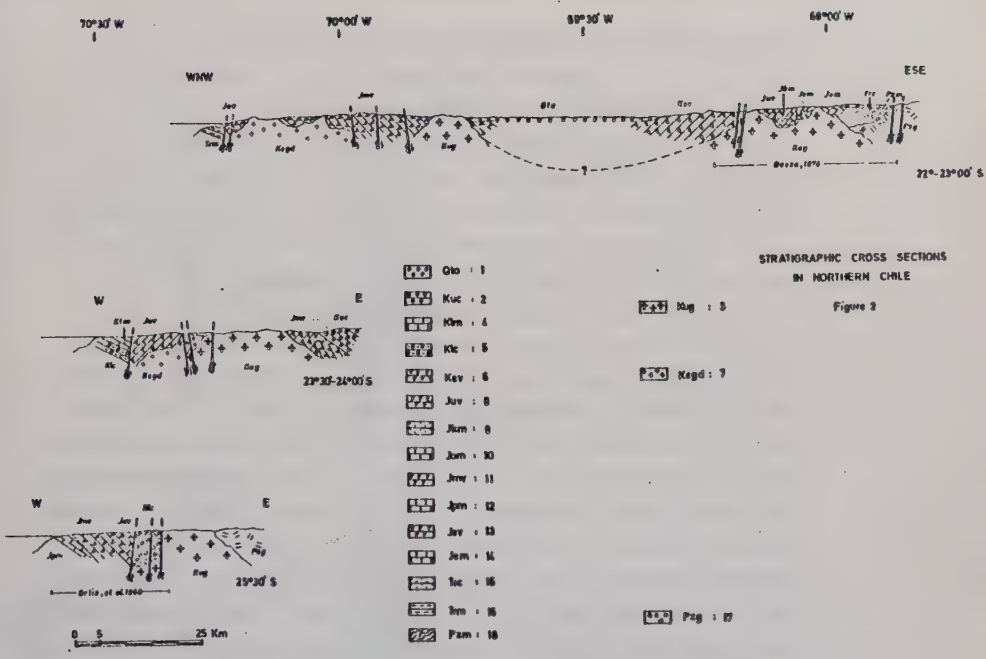

Fig.2. Stratigraphic cross sections in Northern Chile.
1. Quaternary sediments
2. Upper Cretaceous volcanic-sedimentary rocks
3. Upper Cretaceous granitic rocks
4. Lower Cretaceous marine sedimentary rocks
5. Lower Cretaceous continental sedimentary rocks
6. Early Cretaceous volcanic rocks
7. Early Cretaceous granodioritic rocks
8. Upper Jurassic volcanic rocks
9. Kimmeridgian marine sedimentary rocks
10. Oxfordian marine sedimentary rocks
11. Middle Jurassic volcanic rocks
12. Pliensbachian marine sedimentary rocks
13. Early Jurassic volcanic rocks
14. Early Jurassic marine sedimentary rocks
15. Triassic continental sedimentary rocks
16. Triassic marine volcano-sedimentary rocks
17. Paleozoic granitic rocks
18. Paleozoic marine sedimentary rocks.

2. TECTONIC AND PALEOGEOGRAPHIC SETTING

The Andean tectonic cycle began during the Middle to Late Triassic with a stage of distension producing the initial subsidence of a basin oriented NNW - SSE at the present Southwestern continental margin of South America (FRUTOS and TOBAR 1973, FRUTOS 1977). During the initial and intermediate stages of the tectonic cycle (Jurassic to Early Cretaceous), the Andean geosyncline consisted of a eugeosyncline with important syngenetic volcanic episodes, which are well represented in the present Coast Range of Northern Chile. This volcanism has been developed within a volcanic arc of an active continental margin (Pacific type) (Fig. 3). Toward the foreland, a basin received sandstones, limestones and lutites but nearly without volcanics (FRUTOS and TOBAR 1973, MONTANO 1976, BAEZA 1976, FRUTOS 1977). At the end of the Jurassic, the Nevadian diastrophic movements caused a marine regression, leaving only a small Tithonian-Neocomian basin that finally disappeared as a consequence of Sub-Hercynian diastrophism (FRUTOS and TOBAR 1973, FRUTOS 1977). JAMES et al. (1975) suggest that the earliest volcanic rocks of the Central Andean arc were extruded about 185 m.y. ago. The volcanics have initial $^{87}Sr/^{86}Sr$ ration which are identical to those measured in rocks of oceanic island arcs (JAMES et al. 1975, HALPERN 1978). These authors suggest that the earliest magmas of the Andean arc were derived from a descending plate overlying oceanic type asthenosphere or young continental lithosphere at depths less than 100 km.

McNUTT et al. (1975) suggest that the Jurassic volcanic rocks represent magmas produced at a rather early stage of a subduction process, when the melting zone in the oceanic plate was at shallow depth and close to the overlying continental crust. Convergence between continental and oceanic plates was probably most rapid during the initial phases of plate consumption.

During the whole development of the Andean tectonic cycle, active volcanism and plutonism, associated with an evolving subduction zone (oriented NNW - SSE), took place in parallel regions in each period, migrating steadily eastward. In Jurassic times the center of the volcanic activity was located near the present coastline of Northern

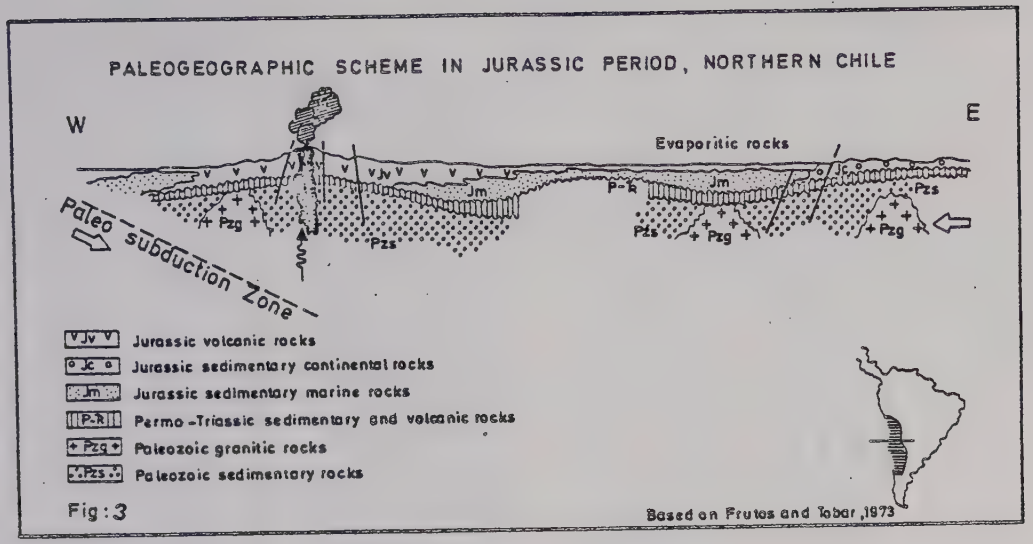
PALEOGEOGRAPHIC SCHEME IN JURASSIC PERIOD, NORTHERN CHILE
W
E
Evaporitic rocks
Jm
P-Tr
Jm
Jc
Pzs
Pzg
Pzs
Pzs
Pzg
Pzg
Paleo subduction Zone
Jurassic volcanic rocks
Jurassic sedimentary continental rocks
Jurassic sedimentary marine rocks
Permo-Triassic sedimentary and volcanic rocks
Paleozoic granitic rocks
Paleozoic sedimentary rocks
Based on Frutos and Tobar, 1973

Fig: 3

Chile, and from there the volcanic belt migrated approximately 200 km eastward to its present position at the crest of the Andes. The axis of magmatism migrated eastward with an increasing rate of about 0.6 mm/yr. in the Early Mesozoic to 1.10 mm/yr. during the mid-Tertiary. In the Miocene, an wide-scale extension of the magmatic activity in the continent resulted in the magmatic eruptions at distances of up to 250 km to the east of the former inner boundary of the orogen, giving rise to a volcanic belt many times broader than those formed earlier. In the Upper Pliocene and the Pleistocene, a rapid westward rejuvenation of volcanism led to the formation of strato-volcanic complexes (DOSTAL et al. 1977).

3. PREVIOUS STUDIES AND AIM OF THIS WORK

DARWIN (1838) during the famous voyage around the earth with the "Beagle" was the first who detected the Jurassic volcanic rocks in Northern Chile. He observed the great thickness of these series and gave them the name "Porphyrformation".

DARAPSKY (1900) in the geological chapter of its book dealing mainly with the mineral deposition in Northern Chile, described the Jurassic volcanic series between Taltal and Paposo (25^{o} to $25^{o}30'$ S), and its relations to the intrusive granitic batholiths and copper mineralization.

STEINMANN (1923) defined the Jurassic volcanic series as "Porphyritic formations" and found that the volcanic rocks had been erupted between Lias and Cretaceous. Lates, in its fundamental book about the "Geologie von Peru" (1929) he delineated and described the volcanic sequences in the extreme Northern part of Chile, in the Arica region, as follows:

> Hier haben während der Jurazeit wiederholt gewaltige Ausbrüche stattgefunden, besonders von Diabasporphyrit, Augitporphyrit und Melaphyr, deren Laven und Tuffe zwischen den marinen Sedimenten eingeschaltet sind. Es ist die sogenannte "Porphyrformation" DARWIN's, später meist "Porphyritformation" genannt. Aber dieser Name ist irreführend und wird am besten durch "Andine Diabas-Melaphyrformation" ersetzt. Diese erscheint aber in der Kordillere von Peru erst in der Unterkreide, während sie in Chile schon im Lias beginnt. (p. 81)

STEINMANN (1923) gave also a petrographic description of the Jurassic and Cretaceous volcanic rocks.

WETZEL (1929), who carried out field investigations in the Coastal Range of Northern Chile, published the first thin slide observations of Jurassic volcanic rocks.

GERTH (1939) presented a description of the Jurassic volcanic series in the Coastal Range of Northern Chile. Field identification and correlation of these lava flows were combined with stratigraphic studies, using clearly observable field characteristics such as color, texture, jointing pattern, erosional forms and position relative to key sedimentary interbeds that served as stratigraphic markers. In the chapter on the

paleogeographic interpretation, GERTH (1939) writes:

> Bei den Laven von konglomeratischer Struktur sind die kantengerundeten Komponenten von Labradorporphyrit nicht durch abgerundetes klastisches Material, sondern durch einen Kristalltuff aus eckigen Mineralsplittern verkittet. Vermutlich ist diese eigentümliche Struktur der Laven durch den explosiven Charakter der submarinen Eruptionen bedingt. Daneben kommen auch konglomeratische Tuffe mit Geröllen aus den gleichen Effusivgesteinen und Bindemittel aus gerolltem, klastischem Material vor, die, als die Eruptionsprodukte bis zur Meeresoberfläche aufgehängt waren, in der Brandungszone vulkanischer Inseln gebildet wurden. (1939, p. 11)

Valuable observations on the Jurassic volcanic rocks were published by BROGGEN (1950) in its "Fundamentos de la Geologia de Chile".

Since about 1960, numerous studies have been published, which deal mainly with stratigraphic and tectonic problems: ORTIZ et al. 1960, HARRINGTON 1961, ALFARO 1974, FRUTOS and TOBAR 1973, BAEZA 1976, MONTANO 1976, FRUTOS 1977, JURGAN 1977.

LOSERT (1974) studied the chemical differentiation of Early Jurassic volcanic rocks in relation to the regional metamorphism in the Southern Tocopilla area. He pointed out that the metamorphism caused large-scale selective re-distribution (differentiation) of Si, Na, Ca, and Sr, while K together with Rb were expelled.

In some previous papers (PALACIOS, 1974 a, b, 1975, 1977) new metamorphic and chemical data of Jurassic lavas were published.

The aim of this work is to integrate metamorphic, petrographic, geochemical and petrological data of Jurassic volcanic rocks of Northern Chile. This study provides metamorphic and petrological data that help to determine the behaviour and the origin of the Jurassic lavas and attempt to resolve questions above development of the Andean volcanism in space and time.

4. WORKING METHODS

For this study, thin sections of about 500 samples were qualitively and quantitatively determined according to common optical methods. An contents of plagioclase were determined for phenocrysts and large microlites using a 4-axis universal stage with methods according to SLEMMONS (1962, 1962 a). 60 samples were analyzed by X-ray diffraction.

Major and trace element data for 42 samples have been performed. Specimens which contain more than 0.5 modal percent of metamorphic minerals have not been analyzed. Rare earth elements data for 13 samples were also carried out.

Major elements have been determined by common wet chemical analytic methods. The precision of the analytical techniques was estimated from the results of a triplicate analysis of the U.S. Geological Survey standard rock G-2. The precisions are generally better than $\pm$ 5%. For TiO_2, MnO and P_2O_5 the precision is better than $\pm$ 10%.

Trace and rare earth elements analytic methods are compiled in Table 1.

TABLE 1: Analytical procedures for the determination of trace and rare earth elements

Element	Method	Precision	Standard
Rubidium	X-ray fluoresc.	4-5%	JG-1 and JB-1 (Geol.Survey Japan)
Strontium	X-ray fluoresc.	4-5%	JG-1 and JB-1 (Geol.Survey Japan)
Barium	X-ray fluoresc.	5%	GA (French) GSP-1 (US Geol. Survey)
Zirconium	X-ray fluoresc.	6%	GA (French) GSP-1 (US Geol. Survey)
Gallium	X-ray fluoresc.	8%	D-455 (synthetic stand.) with W-1 (US Geol. Surv.)
Yttrium	X-ray fluoresc.	8%	BR (French), W-1 and GSP-1 (US Geol. Survey)
Lithium	Atomic absorption	5%	GA (French) GSP-1 (US Geol. Survey)
Chromium	Atomic absorption	5%	GA (French) GSP-1 (US Geol. Survey)
Cobalt	Atomic absorption	7%	GA (French) GSP-1 (US Geol. Survey)
Nickel	Atomic absorption	6%	GA (French) GSP-1 (US Geol. Survey)
Vanadium	Atomic absorption	6%	GA (French) GSP-1 (US Geol. Survey)
Copper	Atomic absorption	9%	JG-1 and JB-1 (Geol. Survey Japan)
Zinc	Atomic absorption	8%	JG-1 and JB-1 (Geol. Survey Japan)
Lead	Atomic absorption	8%	JG-1 and JB-1 (Geol. Survey Japan)
Rare earth elements	Neutron activation	3-10%	BCR-1 (US Geol. Survey)

5. PETROGRAPHY

The Jurassic lava flows show three types of volcanic rock series. These rocks were divided into series A, series B and series C according to petrochemical characteristics. Modal analyses of 42 samples are presented in Table 2.

5.1. Series A

The lavas of the series A are porphyritic and contain combinations of olivine, diopsidic augite and plagioclase; diopsidic augite, plagioclase; diopsidic augite, hornblende, plagioclase; hornblende, biotite, plagioclase; and biotite, plagioclase as phenocrystic minerals. Similar assemblages with modal quartz form the groundmass (Fig. 4; Table 2). The lavas consist of plagioclase, olivine, clinopyroxene, hornblende and biotite set in a groundmass (65-90%) of microlites of plagioclase, clinopyroxenes, hornblende, biotite, quartz and ore minerals. The content of phenocrysts ranges between 10 and 35 per cent. Plagioclase is by far the most abundant mineral (up to 45%) occurring as euhedral to subhedral. Often the plagioclase phenocrysts, which are filled by inclusions of pyroxenes and iron ores, show multiple twinning and zonation.

Olivine is occurring only as phenocrysts, and this mineral is found as euhedral to subhedral and embayed, corroded and iddingsitized crystals.

The more acidic lavas contain phenocrysts of hornblende and biotite, which are strongly pleochroitic. Both show always a beginning transformation into magnetite-hematite at the margins; often the whole crystal is converted into iron ore.

5.2. Series B

The porphyritic texture of the lavas of series B is common and the flows show combinations of olivine, diopsidic augite, plagioclase; olivine, diopsidic augite, hypersthene, plagioclase; diopsidic augite, hornblende, plagioclase; hornblende, biotite, plagioclase; and biotite, plagioclase, as phenocrystic minerals. In addition to the above mentioned assemblages,

the groundmass (about 70-90 per cent of the volume of the rocks) is composed of fine and coarse crystals of plagioclase connected interstitionally to grains of pyroxenes and hornblende. Also existed granoblastic quartz-feldspathic accumulations, as vesicules, infillings or occurrences between the crystals of plagioclase and ferromagnesian minerals (Fig. 4; Table 2).

Plagioclase is the most abundant mineral, and is mineralogically similar to the lavas of the series A. Two different pyroxenes are recognizable: more common is augite, whereas hypersthene occurs in smaller amounts. This orthopyroxene shows often a reaction rim of fine augite. Olivine phenocrysts are partly replaced by clinopyroxene and iddingsite. No microlites of divine occur.

5.3. Series C

The lavas of the series C are porphyritic and contain combinations of olivine, plagioclase; diopsidic augite, olivine, plagioclase; and plagioclase, diopsidic augite as phenocrystic minerals. Similar assemblages with common granoblastic quartzfeldspathic accumulations are present in the groundmass (Fig. 4; Table 2). The groundmass represent about 70-80% of most rocks. Many phenocrysts contain patches (with all probability original glass), suggesting corrosion of intratelluric crystals. Microlites and phenocrysts of plagioclase are euhedral to subhedral; lath-shaped crystals with (010) faces dominant. Microlites commonly aggregate by attaching to mutual (010) faces, and are twinned after albite, Carlsbad and albite-Carlsbad laws in decreasing abundance. Phenocrystals are similarly twinned, but Carlsbad and albite-Carlsbad predominate.

Most of the olivine phenocrystals displays corroded margins and are rimmed or replaced by augite, and Fe oxide, indicating it was in disequilibrium with the melt during the latest stages of crystallization. The opaques minerals are principally hematite, though minor amounts of magnetite and ilmenite are also present.

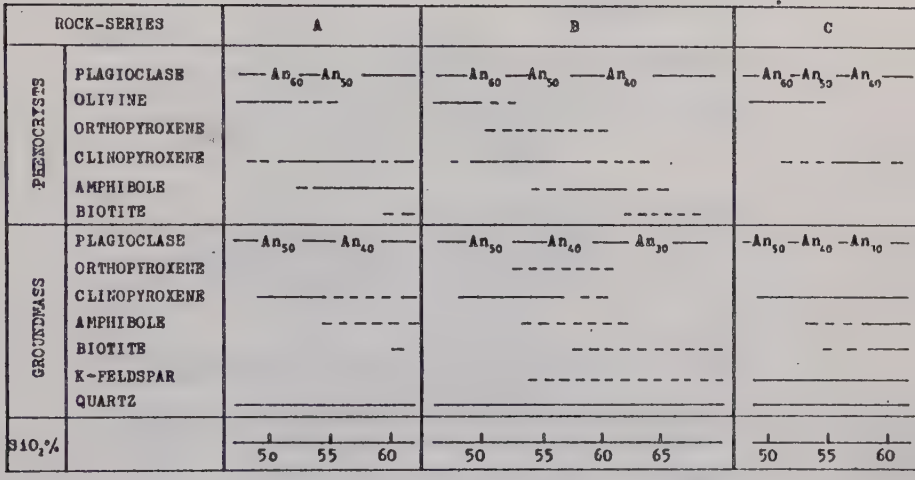

Fig.4. Mineral composition of the three Jurassic volcanic series.

TABLE 2: Petrographic Descriptions of Jurassic Volcanic Rocks
(Location see Fig. 5)

-EARLY JURASSIC-

Sample E-1.- Quartz-andesite.
Phenocrysts of Plagioclase (An 50-53), 18%, clinopyroxene (diopsidic augite) 12%.
Groundmass of Plagioclase (An 44), 40%, clinopyroxene (diopsidic augite) 20%, hematite, quartz, 10%.

Sample E-2.- Quartz-andesite.
Phenocrysts of plagioclase (An 50-53), 20%, clinopyroxene (diopsidic augite) 9%.
Groundmass of plagioclase (An 45), 40%, clinopyroxene 19%, oxide of Fe, quartz, 12%.

Sample E-3.- Quartz-tholeiite hawaiite.
Phenocrysts of plagioclase (An 45), 10%, clinopyroxene, 7%.
Groundmass of plagioclase (An 40), 43%, clinopyroxene, 29%, oxide of Fe, quartz, 11%

Sample E-4.- Mela-olivine-bearing andesite.
Phenocrysts of plagioclase (An 60), 14%, Fe olivine, 3%, clinopyroxene (diopsidic augite) 10%.
Groundmass of plagioclase (An 30), 43%, clinopyroxene, 21%, oxide of Fe, quartz, 9%.

Sample E-5.- Quartz-tholeiite hawaiite.
Phenocrysts of plagioclase (An 50-55), 20%, clinopyroxene, 7%.
Groundmass of plagioclase (An 43), 33%, hornblende, 7%, clinopyroxene, 25%, oxide of Fe, quartz, 8%.

Sample E-6.- Quartz-andesite.
Phenocrysts of plagioclase (An 50), 7%, clinopyroxene (Augite dipsidic), 3%, hornblende, 4%.
Groundmass of plagioclase (An 40-44), 43%, clinopyroxene, 12%, hornblende, 14%, oxide of Fe, quartz, 14%.

Sample E-7.- Tholeiite hawaiite.
Phenocrysts of plagioclase (An 33), 9%, hornblende, 7%.
Groundmass of plagioclase (An 30), 52%, biotite, 18%, oxide of Fe, quartz, 14%.

Sample E-8.- Quartz-lati andesite.
Phenocrysts of plagioclase (An 38), 17%, Fe olivine, 3%.
Groundmass of plagioclase (An ?), 46%, biotite, 16%, K feldspar, oxide of Fe, quartz, 18%.

Sample E-9.- Olivine-bearing andesite.
Phenocrysts of plagioclase (An 60), 20%, Fe olivine, 6%.
Groundmass of plagioclase (An 53), 41%, clinopyroxene (augite), 17%, oxide of Fe, K-feldspar, quartz, 16%.

Sample E-10.- Quartz-latite.
Phenocrysts of plagioclase (An 50-52), 20%, clinopyroxene (diopsidic augite), 9%.
Groundmass of plagioclase (An 43), 31%, clinopyroxene, 10%, K-feldspar, quartz, Fe oxide, 30%.

Sample E-11.- Quartz-latiandesite.
Phenocrysts of plagioclase (An 47-50), 19%, clinopyroxene (augite), 13%.
Groundmass of plagioclase (An 34-36), 37%, clinopyroxene, 10%, Fe oxide, K-feldspar, quartz, 21%.

Sample E-12.- Quartz-latiandesite.
Phenocrysts of plagioclase (An 50), 17%, clinopyroxene (augite), 14%.
Groundmass of plagioclase (An 40), 32%, clinopyroxene (augite), 13%, orthopyroxene (hypersthene), 5%, K-feldspar, Fe oxide, quartz, 19%.

Sample E-13.- Leuco quartz-andesite.
Phenocrysts of plagioclase (An 46), 26%, clinopyroxenes (augite), 5%, hornblende, 3%.
Groundmass of plagioclase (An 36-39), 48%, hornblende, 6%, biotite, 2%, Fe oxide, quartz, 10%.

Sample E-14.- Quartz-latiandesite.
Phenocrysts of plagioclase (An 36-38), 17%, hornblende, 6%, biotite, 3%.
Groundmass of plagioclase (An 29-32), 36%, hornblende, 6%, biotite, 5%, Quartz, K-feldspar, Fe oxide, 27%.

Sample E-15.- Olivine-bearing latiandesite.
Phenocrysts of plagioclase (An 50), 20%, clinopyroxene (augite), 9%, orthopyroxene (hypersthene), 2%.
Groundmass of plagioclase (An 42), 39%, orthopyroxene (hypersthene), 2%, clinopyroxene (augite), 10%, K-feldspar, Fe oxide, quartz, 18%.

Sample E-16.- Quartz-latiandesite.
Phenocrysts of plagioclase (An 50), 16%, clinopyroxene (diopsidic augite), 10%.
Groundmass of plagioclase (An 40), 25%, clinopyroxene, 12%, hornblende, 5%, biotite, 3%, K-feldspar, Fe oxide, quartz, 29%.

-MIDDLE JURASSIC-

Sample M-1.- Mela rhyodacite.
Phenocrysts of plagioclase (An 28-30), 7%, hornblende, 13%.
Groundmass of plagioclase (An ?), 33%, hornblende, 5%, biotite, 14%, K-feldspar, quartz, Fe oxide, 28%.

Sample M-2.- Quartz-latiandesite.
Phenocrysts of plagioclase (An 48-52), 14%, Fe olivine, 3%, clinopyroxene (augite), 8%, orthopyroxene (hypersthene), 3%.
Groundmass of plagioclase (An 40-44), 36%, clinopyroxene (augite), 16%, orthopyroxene (hypersthene), 4%, Fe oxide, quartz, 16%.

Sample M-3.- Leuco olivine hawaiite.
Phenocrysts of plagioclase (An 40), 23%.
Groundmass of plagioclase (An 35), 36%, Fe oxide, quartz, K-feldspar, 41%.

Sample M-4.- Leuco quartz-bearing andesite.
Phenocrysts of plagioclase (An 45), 15%, clinopyroxene (diopsidic augite), 11%, hornblende, 5%.
Groundmass of plagioclase (An ?), 48%, hornblende, 7%, biotite, 6%, Fe oxide, quartz, 8%.

Sample M-5.- Leuco quartz-latiandesite.
Phenocrysts of plagioclase (An 40), 18%, Fe olivine, 2%.
Groundmass of plagioclase (An ?), 35%, K-feldspar, Fe oxide, quartz, 45%.

Sample M-6.- Quartz-latite.
Phenocrysts of plagioclase (An 40), 16%, Fe olivine, 1%, clinopyroxene (diopsidic augite), 9%.
Groundmass of plagioclase (An ?), 35%, clinopyroxene (diopsidic augite), 12%, K-feldspar, Fe oxide, quartz, 27%.

Sample M-7.- Rhyodacite.
Phenocrysts of plagioclase (An 30), 13%, quartz, 8%.
Groundmass of plagioclase (An 25), 34%, quartz, 12%, biotite, 11%, K-feldspar, Fe oxide, 22%.

Sample M-9.- Quartz-latiandesite.
Phenocrysts of plagioclase (An 60), 20%, clinopyroxene (augite), 11%.
Groundmass of plagioclase (An 55), 39%, hornblende, 12%, K-feldspar, Fe oxide, quartz, 18%.

Sample M-10.- Quartz-latiandesite.
Phenocrysts of plagioclase (An 50), 10%.
Groundmass of plagioclase (An 40-42), 43%, K-feldspar, Fe oxide, quartz, 47%.

Sample M-11.- Leuco quartz-bearing latiandesite.
Phenocrysts of plagioclase (An 50), 12%, clinopyroxene (augite), 7%.
Groundmass of plagioclase (An 40), 41%, clinopyroxene (augite), 9%, K-feldspar, Fe oxide, quartz, 31%.

Sample M-12.- Quartz-latiandesite.
Phenocrysts of plagioclase (An 54), 27%.
Groundmass of plagioclase (An 47), 34%, K-feldspar, Fe oxide, quartz, 39%.

Sample M-13.- Quartz-latiandesite.
Phenocrysts of plagioclase (An 42-44), 18%, clinopyroxene (diopsidic augite), 10%.
Groundmass of plagioclase (An 35), 43%, clinopyroxene (diopsidic augite), 11%, K-feldspar, Fe oxide, quartz, 19%.

Sample M-14.- Leuco quartz-bearing tholeiite hawaiite.
Phenocrysts of plagioclase (An 30), 31%.
Groundmass of plagioclase (An ?), 46%, Fe oxide, quartz, 23%.

Sample M-15.- Leuco quartz-latiandesite.
Phenocrysts of plagioclase (An 50), 21%, Fe olivine, 1%.
Groundmass of plagioclase (An ?), 42%, Fe olivine, 3%, Fe oxide, quartz, K-feldspar, 33%.

Sample M-16.- Olivine mugearite.
Phenocrysts of plagioclase (An 60), 21%, olivine, 3%, clinopyroxene (augite), 5%.
Groundmass of plagioclase (An 48-50), 33%, clinopyroxene (augite), 12%, quartz, K-feldspar, Fe oxide, 26%.

Sample M-17.- Leuco quartz-bearing latiandesite.
Phenocrysts of plagioclase (An 35), 32%.
Groundmass of plagioclase (An ?), 31%, K-feldspar, quartz, Fe oxide, 37%.

-UPPER JURASSIC-

Sample U-1.- Leuco quartz-andesite.
Phenocrysts of plagioclase (An 60), 20%,
clinopyroxene (diopsidic augite), 10%.
Groundmass of plagioclase (An 54), 33%,
clinopyroxene (diopsidic augite), 14%,
K-feldspar, Fe oxide, 23%.

Sample U-2.- Quartz-latiandesite.
Phenocrysts of plagioclase (An 45-47), 10%.
Groundmass of plagioclase (An 38-40), 34%,
clinopyroxene (augite), 17%, K-feldspar,
Fe oxide, quartz, 39%.

Sample U-3.- Leuco quartz-latiandesite.
Phenocrysts of plagioclase (An 54-56), 24%,
Fe olivine, 1%.
Groundmass of plagioclase (An 42-45), 33%,
K-feldspar, quartz, Fe oxide, 43%.

Sample U-4.- Quartz-bearing latiandesite.
Phenocrysts of plagioclase (An 47), 18%,
clinopyroxene (diopsidic augite), 6%.
Groundmass of plagioclase (An 38-40), 26%,
clinopyroxene (diopsidic augite), 12%, K-feldspar,
Fe oxide, quartz, 38%.

Sample U-5.- Quartz-latiandesite.
Phenocrysts of plagioclase (An 40-42), 17%,
clinopyroxene (diopsidic augite), 7%.
Groundmass of plagioclase (An ?), 36%, clino-
pyroxene (diopsidic augite), 12%, K-feldspar,
quartz, Fe oxide, 28%.

Sample U-7.- Quartz-bearing latiandesite.
Phenocrysts of plagioclase (An 50), 13%,
clinopyroxene (diopsidic augite), 7%.
Groundmass of plagioclase (An 38-40), 29%,
clinopyroxene (diopsidic augite), 11%,
hornblende, 6%, K-feldspar, quartz,
Fe oxide, 34%.

Sample U-8.- Olivine-bearing andesite.
Phenocrysts of plagioclase (An 40), 26%,
clinopyroxene (diopsidic augite), 6%.
Groundmass of plagioclase (An 32-34), 47%,
clinopyroxene (diopsidic augite), 13%,
Fe oxide, quartz, 8%.

Sample U-11.- Quartz-andesite.
Phenocrysts of plagioclase (An 62), 21%,
clinopyroxene (diopsidic augite), 12%.
Groundmass of plagioclase (An 48), 42%,
clinopyroxene (diopsidic augite), 13%,
Fe oxide, quartz, 12%.

Sample U-12.- Quartz-andesite.
Phenocrysts of plagioclase (An 50), 16%, hornblende, 8%, clinopyroxene (augite), 6%. Groundmass of plagioclase (An ?), 43%, clinopyroxene (augite), 7%, hornblende, 10%, Fe oxide, quartz, 10%.

Sample U-13.- Olivine andesite.
Phenocrysts of plagioclase (An 58-60), 22%, olivine, 6%, clinopyroxene (augite), 5%. Groundmass of plagioclase (An 51-52), 41%, clinopyroxene (augite), 15%, Fe oxide, quartz, 11%.

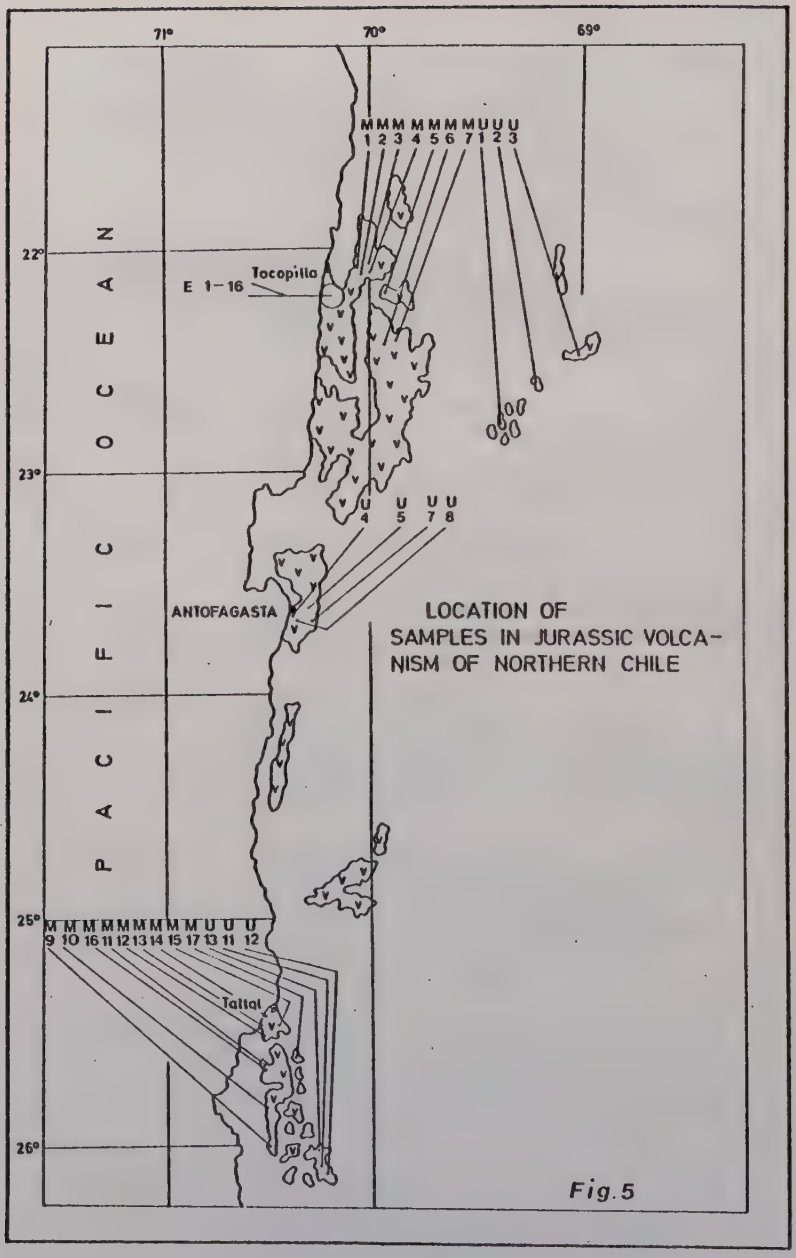
71°
70°
69°
22°
23°
24°
25°
26°
PACIFIC OCEAN
M M M M M M M M U U U
1 2 3 4 5 6 7 1 2 3
E 1–16
Tocopilla
U U U U
4 5 7 8
ANTOFAGASTA
M M M M M M M M M U U U
9 10 16 11 12 13 14 15 17 13 11 12
Taltal
LOCATION OF
SAMPLES IN JURASSIC VOLCA-
NISM OF NORTHERN CHILE

Fig. 5

6. CLASSIFICATION AND NOMENCLATURE OF JURASSIC VOLCANIC ROCKS

The results of the norm calculation in use (CIPW, NIGGLI's molecular norm system) in many cases agree tolerably well with the modal mineral composition. More often, however, large discrepancies arise between the norm and the mode. Especially with regard to the undersaturated volcanics, the results of the CIPW norms show often great differences. This fact was recently pointed out by CHAYES and YODER (1971) and PICHLER and STENGELIN (1973).

The discrepancies between mode and norm are greatly eliminated by the RITTMANN norm method (RITTMANN 1973). The calculation from the chemical analysis yields a mineral composition which would have resulted if the crystallization of the rock had been completed either under volcanic or plutonic conditions. This calculations reflects the mineral assemblages stable at the crystallization temperature of the last fraction of the melt and is therefore based on the real composition of the rock forming minerals and not on ideal normative compounds. The results of the Rittmann norm are expressed in volume percents, the plotted point of a volcanic rock in the Q-A-P-F double-triangle (STRECKEISEN 1967) will determine its petrographic name (PICHLER and STENGELIN 1973).

All chemical analyses of Jurassic volcanic rocks of Northern Chile have been calculated according to the RITTMANN norm method. The denomination of the analysed volcanic rocks is based on the STRECKEISEN system, using the RITTMANN norm calculation.

The results of this calculation are plotted in the Q-A-P-F double-triangle (Fig. 6).

It is clearly recognizable that the rocks are concentrated in three clusters which represent three groups:

- *Series A* is concentrated in the fields 10 and 10*. These rocks are andesites, tholeiite hawaiites and quartz-andesites, respectively. All rocks except samples E-4, E-7, U-8, and U-13 (Table 2) have normative quartz (between 0.1 and 7.6%). Their color index ranges from 12.8 to 42.0, with an average value of 29. Normative sanidine is lacking.
- *Series B* covers the fields 9,9* and 3b. The volcanic rocks of this series are: latiandesites, quartz-latiandesites and rhyodacites.

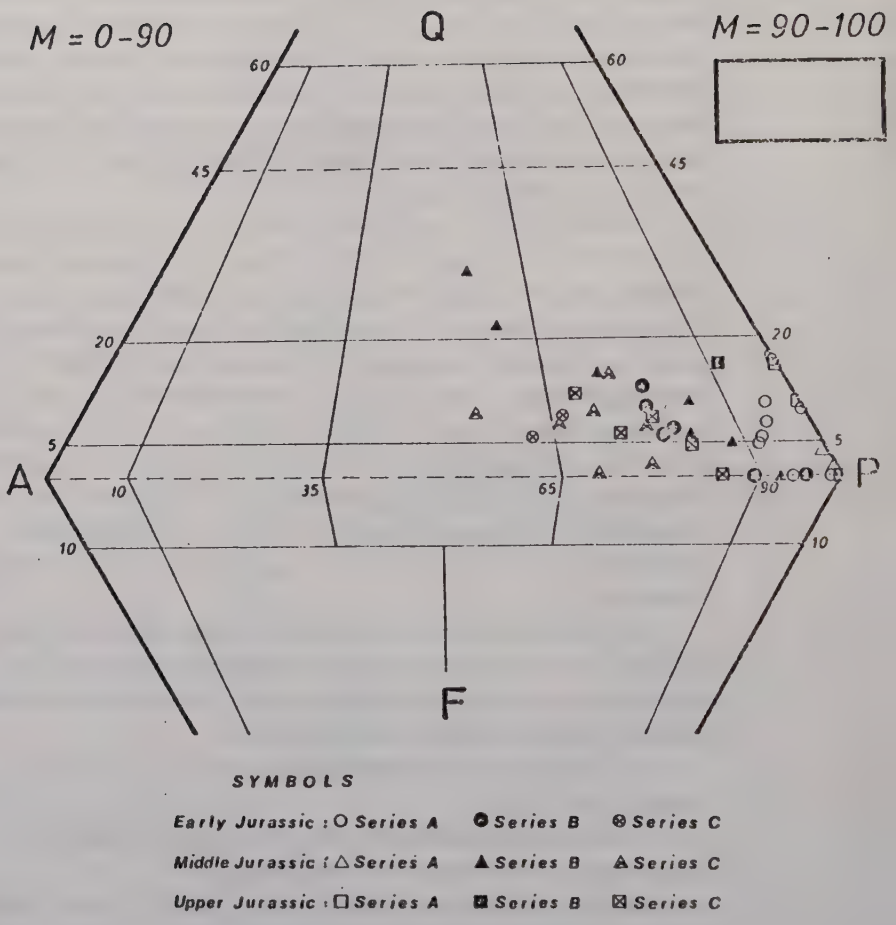

Fig.6. Q-A-P-F double-triangle plot of Jurassic lavas.

Common normative quartz lies between 3.9 and 24.2 (except samples E-9 and E-15). The color index ranges from 12.6 to 27.3 with an average value of 19. In contrast to series A, normative sanidine is always present; its average amounts to 14%.

- *Series C* populates the fields 9,9* and field 8*. All samples (except M-16 and U-7) have normative quartz and the color index ranges from 13.4 to 28.7 with an average value of 20. Normative sanidine average is 21%.

6.1. Comparison with other Magmatic Regions

The series A show a similar distribution in the Q-A-P-F double-triangle as the island arc type volcanic rocks of Kamchatka and the Kurile Islands, Honsyu, Hokkaido, Izu-Marianas. All these rocks are characterized by a concentration near the P (plagioclase) corner in the fields 10 and 10* as stated by PICHLER and STENGELIN (1973) (Fig. 6, 7).

The close similarity of the series B with the main distribution of the Cenozoic volcanic rocks from the Central Andes is clearly demonstrated by Fig. 8.

A clear separation exists between the series C (with a differentiation trend parallel to the A-P line) and the series B. Comparing the distribution of series C it is obvious that a similarity to the alkaline rocks of the Central Andes exists (Fig. 8).

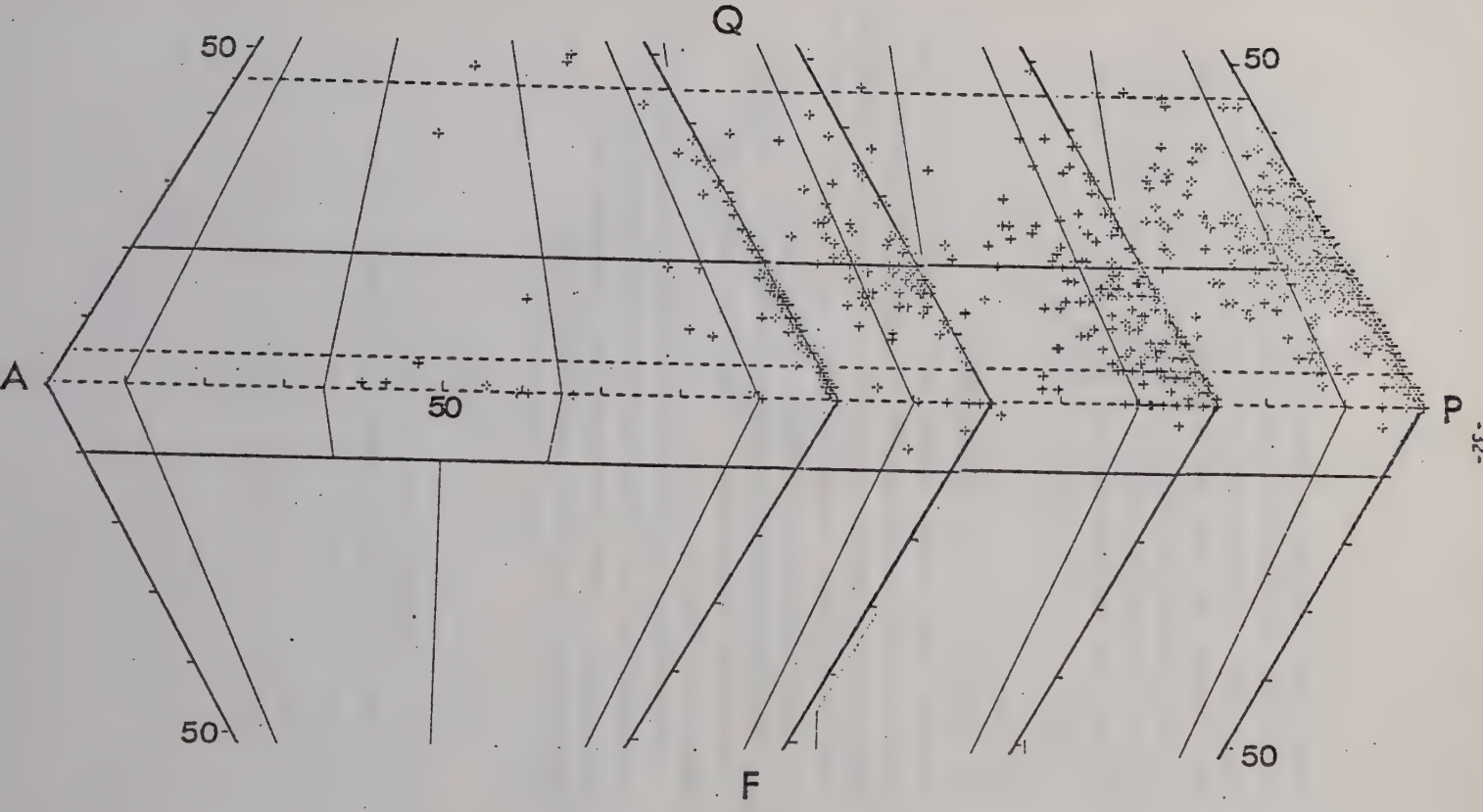

Fig.7. Q-A-P-F double-triangle plot of recent volcanics from: Izu-Marianas (a), Hokkaido (b), Kuriles and Kamtchatka (c), and Honsyu (d). Data from PICHLER and STENGELIN (in press).

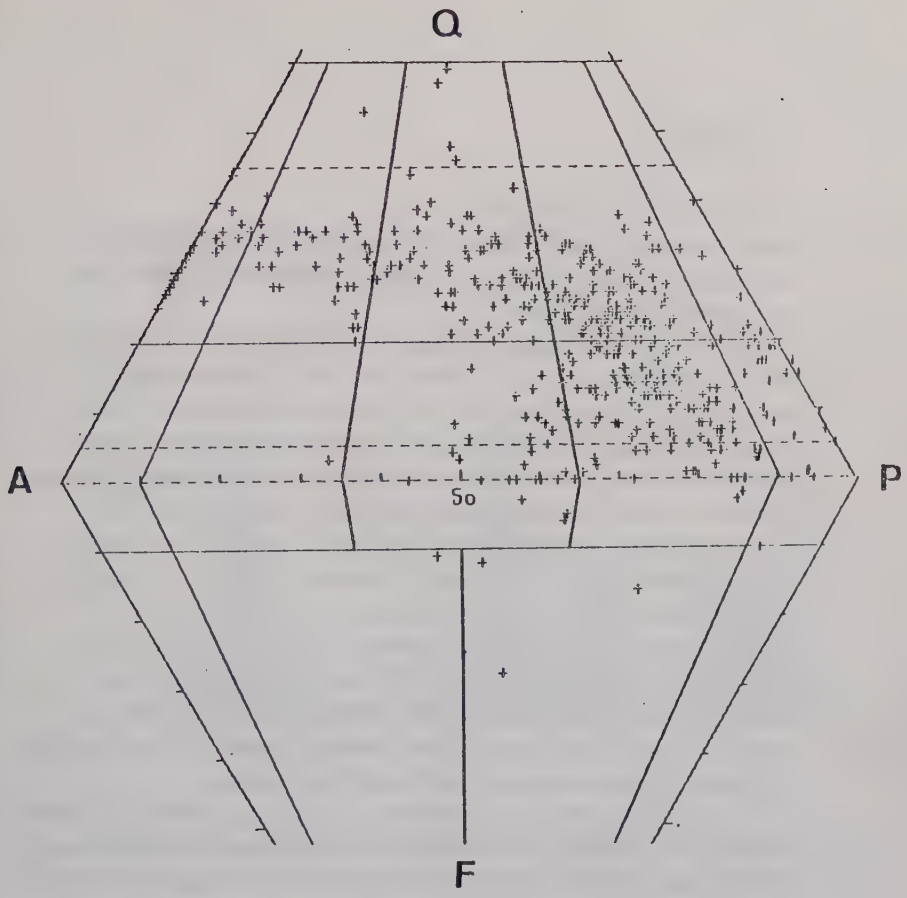

Fig.8. Q-A-P-F double-triangle plot of Cenozoic volcanics from the Central Andes. Data from PICHLER and STENGELIN (in press).

7. GEOCHEMISTRY

7.1. Major Element Chemistry

Major and trace element data (including rare earth abundances) and corresponding norms of 42 new analyses of Jurassic volcanic lavas are given in Tables 3 and 4.

The silica content shows significant differences between the three series (Fig. 9): The series A has silica values between 49.5 and 60%, series B between 52.5 and 67% and series C ranges from 48 to 60%. Moreover series B is characterized by the occurrence of greater relative volumes of intermediate and acidic members than are formed during the crystallization of A and C rock series.

Color index varies inversely with SiO_2 (Fig. 10). At the one extreme, series A with high color index and relatively low SiO_2 is clearly distinguished from the other two rock series.

As observed by IRVINE and BARAGAR (1971), Al_2O_3 is the most significant major element for the distinction between the basic members of the tholeiitic and calc-alkaline series. The samples of series A have a significantly lower alumina content, whereas samples of series B are characterized by higher Al_2O_3 values.

In the K_2O versus SiO_2 plot (Fig. 11 and 12), series A is similar to typical tholeiitic association of modern island arcs: K_2O values are low and remain constant or exhibit depletion trends towards high silica lavas. In series B, K_2O shows a greater slope of enrichment than group A and is similar in this respect to the andesites of the Central Andes. The series C has the highest K_2O values of the three series and is comparable with the alkaline and shoshonitic groups (JAKES and WHITE 1972).

Na_2O shows similar behavior in the three series with a positive relationship to SiO_2 (Fig. 11). CaO varies inversely with silica (Fig. 13); series C is relatively lower in CaO than groups A and B. Fig. 14 shows the K_2O/Na_2O ratio of the Jurassic lavas as a function of the SiO_2 content. Principal divisions of the island-arc volcanic rocks are based on major-element chemistry, particularly the K_2O/Na_2O ratio; this value increase progressively from the tholeiites to calc-alkaline and shoshonitic series. The data show that in series A the K_2O/Na_2O ratios

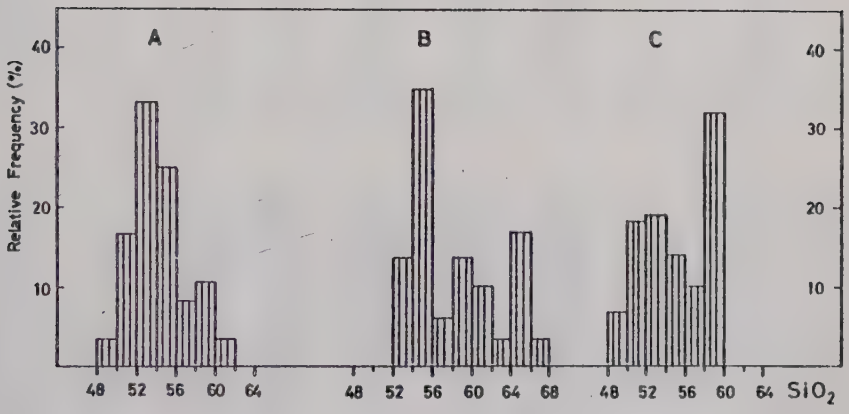

Fig.9. Frequency distribution of SiO_2 in the three different series (A,B,C) of the Jurassic volcanism in Northern Chile.

Table.3. Major element abundances of Jurassic volcanic rocks.

ORIGINAL ANALYSIS	E-1	E-2	E-3	E-4	E-5	E-6	E_7	E-8
SIO2	55.55	53.70	56.82	51.51	57.30	55.52	54.26	61.98
AL2O3	14.00	15.43	14.12	15.49	15.04	14.00	18.96	15.41
FE2O3	1.71	2.20	2.58	1.99	1.01	1.70	9.83	5.62
FEO	8.27	8.59	8.29	6.71	5.07	8.28	0.93	1.71
MNO	0.21	0.17	0.09	0.18	0.10	0.24	0.07	0.07
MGO	5.83	6.29	5.58	10.10	4.52	5.83	1.94	2.52
CAO	8.43	9.10	6.20	10.04	10.88	8.43	1.92	1.69
NA2O	3.88	2.54	3.80	2.21	4.38	3.85	7.03	5.45
K2O	1.20	1.05	1.05	1.01	0.23	1.18	0.52	3.01
TIO2	0.71	0.76	1.08	0.49	1.18	0.72	0.69	0.69
P2O5	0.21	0.21	0.39	0.27	0.29	0.25	0.19	0.24
H2O	0.00	0.00	0.00	0.00	0.00	0.00	3.65	1.70
TOTAL	100.00	100.04	100.00	100.00	100.00	100.00	99.99	100.09
CIPW NORM								
Q	1.32	4.19	7.09	0.00	5.43	1.53	4.91	12.06
OR	7.09	6.21	6.21	5.97	1.36	6.97	3.07	17.79
AB	32.83	21.49	32.16	18.70	37.06	32.58	59.49	46.12
AN	17.24	27.30	18.37	29.36	20.70	17.43	8.23	6.82
DI	19.13	13.30	8.09	15.04	25.54	18.76	0.00	0.00
HY	18.07	22.13	21.39	22.26	5.53	19.32	4.83	6.28
OL	0.00	0.00	0.00	4.22	0.00	0.00	0.00	0.00
MT	2.48	3.19	3.74	2.89	1.46	2.46	1.23	3.74
HM	0.00	0.00	0.00	0.00	0.00	0.00	8.99	3.04
IL	1.35	1.44	2.05	0.93	2.24	1.37	1.31	1.31
AP	0.49	0.49	0.90	0.63	0.67	0.58	0.44	0.56
C	0.00	0.00	0.00	0.00	0.00	0.00	3.90	0.69
RITTMANN NORM								
QUARTZ	3.5	5.4	7.6	0.0	7.0	3.8	0.0	8.6
SANIDINE	4.9	3.3	2.8	3.2	0.0	4.7	0.0	15.9
PLAGIOCLASE	56.8	56.5	59.0	54.8	62.3	56.8	79.3	60.1
CLINOPYROXENE	20.2	14.1	9.5	16.3	27.0	19.8	0.0	0.0
HYPERSTHENE	11.3	17.5	19.4	20.5	1.4	11.6	9.0	10.6
OLIVINE	0.0	0.4	0.0	2.6	0.0	0.0	0.0	0.0
CORDIERITE	0.0	0.0	0.0	0.0	0.0	0.0	5.7	2.3
SPINEL	0.0	0.0	0.0	0.0	0.0	0.0	2.9	0.0
MAGNETITE	2.3	2.0	1.8	1.5	0.9	2.3	1.9	1.3
ILMENITE	0.6	0.9	1.1	0.5	0.8	0.6	0.8	0.8
APATITE	0.4	0.4	0.8	0.6	0.6	0.5	0.4	0.5
COLOUR INDEX	34.4	34.3	29.8	41.4	30.1	34.2	20.3	14.9
Q COORDINATES	5.4	8.2	10.9	0.0	10.1	5.7	0.0	10.2
A STRECKEISEN	7.5	5.1	4.1	5.5	0.0	7.1	0.0	18.8
P DOUBLE-	87.1	86.5	85.0	94.5	89.9	87.1	100.0	71.0
F TRIANGLE	0.0	0.0	0.0	0.0	0.0	0.0	0.0	0.0
A COORDINATES	24.3	17.4	23.0	14.6	30.3	24.1	33.0	47.5
F AFM-	47.9	52.1	50.6	39.5	40.0	48.1	50.9	38.4
M TRIANGLE	27.9	30.5	26.4	45.9	29.7	27.9	10.0	14.1
SIGMA RITTMANN	2.06	1.20	1.70	1.22	1.49	2.02	5.06	3.77
TAU RITTMANN	11.00	13.29	7.02	17.47	7.25	10.46	13.56	19.71

ORIGINAL ANALYSIS	E-9	E-10	E_11	E-12	E-13	E-14	E-15	E-16
SIO2	52.60	53.71	55.76	55.57	59.97	64.44	54.89	56.46
AL203	17.95	14.13	17.73	17.70	15.20	16.64	19.00	15.50
FE203	4.63	5.72	2.36	2.40	3.89	2.39	2.44	3.13
FEO	3.77	5.58	4.96	4.88	4.25	2.66	4.97	6.74
MNO	0.26	0.30	0.22	0.33	0.26	0.07	0.16	0.30
MGO	4.39	4.03	4.22	4.25	1.94	2.52	4.33	4.03
CAO	6.98	5.59	6.02	8.04	4.82	1.69	5.98	5.69
NA2O	4.42	3.33	3.35	3.31	5.19	5.45	4.62	3.33
K2O	1.30	2.78	2.19	2.23	0.52	3.01	1.80	2.78
TIO2	0.94	1.53	0.88	0.90	0.89	0.89	0.94	1.63
P2O5	0.18	0.41	0.29	0.38	0.27	0.24	0.18	0.41
H2O	2.43	2.41	0.00	0.00	2.52	0.00	0.00	0.00
TOTAL	99.85	99.92	100.00	100.00	99.72	100.00	100.31	100.00
CIPW NORM								
Q	1.76	7.14	4.84	4.77	14.88	13.80	0.00	7.30
OR	7.68	16.43	12.94	13.18	3.07	17.79	10.64	16.43
AB	37.40	28.18	28.35	28.01	43.92	46.12	39.09	28.18
AN	25.30	15.40	26.87	26.85	16.64	6.82	25.79	19.14
DI	6.46	8.16	8.96	8.58	4.51	0.00	6.22	5.26
HY	9.90	9.98	12.25	12.54	6.22	7.85	10.74	15.11
OL	0.00	0.00	0.00	0.00	0.00	0.00	2.09	0.00
MT	6.71	8.29	3.45	3.48	5.64	3.47	3.54	4.54
IL	1.79	3.10	1.67	1.71	1.69	1.69	1.79	3.10
AP	0.42	0.95	0.67	0.88	0.63	0.56	0.42	0.95
C	0.00	0.00	0.00	0.00	0.00	1.92	0.00	0.00
RITTMANN NORM								
QUARTZ	0.0	4.1	5.0	4.9	14.6	11.1	0.0	6.7
SANIDINE	3.5	25.9	13.9	14.5	0.0	15.3	8.9	23.2
PLAGICCLASE	73.9	41.8	58.5	57.9	69.6	58.0	71.1	46.9
CLINCPYROXENE	7.1	9.2	9.3	8.9	4.7	0.0	6.4	5.5
HYPERSTHENE	11.0	14.5	10.2	10.6	7.6	7.2	8.9	14.4
OLIVINE	1.2	0.0	0.0	0.0	0.0	0.0	1.6	0.0
CORDIERITE	0.0	0.0	0.0	0.0	0.0	6.2	0.0	0.0
MAGNETITE	2.0	2.0	1.6	1.6	2.0	0.8	1.8	1.6
ILMENITE	1.0	1.6	0.9	0.9	0.9	0.9	1.0	1.7
APATITE	0.4	0.9	0.6	0.8	0.6	0.5	0.4	0.6
COLOUR INDEX	22.2	27.3	22.0	22.0	15.2	15.1	19.7	23.2
Q COORDINATES	0.0	5.7	6.5	6.4	17.4	13.2	0.0	8.9
A STRECKEISEN	4.5	36.1	18.0	18.7	0.0	18.2	11.0	30.6
P DOUBLE-	95.5	58.2	75.5	74.9	82.6	68.7	89.0	60.6
F TRIANGLE	0.0	0.9	0.0	0.0	0.0	0.0	0.0	0.0
A COORDINATES	31.2	28.5	32.4	32.3	36.5	53.3	35.5	30.6
F AFM-	44.8	52.5	42.9	42.9	51.2	30.8	40.5	49.3
M TRIANGLE	24.0	18.9	24.7	24.8	12.4	15.9	24.0	20.2
SIGMA RITTMANN	3.41	3.49	2.41	2.44	1.92	3.34	3.47	2.77
TAU RITTMANN	12.06	5.29	12.29	11.24	8.63	9.90	12.84	5.37

ORIGINAL ANALYSIS	M-1	M-2	M-3	M-4	M-5	M-6	M-7	M-9
SIO2	65.51	54.19	52.65	55.25	58.25	59.60	64.20	52.62
AL2O3	14.26	16.29	18.66	13.23	16.40	16.06	15.89	19.01
FE2O3	3.95	5.32	4.74	6.48	1.82	5.66	3.54	4.27
FEO	1.31	3.49	2.98	2.32	6.25	1.73	2.60	4.08
MNO	0.08	0.14	0.25	0.14	0.06	0.11	0.08	0.17
MGO	2.04	5.12	4.99	3.27	2.16	2.25	1.32	5.13
CAO	2.79	8.35	6.18	4.44	3.83	3.94	2.29	7.27
NA2O	3.49	2.50	4.96	6.02	4.55	4.40	4.43	2.61
K2O	3.87	1.68	1.60	0.91	2.99	3.62	4.11	1.98
TIO2	0.62	0.97	0.80	0.82	1.22	1.22	0.70	0.83
P2O5	0.16	0.25	0.21	0.24	0.36	0.31	0.17	0.19
H2O	1.74	1.76	2.09	1.99	1.99	1.25	0.78	2.64
TOTAL	99.82	99.36	100.11	100.11	99.90	100.15	100.11	99.80
CIPW NORM								
Q	22.04	10.51	0.00	3.13	6.48	10.12	15.92	6.55
OR	22.87	9.33	9.46	5.38	17.67	21.39	24.29	11.70
AB	29.53	21.16	41.97	50.94	38.50	37.23	37.49	22.09
AN	11.82	28.27	23.93	20.03	15.50	13.38	10.25	31.58
DI	0.76	9.14	4.20	0.33	0.97	3.23	0.00	2.58
HY	4.73	9.37	5.83	7.99	13.00	4.11	4.13	14.46
OL	0.00	0.00	3.76	0.00	0.00	0.00	0.00	0.00
MT	2.69	7.71	6.87	5.56	2.64	2.40	5.13	6.19
HM	2.10	0.00	0.00	2.65	0.00	4.01	0.00	0.00
IL	1.18	1.65	1.52	1.56	2.32	2.32	1.33	1.58
AP	0.37	0.58	0.49	0.56	0.83	0.72	0.39	0.44
C	0.00	0.00	0.00	0.00	0.00	0.00	0.40	0.00
RITTMANN NORM								
QUARTZ	24.2	7.1	0.0	0.1	7.1	7.7	18.8	4.5
SANIDINE	24.7	10.9	6.4	0.0	26.2	35.0	27.7	11.9
PLAGIOCLASE	30.6	54.9	75.6	83.2	51.8	42.5	39.4	60.2
CLINOPYROXENE	1.2	10.0	6.1	0.4	1.0	3.5	0.0	2.8
HYPERSTHENE	6.8	14.2	0.0	12.6	10.3	8.1	0.0	17.6
OLIVINE	0.0	0.0	8.6	0.0	0.0	0.0	0.0	0.0
BIOTITE	10.8	0.0	0.0	0.0	0.0	0.0	12.5	0.0
MAGNETITE	1.1	1.6	2.0	2.4	1.5	1.3	1.0	1.6
ILMENITE	0.1	0.9	0.9	0.9	1.3	1.2	0.2	0.9
APATITE	0.3	0.5	0.4	0.5	0.7	0.6	0.3	0.4
COLOUR INDEX	20.1	26.9	17.5	16.2	14.2	14.2	13.7	23.0
Q COORDINATES	30.5	10.7	0.0	0.1	8.4	9.0	21.9	5.8
A STRECKEISEN	31.1	13.7	7.8	0.0	30.8	41.1	32.2	15.6
P DOUBLE-	38.5	75.6	92.2	99.9	60.9	49.9	45.9	78.6
F TRIANGLE	0.0	0.0	0.0	0.0	0.0	0.0	0.0	0.0
A COORDINATES	51.3	23.5	34.4	37.5	42.7	46.6	54.3	25.8
F AFM-	34.5	47.5	39.4	44.8	45.1	40.3	37.3	45.4
M TRIANGLE	14.2	28.9	26.2	17.7	12.2	13.1	8.4	28.8
SIGMA RITTMANN	2.41	1.56	4.45	3.42	3.73	3.87	3.44	2.19
TAU RITTMANN	13.81	12.31	13.56	11.52	7.50	7.62	13.17	15.10

ORIGINAL ANALYSIS	M-10	M-11	M-12	M-13	M-14	M-15	M-16	M-17
SIO2	53.65	56.31	54.98	56.98	59.97	60.19	52.37	59.76
AL2O3	15.79	18.90	17.10	17.48	18.00	18.56	18.54	18.89
FE2O3	9.91	4.95	7.85	3.64	6.54	5.29	2.92	4.33
FEO	1.89	2.19	0.95	3.38	0.37	0.66	5.11	0.83
MNO	0.07	0.03	0.69	0.06	0.02	0.09	0.18	0.36
MGO	8.79	2.33	2.68	2.35	1.08	0.78	5.77	1.26
CAO	6.76	5.68	6.22	5.98	2.14	4.35	7.11	2.06
NA2O	2.70	4.82	3.08	4.16	7.44	4.12	3.48	6.14
K2O	2.33	1.91	2.62	2.45	1.07	2.59	3.11	3.31
TIO2	2.52	0.95	1.47	0.85	0.82	0.65	0.92	0.50
P2O5	0.41	0.18	0.31	0.22	0.26	0.29	0.29	0.25
H2O	3.02	2.03	2.00	2.36	2.42	2.47	0.00	2.50
TOTAL	99.84	99.98	99.95	99.91	100.13	100.04	99.80	100.19
CIPW NORM								
Q	15.98	6.11	11.39	8.23	7.13	16.64	0.00	5.79
OR	13.77	11.29	15.48	14.49	6.32	15.31	18.38	19.56
AB	22.85	40.79	26.06	35.20	62.96	34.86	29.45	51.96
AN	24.08	24.30	25.10	21.79	8.92	19.69	25.78	8.59
DI	4.24	2.11	2.91	5.16	0.00	0.00	6.12	0.00
WO	0.00	0.00	0.00	0.00	0.00	0.00	0.00	0.00
HY	0.00	4.32	5.33	5.29	2.69	1.94	3.61	3.14
OL	0.00	0.00	0.00	0.00	0.00	0.00	9.81	0.00
MT	0.00	4.40	1.05	5.28	0.00	0.54	4.23	2.40
HM	9.91	1.91	7.12	0.00	6.54	4.92	0.00	2.67
IL	4.14	1.30	2.79	1.61	0.82	1.23	1.75	0.95
RU	0.00	0.00	0.00	0.00	0.39	0.00	0.00	0.00
TN	0.83	0.00	0.00	0.00	0.00	0.00	0.00	0.00
AP	0.95	0.42	0.72	0.51	0.60	0.67	0.67	0.58
C	0.00	0.00	0.00	0.00	1.33	1.76	0.00	2.06
RITTMANN NORM								
QUARTZ	12.6	3.9	8.0	7.2	3.4	13.1	0.0	1.8
SANIDINE	17.3	10.1	19.7	17.7	0.0	19.8	23.9	19.3
PLAGIOCLASE	51.4	72.2	53.6	59.7	83.8	54.5	55.9	65.4
CLINOPYROXENE	6.1	2.3	3.2	5.5	0.0	0.0	9.0	0.0
HYPERSTHENE	7.4	8.3	11.3	7.0	5.8	4.6	0.0	4.6
OLIVINE	0.0	0.0	0.0	0.0	0.0	0.0	8.7	0.0
CORDIERITE	0.0	0.0	0.0	0.0	4.4	5.8	0.0	6.8
MAGNETITE	1.6	1.7	1.4	1.7	1.2	0.8	1.9	1.0
ILMENITE	2.8	1.0	1.6	0.9	0.9	0.7	1.0	0.5
APATITE	0.9	0.4	0.6	0.5	0.5	0.6	0.6	0.5
COLOUR INDEX	17.9	13.4	18.0	15.0	12.3	12.0	20.5	12.9
Q COORDINATES	15.5	4.6	9.8	8.5	3.9	15.0	0.0	7.1
A STRECKEISEN	21.3	11.7	24.2	20.9	0.0	22.6	30.3	22.3
P DOUBLE-	63.2	83.7	65.9	70.6	96.1	62.3	69.7	75.5
F TRIANGLE	0.0	0.0	0.0	0.9	0.0	0.0	0.0	0.0
A COORDINATES	30.1	42.4	33.4	42.2	53.6	51.6	32.5	59.8
F AFM-	65.1	42.4	51.0	42.8	39.6	42.4	39.0	32.2
M TRIANGLE	4.7	14.1	15.7	15.0	6.8	6.0	28.5	8.0
SIGMA RITTMANN	2.38	3.48	2.71	3.13	4.27	2.62	4.63	5.33
TAU RITTMANN	4.47	12.46	7.38	12.45	9.78	15.36	12.49	17.00

ORIGINAL ANALYSIS	U-1	U-2	U-3	U-4	U-5	U-7	U-8	U-11
SIO2	56.96	54.95	54.35	52.37	57.84	52.66	49.95	54.19
AL203	18.60	16.39	18.89	16.02	15.37	16.36	17.50	17.09
FE203	3.29	3.09	5.94	4.57	5.18	3.62	3.17	6.92
FEO	3.57	5.40	1.79	5.25	4.33	5.17	5.40	2.32
MNO	0.11	0.12	0.07	0.29	0.09	0.26	0.15	0.09
MGO	3.12	3.38	1.45	4.36	1.69	4.65	7.60	5.32
CAO	7.41	6.59	7.10	8.19	4.76	7.68	9.96	8.03
NA2O	2.80	3.29	3.27	3.14	4.16	3.90	2.99	3.08
K2O	1.45	2.59	2.42	1.76	2.62	1.73	0.57	0.48
TIO2	1.26	1.10	1.30	1.36	1.73	1.45	0.69	0.88
P2O5	0.29	0.29	0.39	0.37	0.35	0.27	0.23	0.16
H2O	1.21	1.78	2.88	1.69	2.07	2.09	1.60	1.62
TOTAL	100.07	100.08	99.85	99.97	100.19	99.84	99.81	100.18
CIPW NORM								
Q	14.73	5.51	10.43	5.90	12.69	1.73	0.00	11.35
OR	8.57	15.31	14.30	10.40	15.48	10.22	3.37	2.84
AB	23.69	27.34	27.67	26.57	35.20	33.00	25.30	26.06
AN	33.90	23.34	29.72	24.42	15.53	22.03	32.65	31.33
DI	0.77	5.58	2.30	11.02	4.62	11.52	12.24	5.76
HY	9.36	12.38	2.54	8.76	3.00	10.63	14.94	10.58
OL	0.00	0.00	0.00	0.00	0.00	0.00	3.28	0.00
MT	4.77	4.47	2.23	6.63	7.51	5.25	4.60	5.22
HM	0.00	0.00	4.40	0.00	0.00	0.00	0.00	3.32
IL	2.39	2.09	2.47	3.72	3.29	2.75	1.31	1.67
AP	0.67	0.67	0.90	0.86	0.81	0.63	0.53	0.37
RITTMANN NORM								
QUARTZ	13.3	4.6	7.7	3.4	10.1	0.0	0.0	7.9
SANIDINE	6.0	18.3	16.5	11.3	22.3	10.4	0.0	0.0
PLAGIOCLASE	64.7	54.3	62.0	56.6	50.4	61.5	66.9	65.9
CLINOPYROXENE	0.8	5.9	2.6	12.3	5.1	12.7	13.4	6.4
HYPERSTHENE	12.4	13.3	7.8	12.2	8.0	11.8	12.0	16.9
OLIVINE	0.0	0.0	0.0	0.0	0.0	0.0	4.8	0.0
MAGNETITE	0.9	1.4	1.1	1.4	1.6	1.5	1.6	1.6
ILMENITE	1.4	1.2	1.4	2.0	1.8	1.4	0.7	1.0
APATITE	0.6	0.6	0.8	0.8	0.7	0.6	0.3	0.3
COLOUR INDEX	15.5	21.7	13.0	27.9	16.5	27.4	32.6	25.9
Q COORDINATES	15.8	5.3	3.0	4.8	12.1	0.1	0.0	10.8
A STRECKEISEN	7.1	24.3	19.1	15.9	26.9	14.5	0.0	0.0
P DOUBLE-	77.1	69.4	71.9	79.3	60.9	85.4	100.0	89.2
F TRIANGLE	0.0	0.9	0.0	0.0	0.0	0.0	0.0	0.0
A COORDINATES	30.3	32.4	39.7	25.9	38.6	29.7	18.2	20.3
F AFM-	47.4	45.7	50.2	51.0	51.7	45.8	43.0	49.3
M TRIANGLE	22.3	21.9	10.1	23.1	9.6	24.5	38.8	30.4
SIGMA RITTMANN	1.29	2.39	2.85	2.56	3.10	3.28	1.82	1.13
TAU RITTMANN	10.19	9.96	9.24	5.53	5.39	7.24	15.77	13.47

ORIGINAL ANALYSIS	U-12	U-13
SIO2	56.16	51.86
AL2O3	16.64	18.40
FE2O3	5.43	2.19
FEO	3.14	5.84
MNO	0.12	0.15
MGO	4.52	7.60
CAO	7.56	8.58
NA2O	3.09	3.99
K2O	0.37	0.37
TIO2	0.92	0.69
P2O5	0.21	0.13
H2O	1.76	0.00
TOTAL	99.92	100.00

CIPW NORM		
Q	15.65	0.90
OR	2.19	3.37
AB	26.15	33.76
AN	30.44	30.61
DI	4.43	8.35
HY	9.20	7.74
OL	0.00	10.75
MT	7.84	3.18
HM	0.02	0.00
IL	1.75	1.31
AP	0.49	0.30

RITTMANN NORM		
QUARTZ	12.9	0.0
PLAGIOCLASE	64.1	72.4
CLINOPYROXENE	4.9	9.4
HYPERSTHENE	15.2	7.3
OLIVINE	0.8	6.2
MAGNETITE	1.5	1.7
ILMENITE	1.0	0.7
APATITE	0.4	0.3
COLOUR INDEX	22.6	27.3
Q COORDINATES	16.8	0.0
A STRECKEISEN	0.0	0.0
P DOUBLE-	83.2	100.0
F TRIANGLE	0.0	0.0
A COORDINATES	21.5	22.7
F AFM-	50.5	39.5
M TRIANGLE	28.0	37.8
SIGMA RITTMANN	0.91	2.35
TAU RITTMANN	11.99	17.57

Samples of series A: E-1;E-2;E-3;E-4;E-5;E-6;E-7;E-13;M-4;M-14; U-8;U-11;U-12;U-13.

Samples of series B: E-8;E-9;E-11;E-12;E-14;E-15;M-1;M-2;M-3; M-7;M-9;M-11;M-15;U-1.

Samples of series C: E-10;E-16;M-5;M-6;M-10;M-12;M-13;M-16;M-17; U-2;U-3;U-4;U-5;U-7.

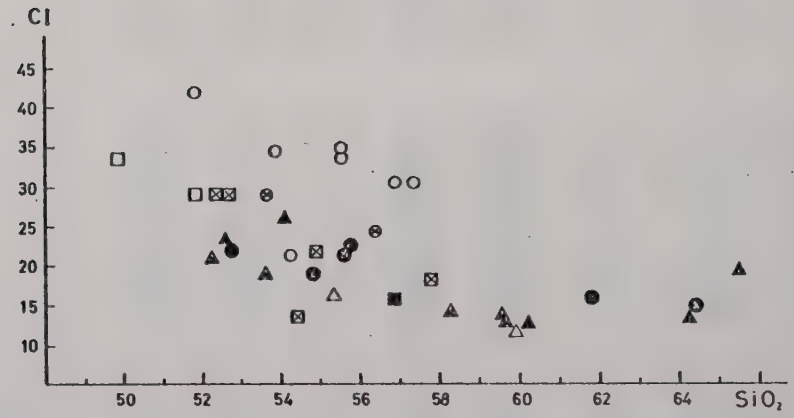

SYMBOLS

Early Jurassic : ○ Series A ● Series B ⊗ Series C

Middle Jurassic : △ Series A ▲ Series B ⊠ Series C

Upper Jurassic : □ Series A ■ Series B ⊠ Series C

Fig.10. Colour Index (CI) versus SiO_2 (in wt.%).

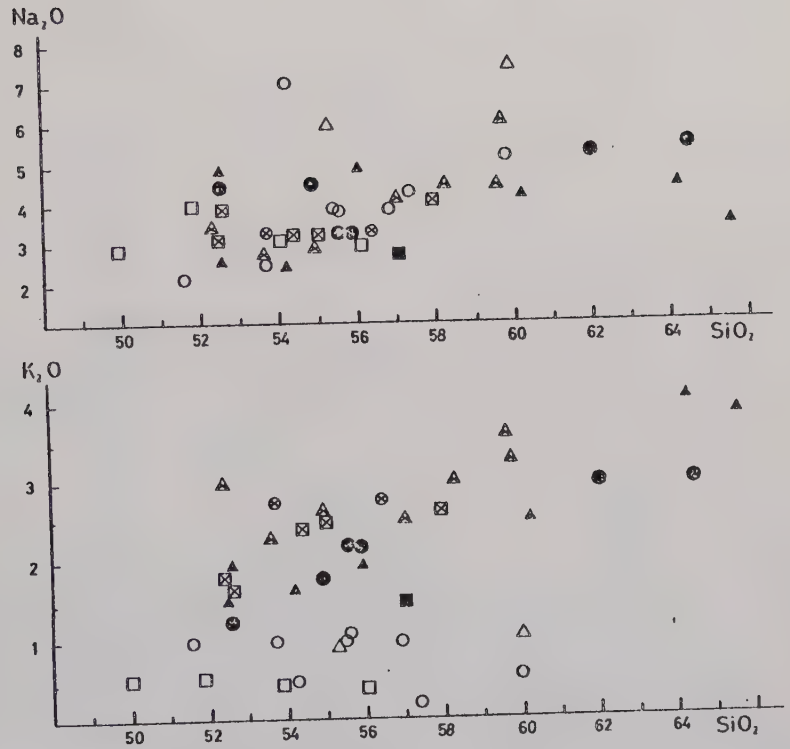

SYMBOLS

Early Jurassic :	○ Series A	● Series B	⊗ Series C
Middle Jurassic :	△ Series A	▲ Series B	⊠ Series C
Upper Jurassic :	□ Series A	■ Series B	⊠ Series C

Fig.11. Na_2O and K_2O versus SiO_2 (in wt.%).

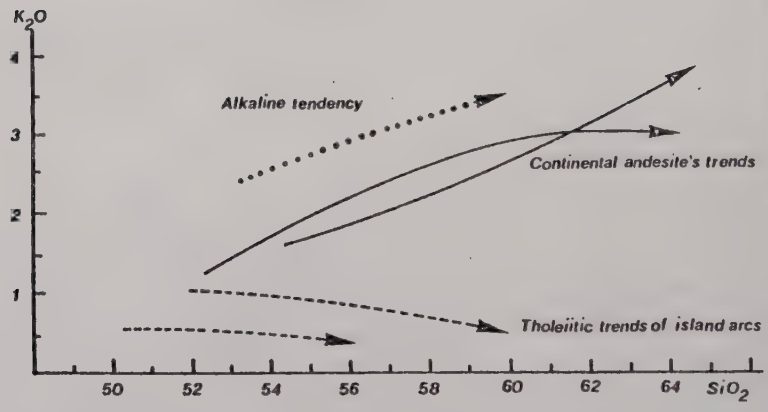

Fig.12. K_2O - SiO_2 diagram showing characteristic trends of the Jurassic volcanic series.

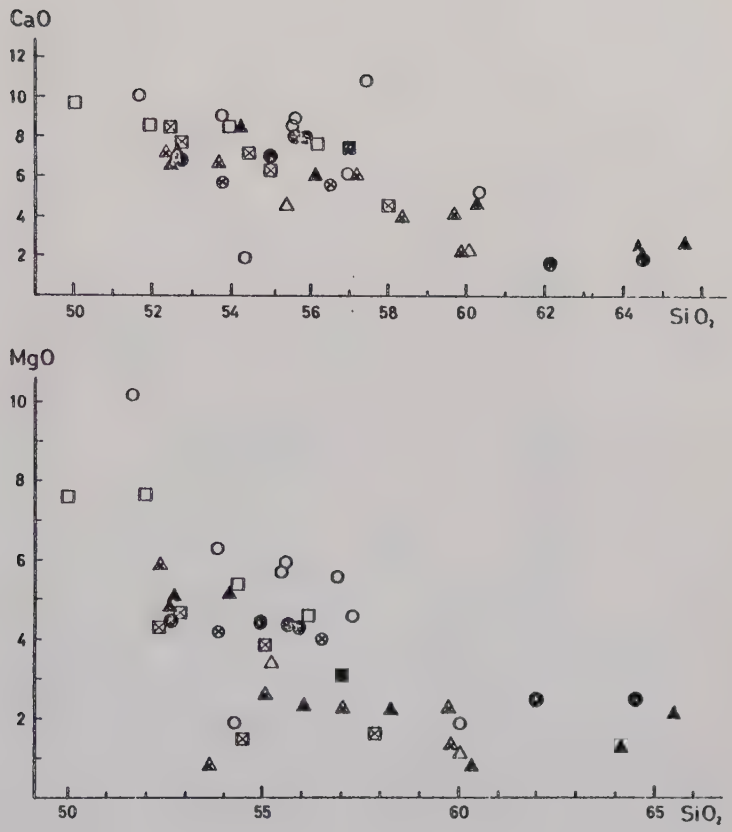

Fig.13. CaO and MgO versus SiO_2 (in wt.%).

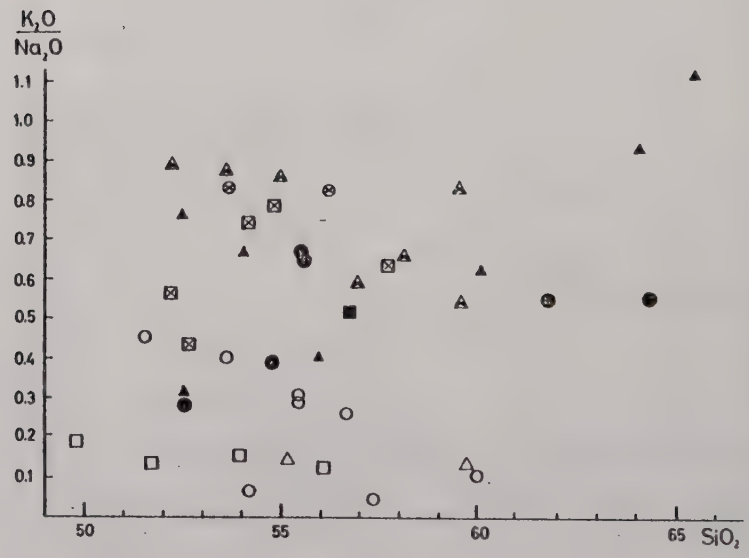

SYMBOLS

Early Jurassic : ○ Series A ● Series B ⊗ Series C

Middle Jurassic : △ Series A ▲ Series B ⧋ Series C

Upper Jurassic : □ Series A ■ Series B ⊠ Series C

Fig.14. K_2O/Na_2O versus SiO_2 (In wt.%).

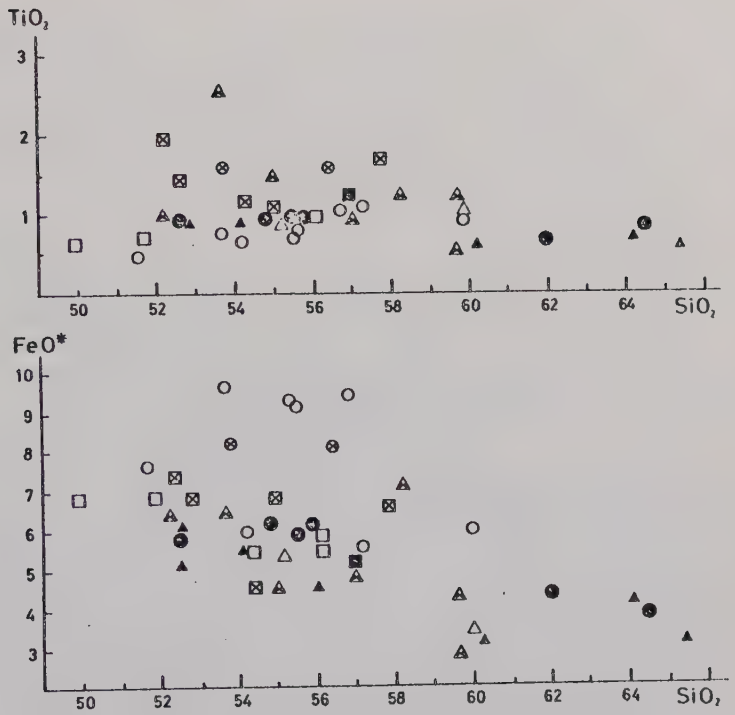

SYMBOLS

Early Jurassic : ○ Series A ● Series B ⊗ Series C

Middle Jurassic : △ Series A ▲ Series B ⊠ Series C

Upper Jurassic : □ Series A ■ Series B ⊠ Series C

Fig.15. TiO_2 and FeO (Fe total as FeO) versus SiO_2 (in wt.%).

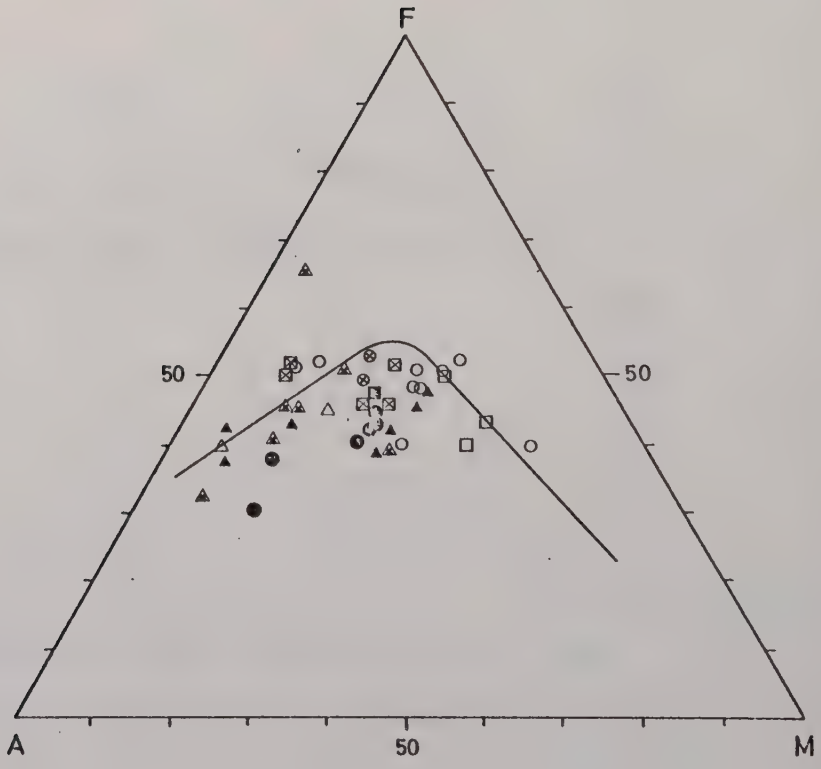

SYMBOLS

Early Jurassic :	○ Series A	◐ Series B	⊗ Series C
Middle Jurassic :	△ Series A	▲ Series B	⊗ Series C
Upper Jurassic :	□ Series A	■ Series B	⊠ Series C

Fig.16. AFM diagram of Jurassic volcanic rocks.

are notably low. The close relationship of series B with the modern volcanic rocks of calc-alkaline associations is further demonstrated in Fig. 14, in which a continuous transition from low to high K_2O/Na_2O ratios is obvious. Series C has higher K_2O/Na_2O ratios. The K_2O/Na_2O ratios ranges from 0.04 to 0.45 for the analysed samples of series A, from 0.29 to 1.10 for the lavas of series B, and from 0.23 to 0.94 for the series C. The average value is 0.21 for the series A, 0.60 for the series B,and 0.64 for series C. The values of these ratios are similar to those of the tholeiitic and calc-alkaline series, respectively of the circum-Pacific island arcs (JAKES and WHITE 1972).

MgO varies inversely with SiO_2 (Fig. 13). At the one extreme, series A with high MgO and relatively low SiO_2 contents, is clearly distinguished from series B and C.

Values of FeO (= total iron as FeO) are shown in Fig. 15. Series A show enrichment in FeO with increasing SiO_2, whereas series B and C decreases monotonically. The TiO_2 content shows similar variations as FeO (Fig. 15). In series A, TiO_2 increases with SiO_2, whereas series B and C show monotonically decreasing TiO_2 contents. For the range $SiO_2 > 57\%$, points of A, B and C rock series are mixed, whereas for lower SiO_2 values C series tend to have higher TiO_2 contents than B and A series. Group A shows lower TiO_2.

Fe and Ti are mostly concentrated in magnetite. Under a high oxygen fugacity, most of the magnetite would crystallize in a relatively early stage, leading to depletion of the residual magma in Fe and Ti and enrichment in SiO_2. This trend is typical for the series B (normal calc-alkaline trend). On the other hand, under a lower oxygen fugacity, crystallization of magnetite would be delayed, and hence Fe and Ti are not so strongly removed from magma as in the calc-alkaline series. This should be the series A trends.

The AFM plot (Fig. 16) shows a clear iron enrichment, relative to MgO and alkalies for the series A and C. The trend for the series B is similar to calc-alkaline suites.

7.2. Trace Element Chemistry

Trace element data are shown in Fig. 17 to 22 and in Table 4.

In general, Rb, Ba, and Sr show the largest variations in the three Jurassic rock series. Rubidium increases from 10 to 70 ppm, 25 to 150 ppm and 25 to 120 ppm in the series A, B and C, respectively (Fig. 17). GAST (1968) has shown that the K/Rb ratio is often a useful parameter for recognizing the fractionation of rock suites. According to GAST (1965), the K/Rb ratio is constant in many common rocks (K/Rb $\sim$300). The Jurassic volcanic series are characterized by a strong decrease of the K/Rb ratio from the basic to the acid members (Fig. 18). A series with low values of K/Rb ratio is clearly distinguished from all other suites. At the other extreme series C shows high K/Rb values. The behavior of barium is similar to that of rubidium (Fig. 17); series A has lower contents of Ba than series B and C. The strong Sr variations result from the distinct fractionation of the feldspars. KOLBE and TAYLOR (1966), HALL (1967), RHODES (1969), and others found a decrease of Sr with increasing SiO_2 in calc-alkaline plutonic rocks. Similar trends are observed within the tholeiitic association in island arc rocks (JAKES and WHITE 1972). In typical calc-alkaline suites of island arcs, however, such trends are not clear (BAKER 1968). In high-K calc-alkaline rocks (e.g. Eastern Papua, JAKES and SMITH 1970) the converse is found, i.e. increasing Sr with increasing SiO_2. Fig. 17 shows Sr values in the three series: Sr decreases with increasing silica content. Group B has higher values than the other series. The pattern is therefore on of progressive depletion of Sr in the melt. However, the Sr behavior in Jurassic lavas is not contrary with the rule that plagioclase/matrix Sr distribution coefficients rise rapidly with increasing proportions of albite molecule (JENSEN 1973). EWART and TAYLOR (1969) found a strong tendency for maximum concentration of Sr in the compositional range of An_{40-55} in andesitic and rhyolitic rocks of the Taupo volcanic zone, despite increasing distribution factors with decreasing An content.

Cr and Ni are easily affected by removal or accumulation of ferromagnesian mineral phases, mainly of olivine. The abundances of Cr, Ni, and V show an inverse correlation with SiO_2 (Fig. 19). There

TABLE 4: Trace element abundances in Jurassic volcanic rocks

ELEMENT (ppm)	E-1	E-2	E-3	E-4	E-5	E-6	E-7	E-8	E-9	E-10	E-11
Li	30	37	38	36	32	30	14	13	17	19	21
Rb	74	50	65	40	24	72	10	80	25	70	60
Sr	496	302	188	305	323	400	70	120	215	190	460
Ba	270	294	259	292	299	301	37	140	169	519	422
Cr	140	160	170	243	217	138	14	85	47	38	52
Co	25	41	19	40	18	25	32	11	29	23	23
Ni	30	47	43	78	46	30	22	24	31	31	36
V	253	231	255	220	280	255	245	154	259	380	187
Cu	86	56	65	155	80	68	36	54	115	68	128
Zn	105	83	49	128	51	102	46	65	63	179	88
Ga	15	16	17	13	16	14	22	22	21	21	23
Y	12	12	13	13	13	14	19	25	25	41	27
Zr	58	55	50	47	51	60	81	200	91	212	152
Mo	3	4	8	15	8	11	8	13	16	15	20
Pb	60	32	32	41	31	60	45	35	35	54	38
La		6.7		7.2					9.7	24.2	20.4
Ce		17.2		15.3					22.8	50.3	41.7
Nd		11.4		8.6					12.9	30.1	22.8
Sm		2.4		2.4					3.8	7.4	4.9
Eu		0.8		0.8					1.2	2.0	1.3
Gd		2.0		2.0					5.4	9.0	5.0
Tb		0.3		0.3					0.7	1.1	0.7
Dy		2.2		1.7					4.7	6.5	3.4
Tm				0.3					0.4	0.5	0.3
Yb		1.2		1.1					2.6	4.0	2.3
Lu		0.1		0.3					0.5	0.7	0.4

ELEMENT (ppm)	E-12	E-13	E-14	E-15	E-16	M-1	M-2	M-3	M-4	M-5	M-6
Li	20	15	14	16	18	20	13	73	12	18	36
Rb	65	10	80	25	70	150	35	35	15	70	110
Sr	440	70	120	215	190	150	340	550	400	420	160
Ba	423	36	135	165	500	333	268	181	111	709	674
Cr	53	178	207	233	203	42	88	56	51	106	112
Co	29	26	19	22	28	19	29	19	22	20	11
Ni	35	23	24	31	37	25	47	31	39	25	38
V	172	240	156	261	375	110	253	193	188	165	90
Cu	117	40	56	115	68	52	267	153	118	38	74
Zn	80	46	65	63	179	53	100	92	90	80	107
Ga	23	22	22	21	21	17	18	19	19	22	14
Y	27	19	25	25	40	35	22	22	22	50	21
Zr	153	81	203	90	210	216	119	66	99	291	121
Mo	16	6	10	15	10	21	21	5	25	5	3
Pb	32	45	34	36	50	35	48	22	38	22	30
La							13.9		9.7		42.7
Ce							28.9		20.6		88.1
Nd							17.7		14.9		44.5
Sm							4.3		3.5		9.4
Eu							1.1		1.1		2.1
Gd							4.7		4.0		9.1
Tb							0.6		0.6		1.4
Dy							3.3		3.5		7.2
Tm							0.3		0.3		0.7
Yb							2.2		2.3		5.4
Lu							0.4		0.4		0.7

ELEMENT (ppm)	M-7	M-9	M-10	M-11	M-12	M-13	M-14	M-15	M-16	M-17
Li	17	35	28	21	40	43	8	28	35	9
Rb	145	65	60	50	105	90	35	50	45	110
Sr	180	400	80	670	130	620	40	480	390	160
Ba	689	270	215	347	413	591	98	511	276	674
Cr	18	63	33	66	27	40	44	48	89	130
Co	67	27	26	24	28	25	18	20	76	17
Ni	13	50	32	44	27	26	24	29	73	45
V	55	220	349	143	237	176	133	79	226	105
Cu	105	174	55	88	69	166	99	99	51	60
Zn	100	128	75	39	222	94	62	63	100	107
Ga	21	20	22	22	24	20	18	20	22	14
Y	56	20	58	20	46	28	34	28	35	21
Zr	408	93	281	103	215	111	148	169	146	121
Mo	4	17	15	18	10	4	18	22	6	4
Pb	36	35	42	45	48	35	32	32	30	35
La		10.3	23.4							
Ce		23.1	53.6							
Nd		15.1	36.1							
Sm		3.5	8.8							
Eu		1.2	2.1							
Gd		2.5	10.6							
Tb		0.5	1.4							
Dy		3.5	9.7							
Tm		0.3	0.7							
Yb		1.8	5.1							
Lu		0.3	0.7							

ELEMENT (ppm)	U-1	U-2	U-3	U-4	U-5	U-7	U-8	U-11	U-12	U-13
Li	33	18	30	20	24	23	18	39	13	19
Rb	85	55	20	35	76	25	10	10	10	12
Sr	650	300	500	230	100	220	250	230	390	260
Ba	553	571	699	209	232	344	69	106	127	59
Cr	36	18	33	66	38	41	97	172	86	91
Co	11	22	25	24	28	66	33	19	19	87
Ni	14	20	25	56	27	34	81	43	53	80
V	99	206	146	319	165	253	212	248	168	210
Cu	60	68	92	53	52	50	50	67	65	45
Zn	87	91	101	107	139	78	81	49	50	101
Ga	25	21	21	22	20	19	19	19	19	19
Y	28	34	39	44	52	38	14	20	26	13
Zr	144	211	228	199	298	161	49	72	207	47
Mo	3	6	25	6	14	5	3	11	15	3
Pb	31	27	35	35	36	31	29	32	32	30
La	21.1	22.2		14.4						
Ce	43.2	44.8		35.4						
Nd	27.1	23.7		25.1						
Sm	4.9	5.3		6.4						
Eu	1.5	1.2		1.9						
Gd	4.9	5.5		6.8						
Tb	0.8	0.8		1.1						
Dy	3.2	4.2		6.9						
Tm	0.4	0.4		0.5						
Yb	2.7	3.0		3.8						
Lu	0.4	0.5		0.7						

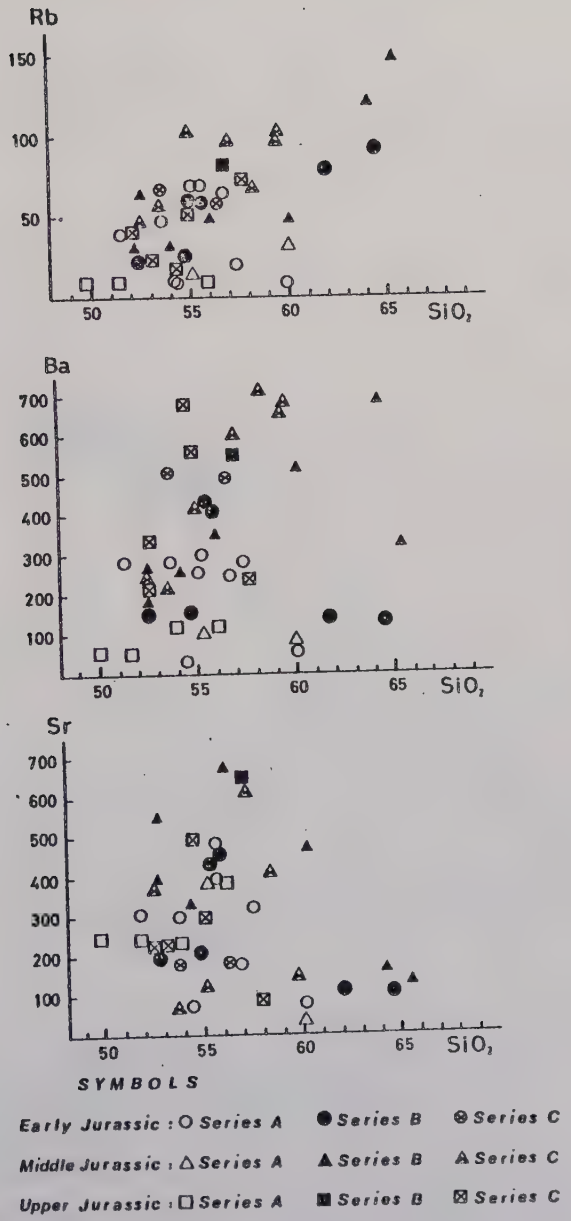

Fig.17. Rb,Ba and Sr (in ppm) versus SiO_2 (in wt.%).

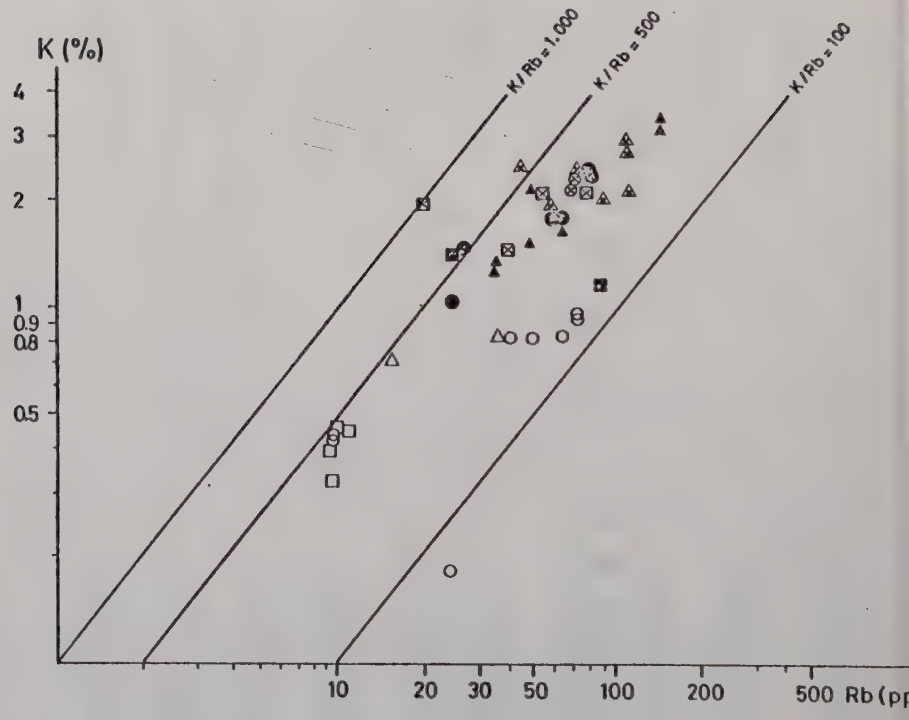

Fig.18. Potassium (in wt.%) versus rubidium (in ppm).

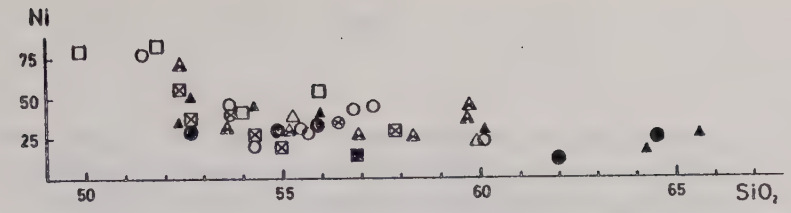

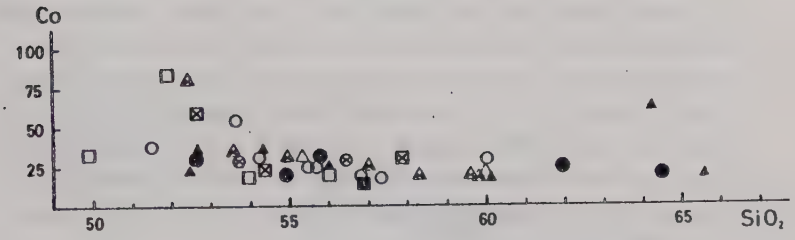

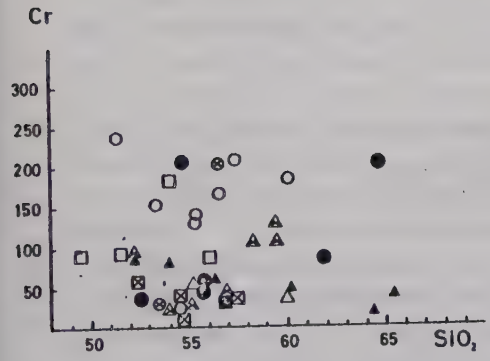

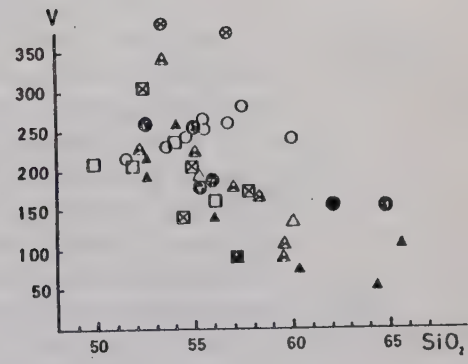

SYMBOLS

Early Jurassic :	○ Series A	● Series B	⊗ Series C
Middle Jurassic :	△ Series A	▲ Series B	⊠ Series C
Upper Jurassic :	□ Series A	■ Series B	⊠ Series C

Fig.19. Ni,Co,Cr and V (in ppm) versus SiO_2 (in wt.%) plot of Jurassic volcanic rocks.

is a wide range of abundance even for one rock association within a particular region (BAKER 1968), but, in general, ferromagnesian trace element concentration in island arc rocks are low. The abundances of these trace elements in calc-alkaline rocks are normally low, but in rocks with less than 54 percent SiO_2, Cr and Ni are sometimes high (JAKES and WHITE 1972). Series A shows higher Cr and Ni values than the other rock-series. Their enrichment seems to be the result of gravitative differentiation by which olivine and clinopyroxene are accumulated. Series B and C present approximately similar Cr and Ni concentrations. In contrast to Cr and Ni behaviour, V contents increase in series A with SiO_2. In this case vanadium shows a similar behaviour to FeO and TiO_2. These data support also the idea that magnetite was not so strongly removed from magma in series A.

The transition from low SiO_2 to high silica volcanics is accompanied by strong cobalt depletion (Fig. 19). The content of Co is similar in the three series, and the only anomalies being shown by a few samples of series B, in which high cobalt values for their concentrations of SiO_2 are present.

Zr shows likewise a regular pattern of variation (Fig. 20). There is a positive correlation between Zr and SiO_2, and zirconium indicates in the Jurassic volcanic rocks well its "residual character". However, the pattern of Zr increase with fractionation is not universal. LAMBERT et al. (1974) have found a progressive decline of Zr, as well as Y, in calc-alkaline lavas ranging from 60 to 75% SiO_2. The Zr content in series A is less than that of series B and C, and group C has the higher values.

The regular increase in yttrium from basic to high silica lavas in series B and C, is shown in Fig. 20; however, in group A remain approximately constant.

Gallium values remain constant with SiO_2 increase in the three volcanic suites, and series A shows the lower abundance in this element (Fig. 20).

Cu, Zn, and Pb in Jurassic series exhibit depletion towards high silica lavas (Fig. 21).

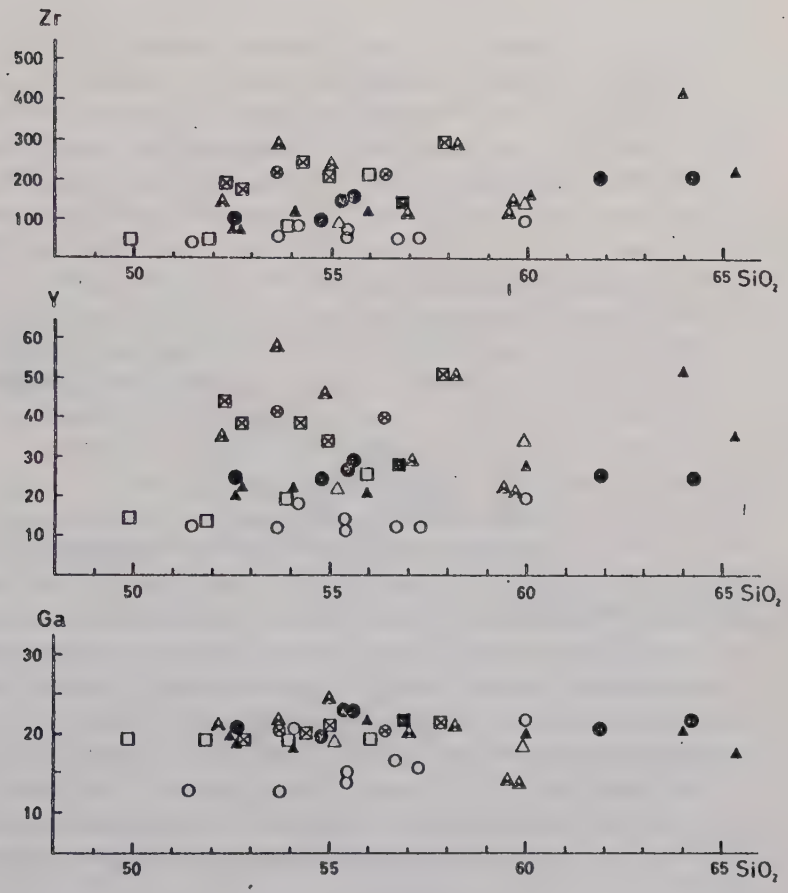

SYMBOLS

Early Jurassic :	○ Series A	● Series B	⊗ Series C
Middle Jurassic :	△ Series A	▲ Series B	⊠ Series C
Upper Jurassic :	□ Series A	■ Series B	⊠ Series C

Fig.20. Zr,Y and Ga (in ppm) versus SiO_2 (in wt.%).

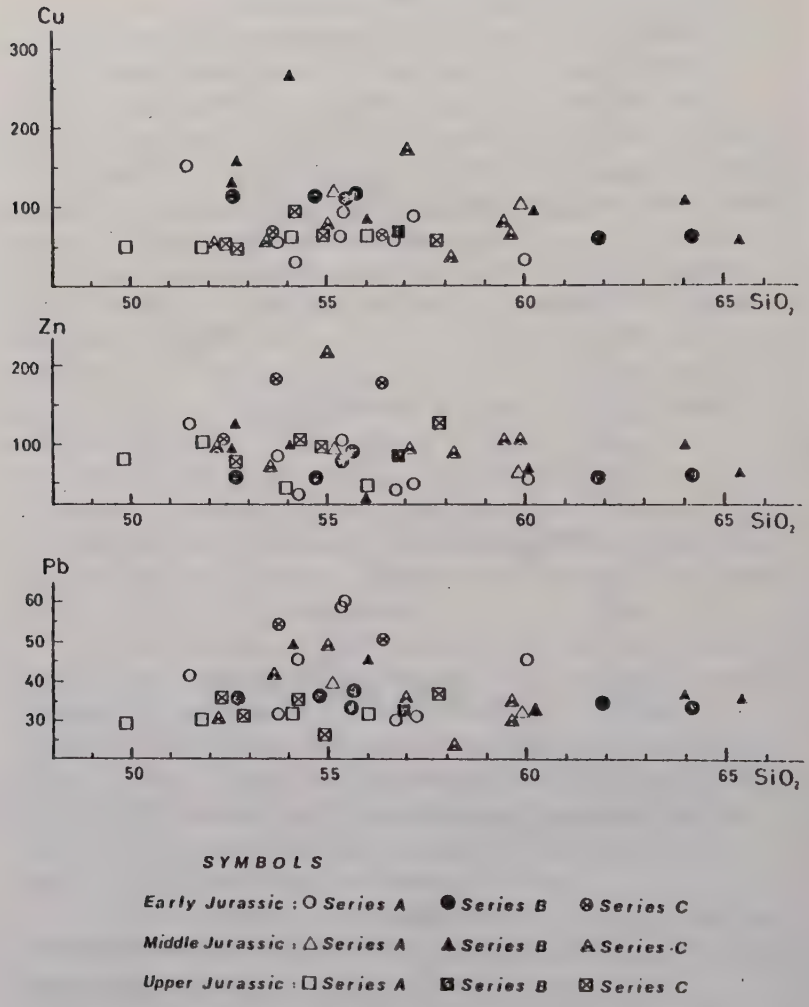

Fig.21. Cu,Zn and Pb (in ppm) versus SiO_2 (in wt.%).

The REE abundance pattern of series A is shown in Fig. 22. The concentrations are relatively low, showing between 5 to 20-fold enrichment relative to chondrites. There is a scatter in light rare earth element concentrations, and each sample has its greatest enrichment relative to chondrites in the La-Eu range. All but one have quite uniform abundances of the heavier elements (Tb-Yb) and the La/Yb ratio are 4.2-6.8.

The REE patterns of series B show a moderate enrichment in light-REE and only small fractionation of heavy-REE features which are typical for calc-alkaline rocks of island arcs (Fig. 22) (TAYLOR 1969, GILL 1970, YAJIMA et al. 1972, LOPEZ et al. 1977). The La/Yb ratios range between 3.7 and 8.8.

The REE concentrations in samples of series C (Fig. 22) show relative enrichment of the lighter elements. La/Yb ratios are 3.7-7.9. Probably the most significant aspect of the series C is the behaviour of Eu. At oxygen fugacities of andesitic magmas ($fO_2 = 10^{-7.2} - 10^{-8.2}$ at 1,200° C; FUDALI 1965, DRORY and ULMER 1974) plagioclase fractionation would cause significant Eu depletion (WEILL and DRAKE 1973, DRAKE 1975). The negative Eu anomalies of these rocks would then have to be due to the intensive fractionation of plagioclase, although the possibility of the presence of plagioclase in the residue after small degrees of melting cannot be discarded. The progressive development of negative Eu anomalies in conjunction with decreasing Al_2O_3, CaO and Sr is entirely consistent with continuous removal of plagioclase as a crystallizing phase (PALACIOS and SCHOCK, in prep.).

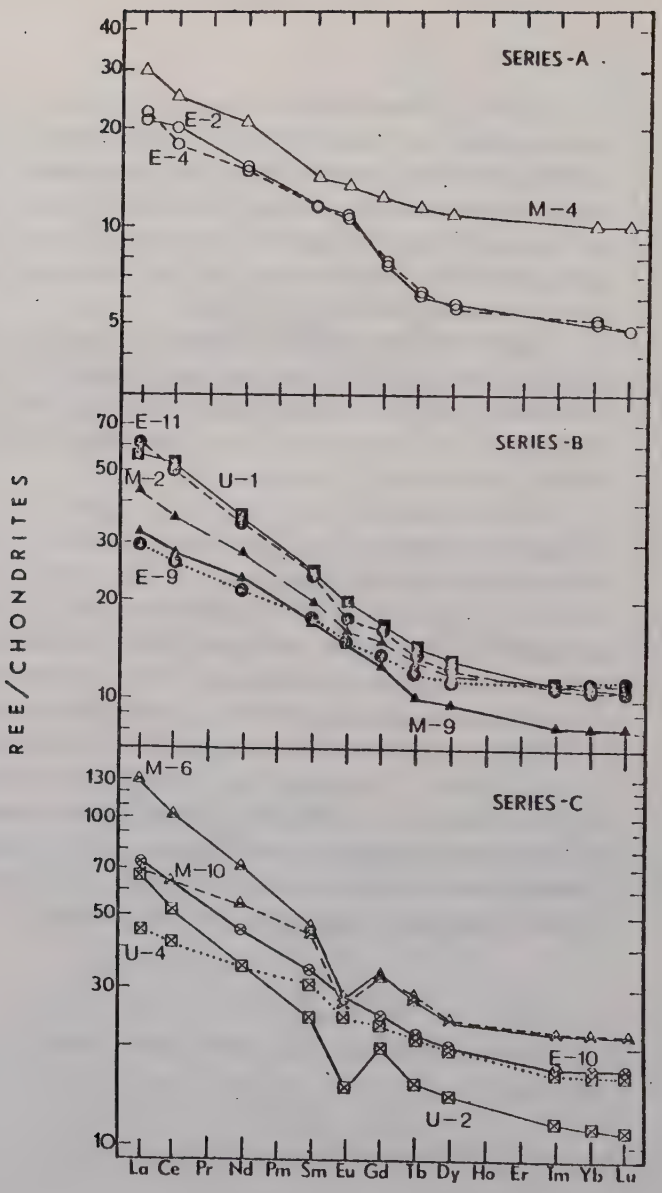

Fig.22: REE abundances in the Jurassic volcanic series normalized to a chondrite average (Frey et al. 1968).

8. PETROGENESIS OF JURASSIC VOLCANIC SERIES

8.1. Series A. - Partial Melting of Upper Mantle

An origin by partial melting of mantle peridotite which has gained water from the dehydration of downgoing oceanic crust is discussed for tholeiitic basalts and basaltic andesites in island arcs by NICHOLLS and RINGWOOD (1972). Depths to the Benioff zone beneath the volcanoes which erupt lavas of the island arc tholeiitic association fall within the range 80-120 km. The mean temperature of downgoing oceanic crust at these depths is probably $< 600^{o}$ C (OXBURGH and TURCOTTE 1970), so that dehydration occurs below the basalt-amphibolite-eclogite solidus (HILL and BOETTCHER 1970), and partial melting does not occur. Water therefore may escape into the overlying part of the mantle. Partial melting of hydrous peridotitic mantle and magma segregation were thought to take place not immediately above the Benioff zone, but at shallower depths in rising diapirs originating from the vicinity of the Benioff zone (NICHOLLS and RINGWOOD 1972, NICHOLLS 1974). NICHOLLS and RINGWOOD (1973) propose that 10 - 30% melts of hydrous peridotite are quartz-tholeiite which differentiate by olivine fractionation to form the island-arc tholeiitic series.

We find that a two-stage model can explain the composition of the series A, assuming that the peridotite source has REE abundances equal to twice chondrites and using reasonable REE mineral / liquid partition coefficients (see Tables 5 and 6) Fig. 23 and 24: Sample M-4: 10% of garnet-free peridotite melting (15% cpx, 25% opx, 60% ol; with a melting proportion of cpx: opx: ol=2:1:1), followed by fractional crystallization of olivine (Fo_{80}, 20%) and clinopyroxene (Augite, 6%).

Samples E-2 and E-4: 10% of garnet peridotite melting (15% cpx, 25% opx, 57% ol, 3% gt; with a melting proportion of cpx:opx: ol=2:1:1), followed by fractional crystallization of olivine (Fo_{80}, 9%) and clinopyroxene (augite, 2%).

The models were calculated using equation 15 of SHAW (1970). It is obvious that in this model the results depend of the peridotite composition and mineralogy and mineral liquid partition coefficients, however, the results establish the possibility of a two-stage model (partial peridotite melting followed by mineral fractionation).

8.2. Series B and C. - Partial melting of eclogite at 100-170 km

Basaltic oceanic crust subducted below the Jurassic volcanoes was in the eclogite facies. Partial melting of such an eclogite at 20-40 kb or 70-170 km depth would initially yield calc-alkaline series (GREEN and RINGWOOD 1968, RINGWOOD 1974).

Relative to the Jurassic series B and C, a melt formed by 30-40% fractional melting of eclogite has 1/20 Rb, 1/10 Ba, 1/3 K_2O and Cr, 1/2 Co and 2 Ni. GILL (1974) and DeLONG (1974) have shown that the eclogite model cannot explain the high abundances of K, Rb and Ba, and low content of Ni in calc-alkaline lavas of the Fijian and Aleutian arc respectively. A calculation of a partial melting model for REE, taking the composition of the Nazca Plate tholeiite as representative of the eclogite source, cannot account for the REE pattern in the Jurassic series B and C of Northern Chile, and on the basis of major, trace and rare earth elements geochemistry is discarded the partial melt of the subducted basaltic ocean crust as model for the genesis of the calc-alkaline suite. The posterior evolution of these series by low-pressure fractionation involving clinopyroxene, olivine and plagioclase would not provide a sufficient Rb, Ba and K_2O enrichment. Some types of marine alteration can cause significant enrichment in Rb and light-REE in the ocean floor basalts. But, the enormous volumes of volcanic flows require that large portions of ocean floor basalts must be altered. However, numerous recent papers have shown that less than 1% of the basalt core is altered to the degree required. Besides, isotope studies (CHURCH 1973) indicate that the oceanic sediments contribution to the calc-alkaline magmas was very limited ($< 2\%$) and was probably insufficie to account for the observed enrichment.

Partial melting of hydrous upper mantle

Recent experimental evidence suggest that the melting of hydrous upper mantle peridotite could have played an important role in the genesis of calc-alkaline magmas (KUSHIRO et al. 1972, MYSEN et al. 1974, MYSEN and BOETTCHER, 1975). However, the partial melting of peridotite cannot expl the high content of K and Rb in the Jurassic series B and C, unless very low degrees of melting ($\lesssim 5\%$) are invoked, followed by fractionation of olivine, spinel and pyroxene to account for the low compatible trace element abundances.

The geochemical patterns of the Jurassic series B and C (Fig. 23 and 24) agree with a derivation by low degrees of partial melting of a peridotite mantle, followed by fractionation of olivine, clinopyroxene and plagioclase.

Series B

Samples M-9 and E-9: 7% of garnet-free peridotite melting (15% cpx, 25% opx, 60% ol; with a melting proportion of cpx:opx:ol=2:1:1), followed by fractional crystallization of olivine (Fo_{80}, 11%), clinopyroxene (augite, 6%).

Samples E-11, M-2 and U-1: 3% of garnet-free peridotite melting (15% cpx, 25% opx, 60% ol; with a melting proportion of cpx:opx:ol=2:1:1), followed by fractional crystallizations of olivine (Fo_{80}, 12%) and clinopyroxene (augite, 6%).

Series C

Samples M-6 and M-10: 2% of garnet-free peridotite melting (15% cpx, 25% opx, 60% ol; with a melting proportion of cpx:opx:ol=2:1:1), followed by fractional crystallizations of olivine (Fo_{80}, 20%), clinopyroxene (augite, 2%) and plagioclase (An_{60}, 30%).

Sample U-2: 2% of garnet-free peridotite melting (15% cpx, 25% opx, 60% ol; with a melting proportion of cpx:opx:ol=2:1:1), followed by fractional crystallization of olivine (Fo_{80}, 11%), clinopyroxene (augite, 6%) and plagioclase (An_{60}, 13%).

Sample U-4: 5% of garnet-free peridotite melting (15% cpx, 25% opx, 60% ol; with a melting proportion of cpx:opx:ol=2:1:1), followed by fractional crystallization of olivine (Fo_{80}, 25%), clinopyroxene (augite, 5%) and plagioclase (An_{60}, 10%).

Sample E-10: 2% of garnet-free peridotite melting (15% cpx, 25% opx, 60% ol; with a melting proportion of cpx:opx:ol=2:1:1), followed by fractional crystallization of olivine (Fo_{80}, 24%), clinopyroxene (augite, 4%) and plagioclase (An_{60}, 10%).

These models were calculated assuming that the peridotite source has REE abundances equal to twice chondrites, (for REE mineral/liquid partition coefficients, see Tables 5 and 6) and using equation 15 of SHAW (1970).

However, because the controversy regarding the SiO_2 content of melts formed by melting of hydrous peridotite (MYSEN et al. 1974, MYSEN and BOETTCHER 1975), and the possible difficulty of extracting small amounts of melts from large amounts of a rigid mantle, several problems remain.

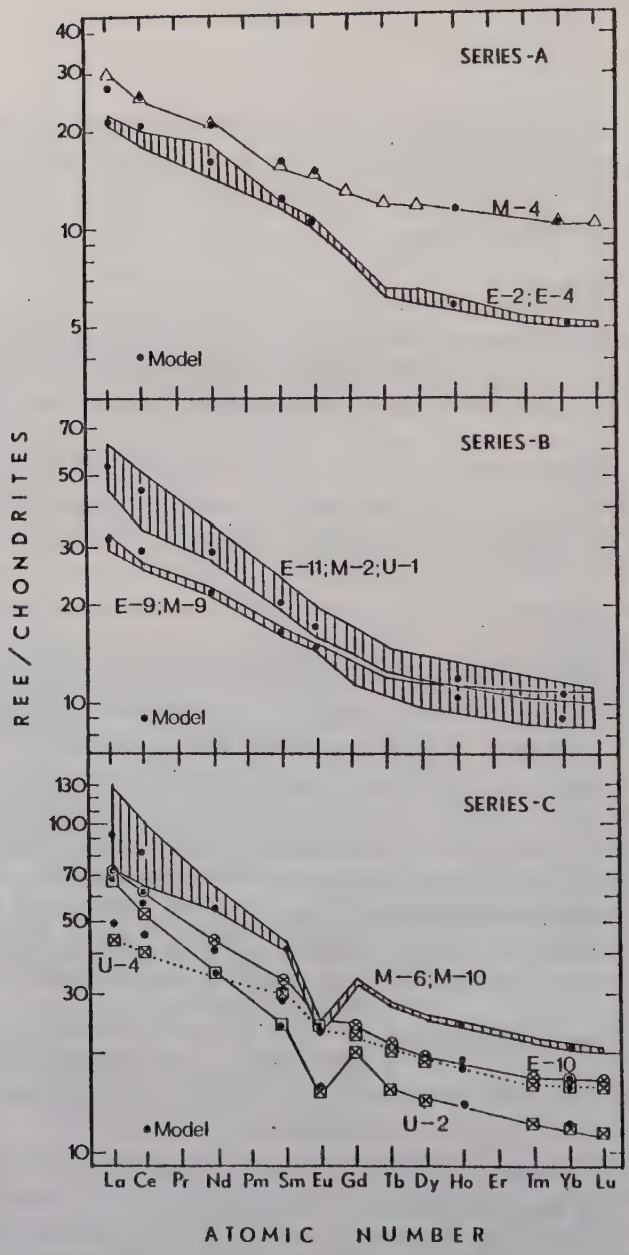

Fig.23: REE abundances in the Jurassic series and in the calculated models normalized to a chondrite average. (Frey et al. 1968).

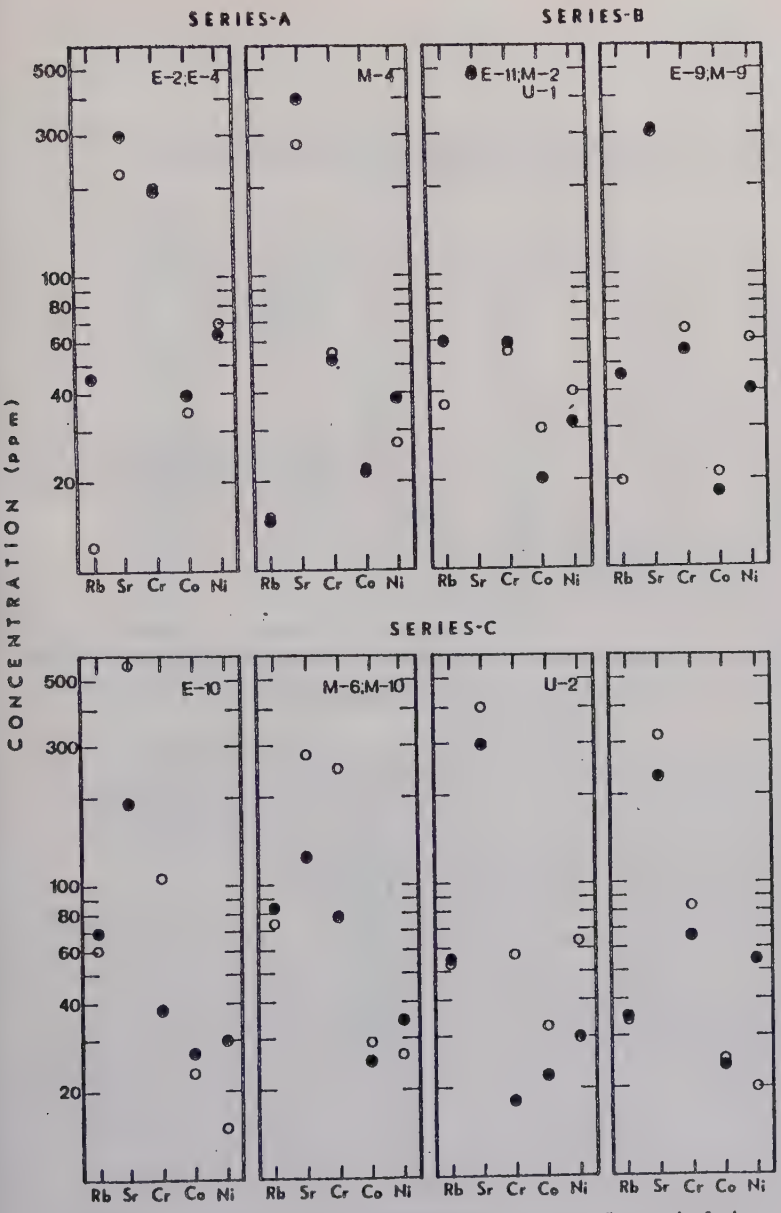

Fig.24. Comparison of observed trace element data (full circles) to concentrations expected in models (indicated by open circles).

TABLE 5: Solid/Liquid Partition coefficients used in this study From ARTH (1976) and FREY et al. (1978).

	Cpx	Opx	Ol	Gt	Pl
La	0.1	0.03	0.01	0.005	0.1
Ce	0.15	0.031	0.01	0.007	0.1
Nd	0.35	0.034	0.01	0.03	0.1
Sm	0.55	0.047	0.01	0.25	0.1
Eu	0.6	0.06	0.01	0.35	1.3
Ho	0.65	0.2	0.01	5	0.1
Yb	0.61	0.45	0.01	9	0.1
Lu	0.6	0.6	0.01	10	0.1
Cr	30	1	1	20	0.06
Co	2	2	3	4	0.06
Ni	3	3	10	0.7	0.01
Rb	0.05-0.001	0.01	0.01	0.03	0.1-0.03
Sr	0.15-0.05	0.01	0.01	0.008	3.0-2.04

TABLE 6: Trace element content (ppm) of peridotite used in modelling. REE are equal to twice a chondrite average (FREY et al. 1968, FREY et al. 1978).

	Upper mantle peridotite
La	0.66
Ce	1.76
Nd	1.20
Sm	0.36
Eu	0.14
Ho	0.14
Yb	0.40
Lu	0.07
Cr	2200
Co	110
Ni	1500
Rb	1
Sr	20

9. COMPARISON WITH OTHER VOLCANIC SUITES

A: Tholeiitic series (series A)

In general, there exists a good geochemical similarity of the series A with tholeiitic rocks of the island arc type (Table 7). The latter show higher values of K, Sr, Rb, Cr and Ni.

B: Calc-alkaline suites (series B)

In previous papers, (PALACIOS 1974 a and b; 1975) it was emphasized that a clear chemical similarity between the calc-alkaline rocks of Jurassic series and the high-K andesites of island arcs exists. This similarity is shown in Table 8. Only the average of the major elements Al and Mg differs. The differences in Fe, Ca, Li, Cr, Co, Cu, Sr, Y, Ba and V values between series B and the Cenozoic quartz-latiandesites from the Central Andes is compiled in Table 8 . Great discrepancies are obvious between the rocks of the Central Andes and those of the calc-alkaline island arc suite. This fact was recently indicated by KLERKX et al. (1977) and JAKES and WHITE (1972).

C: Group with alkaline affinities (series C)

A comparison with other volcanic series suggest the idea that the series C is atypical. In Table 9 is presented a compilation of information. In contrast to the calc-alkaline series, the potassium and rubidium values of series C are higher and comparable with those of shoshonitic association. Strontium and barium concentrations however, are similar to those of typical calc-alkaline rock series. Nevertheless, there exists a good geochemical similarity in major elements, Cr, Ni, Cu, Rb, Zr between series C with alkaline rocks of Central Andes (Antizana, Tungurahua and El Chaco volcanoes of Ecuador (HÜRMANN and PICHLER 1978).

TABLE 7: Statistical comparison of the geochemistry of theoleiitic rocks (FeO calculated as total iron)

Oxides (wt. %)	1	2	3
SiO_2	55.4	51.6	57.4
Al_2O_3	16.2	15.9	15.6
FeO	6.7	9.5	6.6
MgO	4.9	6.7	3.4
CaO	7.0	11.7	6.6
Na_2O	4.4	2.4	4.2
K_2O	0.7	0.4	0.4
TiO_2	0.8	0.8	1.2
Elements (ppm)			
Li	24	-	-
Cr	129	50	15
Co	31	-	-
Ni	45	30	20
Cu	66	-	-
Zn	77	-	-
Ga	18	-	-
Rb	31	5	6
Sr	265	200	220
Y	14	-	-
Zr	79	70	70
Ba	166	75	100
V	217	270	175

1. Average of series A (14 samples) of Northern Chile
2. Average of theoleiitic basalts of island arcs (JAKES and WHITE, 1972)
3. Average of tholeiitic andesites of island arcs (JAKES and WHITE, 1972)

TABLE 8: Statistical comparison of the geochemistry of calc-alkaline series (FeO calculated as total iron)

Oxides (wt. %)	1	2	3	4
SiO_2	57.8	58.5	59.6	59.4
Al_2O_3	17.4	16.2	17.4	17.0
FeO	5.0	4.7	3.9	5.7
MgO	3.3	4.1	3.9	3.3
CaO	5.5	5.6	5.9	5.8
Na_2O	4.0	3.6	4.4	4.0
K_2O	2.3	2.7	2.0	2.4
TiO_2	0.8	0.8	0.8	0.8
Elements (ppm)				
Li	24	-	-	12
Cr	78	-	25	35
Co	30	-	-	19
Ni	28	-	18	32
Cu	113	-	-	44
Zn	78	-	-	87
Ga	21	-	-	-
Rb	68	-	30	64
Sr	356	-	385	648
Y	27	-	21	10
Zr	157	-	110	197
Ba	329	-	270	914
V	167	-	175	136

1. Average of series B (14 samples) of Northern Chile
2. Average of calc-alkaline high-K andesites of island arcs (JAKES and WHITE, 1972)
3. Average of calc-alkaline andesites of island arcs (JAKES and WHITE, 1972)
4. Average of quartz-latiandesites from the Central Andes (PICHLER and STENGELIN, in prep.).

TABLE 9: Statistical comparison of the geochemistry of "alkaline" suites (FeO calculated as total iron)

Oxides (wt. %)	1	2	3
SiO_2	55.6	53.7	56.9
Al_2O_3	16.7	15.8	15.2
FeO	6.0	6.3	5.8
MgO	2.9	6.4	4.4
CaO	5.8	7.9	6.3
Na_2O	3.8	2.4	4.0
K_2O	2.7	2.6	2.8
TiO_2	1.4	1.1	1.1
Elements (ppm)			
Li	26	-	16
Cr	69	30	74
Co	32	-	15
Ni	36	20	40
Cu	72	-	84
Zn	119	-	-
Ga	20	-	-
Rb	67	75	95
Sr	263	700	870
Y	39	-	50
Zr	200	50	204
Ba	473	1,000	1,178
V	228	200	139

1. Average of series C (14 samples) of Northern Chile
2. Average of shoshonitic series of island arcs (JAKES and WHITE, 1972)
3. Average of alkaline volcanic rocks from Ecuador (HÖRMANN and PICHLER, in prep.).

10. DEPTH OF THE JURASSIC PALEOSEISMIC ZONE AND CRUSTAL THICKNESS

The variation of the K_2O content in the calc-alkaline association of the recent circum-Pacific island arcs has been related to the depths of the inclined Benioff zone beneath the volcanoes (DICKINSON and HATHERTON, 1967; HATHERTON and DICKINSON, 1968, 1969; DICKINSON 1975). In the diagram used (HARKER's diagram) for the variation of the K_2O/SiO_2 ratio, the absolute values of K_2O are taken at 55% and 60% SiO_2 or at 57.5% SiO_2. This method has been applied also for ancient calc-alkaline rocks to calculate the position and inclination of paleoseismic zones (DICKINSON 1970; LIPMAN et al., 1971). A sufficient number of analysis for the single volcanic series is required in the application of the method proposed by DICKINSON and HATHERTON (1967). Obviously, this is easily possible for active volcanoes, while it becomes more complicated for older volcanoes.

However, we can calculate the depth of paleoseismic zone using the K_2O-SiO_2/depth Benioff zone relation as proposed by HUTCHINSON (1976): Depth to the Benioff zone (Km) = 397 - (5.26 ×% SiO_2) + (35.04 ×% K_2O) - Correlation coefficients = 0.87 (level of significance < 0.001). The standard error of depth estimate is about 30 Km.

These relations were calculated by HUTCHINSON (1976) using the chemical and geophysical data of the Indonesian active volcanic arc. The data obtained with this method suggest a depth of paleoseismic zone beneath the Jurassic volcanoes of Northern Chile of about 150 km (using the geochemical data of this work, LOSERT (1974) and PALACIOS (1974b, 1975)).

The development of continental-type crust is accompanied by an increase in the proportion of more silicic volcanic rocks, and the average SiO_2 percentage of all the volcanic rocks (MIYASHIRO 1974).

Fig. 25 shows the relation between the average SiO_2 content in the volcanic arcs (tholeiitic and calc-alkaline series mixed) and continental margins, and crustal thickness. According to these calculated data, the continental crust during the Jurassic in Northern Chile may have been between 15 and 25 km thick.

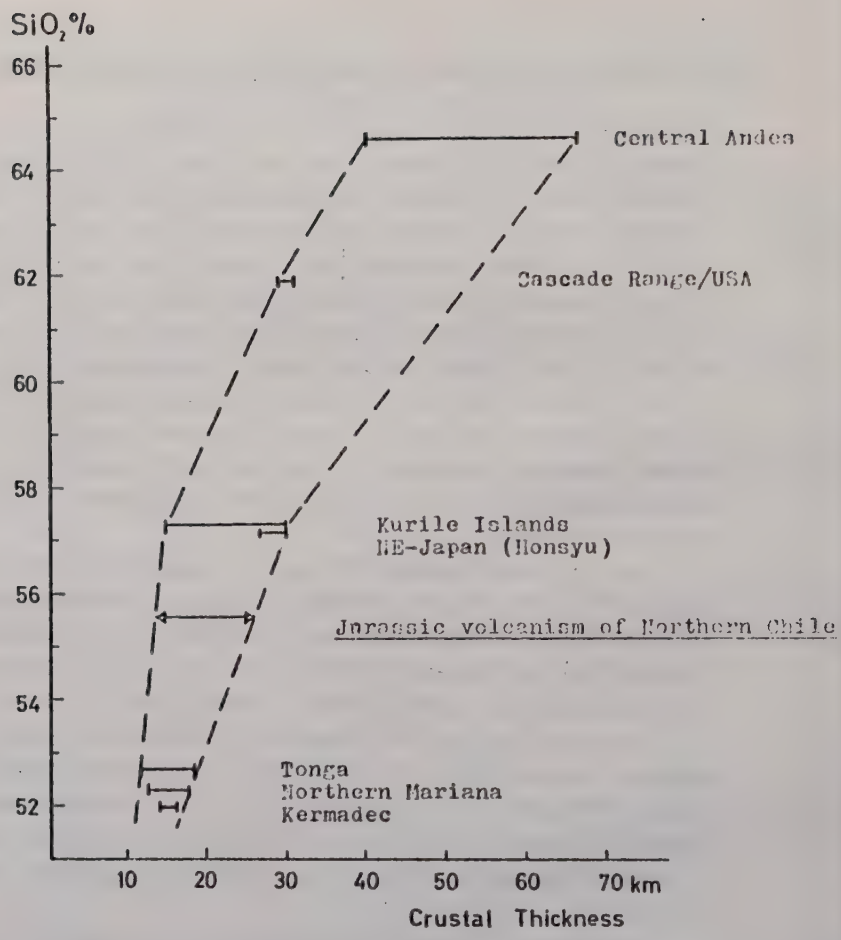

Fig.25. Relation between the average SiO_2 content in volcanic rocks (tholeiitic and calc-alkaline series mixed) of island arcs and continental margins and crustal thickness. Data from MIYASHIRO (1974) and LE PICHON (1968).

11. REGIONAL METAMORPHISM

11.1 Regional Metamorphism in Jurassic volcanic rocks

The Jurassic volcanic rocks have mineral assemblages typical for low-grade regional metamorphism. The typical features of this metamorphism are: recrystallization, transformation of pyroxenes into chlorite, actinolite and epidote, albitization of plagioclase and the evidence of biotite, chlorite, calcite, white mica, prehnite, pumpellyite and quartz in vesicles and cracks. In the whole stratigraphic suite secondary minerals replace the primary ones or fill amygdules and open fractures. Often the matrix of the flows, dikes and sedimentary intercalations is full of this low-grade metamorphic mineral. Patterns of metamorphism are regular and persistent and occur generally in the lower and upper parts of each lava flow and in sedimentary intercalations. In the central parts of the flows, however, evidences of metamorphism are rare.

Prehnite is fibrous and forms radial crystals in amygdules of altered flows. Pumpellyite occurs in spherulitic crystals in amygdules, and replaces pyroxene and hornblende; it is found in the matrix of interbedded sediments. Epidote occurs mostly in vesicules and veinlets. Actinolite is present in flaky crystals in veinlets, amygdules and replaces pyroxene and hornblende in altered volcanic rocks. White mica (muscovite and sericite) are flaky aggregates in amygdules formed by transformation of feldspar and in part of ferromagnesian minerals. Chlorite and biotite crystals were identified by X-ray and thin section analysis; these minerals derive from the transformation of ferromagnesian minerals. Chlorite shows abnormal violet interference colour.

A summary of the metamorphic-petrographic features is given in Table 10.

Table 10 shows that the Jurassic lavas can be divided according to their mineral assemblages into four low-grade metamorphic zones:

1) Epidote-prehnite-pumpellyite
2) Chlorite-calcite
3) Actinolite-chlorite
4) Biotite.

These metamorphic zones occur in parallel belts from West to East (Fig. 26).

TABLE 10: Typical low-grade metamorphic mineral assemblages in the Jurassic volcanic rocks of Northern Chile

	Epidote-Prehnite-Pumpellyite Zone	Chlorite-Calcite Zone	Actinolite-Chlorite Zone	Biotite Zone
EPIDOTE	XXXXXXXXXXXXX	XXXXXXXXXXXX	X X X	XXXXXXXXXX
WHITE MICA	X X X X	XXXXXXXXXXXXX	XXXXXXXXXXXXX	XXXXXXXXXX
CHLORITE	XXXXXXXXXXXXX	XXXXXXXXXXXXX	XXXXXXXXXXXXX	X X X X X
BIOTITE			X X X X	XXXXXXXXXX
ACTINOLITE	X X X X		XXXXXXXXXXXXX	X X X X X
PREHNITE	XXXXXXXXXX			
PUMPELLYITE	XXXXXXXXXX			
CALCITE		XXXXXXXXXXXXX	XXXXXXXXXXXXX	XXXXXXXXXX
ALBITE	XXXXXXXXXXXXX	XXXXXXXXXXXXX	XXXXXXXXXXXXX	XXXXXXXXXX
HEMATITE	XXXXXXXXXXXXX	XXXXXXXXXXXXX	XXXXXXXXXXXXX	XXXXXXXXXX
SPHENE	XXXXXXXXXX			
QUARTZ	XXXXXXXXXXXXX	XXXXXXXXXXXXX	XXXXXXXXXXXXX	XXXXXXXXXX

The western metamorphic zone, with epidote, prehnite and pumpellyite, is developed in the Tocopilla area (22^{o} 06´S/70^{o}12´W) where Early Jurassic volcanic rocks occur. More to the south, in the Antofagasta area (23^{o}38´S/70^{o}24´W), the same metamorphic phenomena have affected Upper Jurassic volcanics (Fig. 9). Characteristica for this metamorphic zone is the formation of secondary quartz, low-temperature albite and hydrous minerals like prehnite, pumpellyite, chlorite, actinolite and epidote. Assemblages of these minerals were formed by low-temperature regional metamorphism involving high-temperature pyroxene, olivine and calcium-rich plagioclase. Considerable calcium metamorphic differentiation took place in the relatively highest-grade epidote-bearing rocks. In addition to the formation of the above mentioned minerals, this metamorphic zone is characterized by the resistence of clinopyroxene against alteration, by the formation of sphene as the only stable titanium mineral and by the almost complete immobility of iron and its incomplete oxidation to t trivalent form (LOSERT 1974).

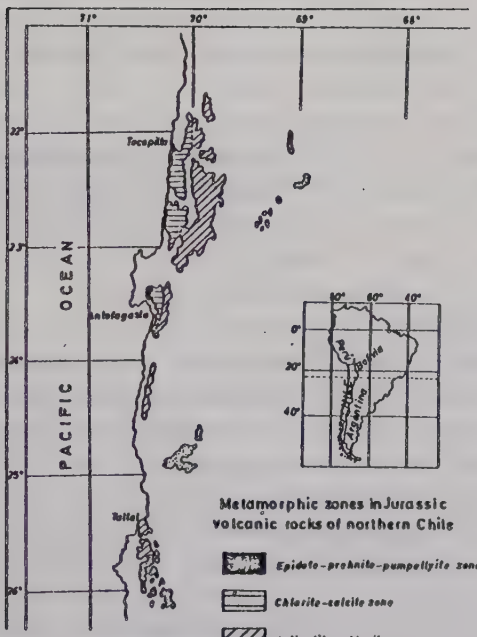
71°
70°
69°
68°
22°
23°
24°
25°
26°
PACIFIC OCEAN
Tocopilla
Antofagasta
Taltal
80°
60°
40°
0°
20°
40°
Peru
Bolivia
Argentina
Chile
Metamorphic zones in Jurassic volcanic rocks of northern Chile
Epidote-prehnite-pumpellyite zone
Chlorite-calcite zone
Actinolite-chlorite zone
Biotite zone
based on Palacios, 1977

Fig : 26

East of this zone the chlorite-calcite belt is developed. This zone is characterized by chlorite, calcite, low-temperature albite, epidote, white mica, quartz and hematite (Table 10, Fig. 26).

The third zone comprises rocks with actinolite, chlorite, calcite, white mica, low-temperature albite, quartz, hematite and rarely epidote and biotite. Abundant actinolite and the occassional occurrence of metamorphic biotite are characteristic for this zone.

Typical for the eastern metamorphic zone is the formation of secondary biotite and lesser amounts of chlorite (Table 10). The mineral assemblages of zone 4 is calcite, white mica, biotite, low-temperature albite, epidote, quartz, hematite and subordinate actinolite and chlorite.

11.2. Discussion

On account of the different metamorphic mineral assemblages (Table 10) four metamorphic zones within the Jurassic lavas can be distinguished. These zones are distributed from west to east in small belts parallel to the present coast of Northern Chile (Fig. 26):

Zone 1 : Epidote, prehnite and pumpellyite
Zone 2 : Chlorite and calcite
Zone 3 : Actinolite and chlorite
Zone 4 : Biotite

Prehnite-pumpellyite-bearing assemblages are considered by some petrologists to indicate metamorphic conditions of relatively high total pressure and low temperature. These are benchmarks for MIYASHIRO's low-temperature metamorphic trend (MIYASHIRO 1961; SEKI 1969; HASHIMOTO 1966). MIYASHIRO (1961) indicates pumpellyite-bearing assemblages in the lowest grade of a high-pressure/low-temperature metamorphic belt. Here in basic rocks the common mineral assemblage is: sodic plagioclase, pumpellyite, chlorite, stilpnomelane and quartz, showing that in this zone uncomplete metamorphic features are developed. Available experimental data support that the prehnite-pumpellyite mineral assemblages are stable under high-pressure/low-temperature conditions (NITSCH 1971; STRENS 1968; HINRICHSEN and SCHÜAMMANN 1969). Prehnite and pumpellyite-bearing low-grade metamorp

rocks have world-wide distribution, especially in recent orogenic belts, e.g. around the Pacific, within the Tethyian belt, and in the Caribbean region. If one superimposes a world map depicting the prehnite and pumpellyite-bearing assemblages formed in Mesozoic and Cenozoic metamorphism on a map of contemporary deep-focus earthquake epicenters, a striking correspondence appears. The zones of deep-focus earthquakes are considered loci of plate boundary subduction, where cold, high-pressure materials is formed in downgoing slabs. Significant prehnite and pumpellyite-bearing pre-Mesozoic rocks, are occurring in the Tasmanian geosyncline of New South Wales, the Keweenawan belt and the northern Appalachian region. Glaucophane schist belts, contain rocks of distinctive metamorphic facies ranging from low-grade laumontite and analcime-bearing zeolitic rocks to prehnite-pumpellyite and blueschist $\pm$ greenschist mineral assemblages. Higher metamorphic conditions of this type form albite amphibolites and eclogites (type C of COLEMAN et al., 1965; ERNST 1973). Thus, it is possible to consider the epidote, prehnite, pumpellyite zone as relict metamorphic assemblages that could be assigned to a high-pressure/low-temperature type metamorphism.

To the east, the chlorite-calcite and actinolite-chlorite zones are developed. In these metamorphic zones, abundant chlorite is characteristic.

The biotite zone belongs to the most eastern metamorphic area. Biotite replaces here the chlorite. In the high pressure metamorphic assemblages, the temperature was not high enough to form biotite. However, chlorite is a common mineral. The transition of chlorite to biotite has been considered to be typical for increasing temperatures. In the kyanite-sillimanite metamorphic rocks, biotite occurs in middle and high grades (MIYASHIRO 1961). Notwithstanding the lowest temperature for the biotite formation varies with pressure, the above relations suggest that the biotite-bearing rocks belong to a relative high temperature metamorphic zone. If we accept that the western belt (epidote-prehnite-pumpellyite zone) belongs to a high-pressure/low-temperature metamorphic area, and the eastern belt (biotite zone) suggest a relative high-temperature metamorphic terrain, it is possible to interpret this metamorphism as related to a continental margin tectonic setting during the Mesozoic in Northern Chile.

11.3. Changes of the Chemical Composition by Regional Metamorphism

There are numerous available descriptions of the chemical effects of metamorphism (e.g. VALLANCE 1960, 1965 and 1974; SMITH 1968; CANN 1969; REED and MORGAN 1971; SMITHERINGALE 1972; JOLLY and SMITH 1972; PEARCE and CANN 1973; WOOD et al. 1976; BARRON 1976; FLOYD and WINCHESTER 1978). However, these reports suggest that the rocks maintain their subalkaline and iron enriched nature, ferromagnesian trace elements change little and rare earth abundances and distribution patterns are not affected.

12. PALEOVOLCANISM IN CENTRAL CHILE

12.1. Geological Setting

In central Chile, an extensive Mesozoic volcanic activity was developed along the western margin of South America, where Jurassic, Cretaceous and Early Tertiary volcanic and sedimentary rocks accumulated to a total thickness of many kilometers (Fig. 27). The Jurassic series (Lias to Lower Dogger) has a thickness of 7,000 m and the strata are formed mainly by volcanic flows with minor intercalations of marine sediments (CORVALAN 1967). According to GERTH (1935), BROGGEN (1950) and MUNOZ CRISTI (1968) the volcanic rocks have been formed within a volcanic islands which limited the Jurassic sedimentary basin to the West. The Lower Cretaceous volcanic sequence consists mainly of acidic and intermediate volcanic rocks with several lenticular marine sedimentary intercalations (VERGARA 1972). The maximum thickness of the Lower Cretaceous series is 13,000 m and occurs in the Coastal Range of Chile (VERGARA 1972). This author suggests that this series was mainly produced by an "island arc type" volcanism.

In the Lower Cretaceous a cycle of continental and volcanic sedimentation existed, represented by the "Abanico and Farellones" formations of Upper Cretaceous and Lower Tertiary age, respectively (VERGARA 1965). The Upper Cretaceous sequence reaches 6,000 m in thickness (500 m of rhyolitic flows and 5,500 m of volcanoclastic andesitic rocks) (VERGARA 1969). Fig. 28 shows a cross section through the Andean Belt at $34^{o}30'S$.

The Mesozoic lavas show a mineralogical association of altered rocks, attributed to "burial metamorphism" by LEVI and CORVALAN (1964) and LEVI (1969, 1970). However, VERGARA (1969) pointed out that quantitative differences between the rock metamorphism of the Lower Cretaceous and the Upper Cretaceous series are existing. LEVI (1969, 1970) has shown that in the Lower Cretaceous lava flows from central Chile petrochemical differences between the dense lower parts and the more porous upper parts of the lava flows are typical. Here, from the lower to the upper part of each volcanic level an increase of Na, K, CO_2 and H_2O content and at same time a decrease of Ca exist. LEVI has attributed these changes to "burial metamorphism"; NISTERENKO and CHAVEZ (1971) suggested that this metasomatism is due to regional hydrothermal alteration.

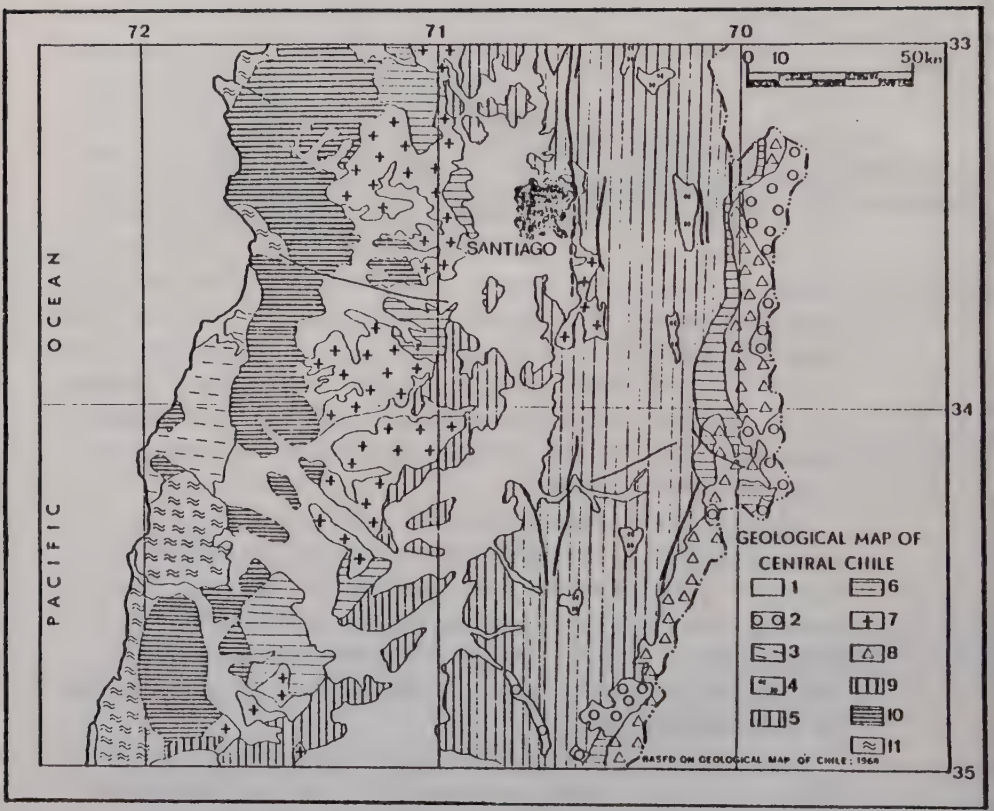

Fig.27:Geological map of Central Chile.
1. Quaternary continental sedimentary rocks.
2.Quaternary volcanic rocks.
3.Tertiary marine and continental sedimentary rocks.
4.Tertiary granitic rocks.
5.Cretaceous volcanic rocks.
6.Cretaceous marine sedimentary rocks.
7.Cretaceous granitic rocks.
8.Jurassic marine sedimentary and volcanic rocks.
9.Triassic continental sedimentary and volcanic rocks.
10.Paleozoic granitic rocks.
11.Paleozoic metamorphic rocks.

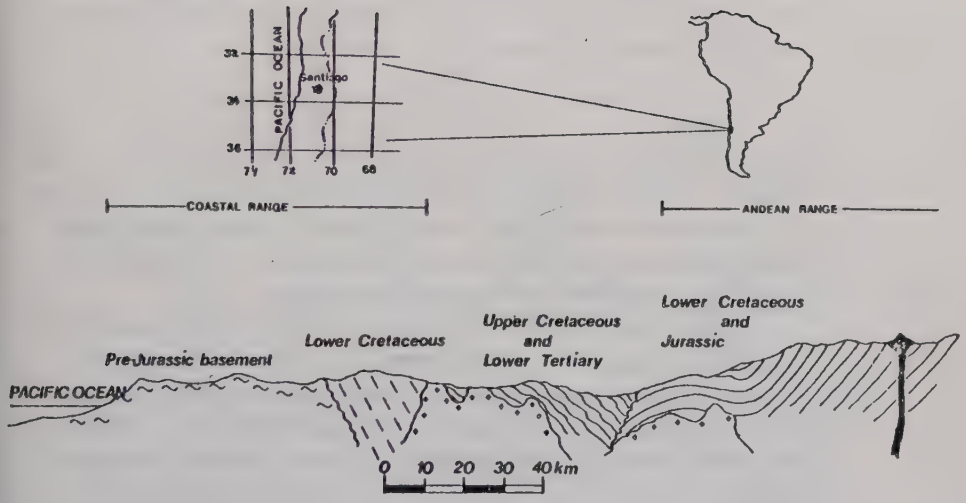

Fig. 28. Profile throug the Andean Belt at 34° 30'S.
(According to VERGARA, 1972).

VERGARA (1972) found that the Mesozoic volcanism in central Chile is mainly of "aluminous-andesitic nature with strong affinity to calc-alkaline character". The intrusive-effusive alkaline complex of Mesozoic age from the Andean foreland in Argentina (Sierra de Córdova: $31^{o}48'S/64^{o}31'W$; GORDILLO and LENCINAS 1967, 1968) shows that a petrologic polarity existed during this era (VERGARA 1972). The assymetry could be used to infer that this region was a contact plate zone during the Mesozoic age (VERGARA 1972).

12.2. Chemistry

Diagrams for the major elements, AFM and Q-A-P-F double-triangle plots for representative analytical data of Mesozoic volcanic rocks from central Chile are given in Fig. 29 to 32. These data were taken from OYARZUN and VILLALOBOS (1969) and VERGARA (1972).

Although the available data for the Jurassic-Cretaceous volcanic rocks of central Chile (Southern Andes) are very limited, the geochemical patterns suggest that these rocks are demonstrably similar to the Jurassic series A, B and C of Northern Chile. The data show that three different series of Mesozoic igneous activity occurred in central Chile:

1) The first association is comparable to the series A of Northern Chile and to the tholeiitic series, in spite of lower values of Ca and Mg.
2) The second association belongs to the calc-alkaline suite and is distinguished by moderate K_2O-SiO_2 increase and lower potassium values than series B of Jurassic flows of Northern Chile.
3) The third association consists of rocks with high contents of potassium and low magnesium values.

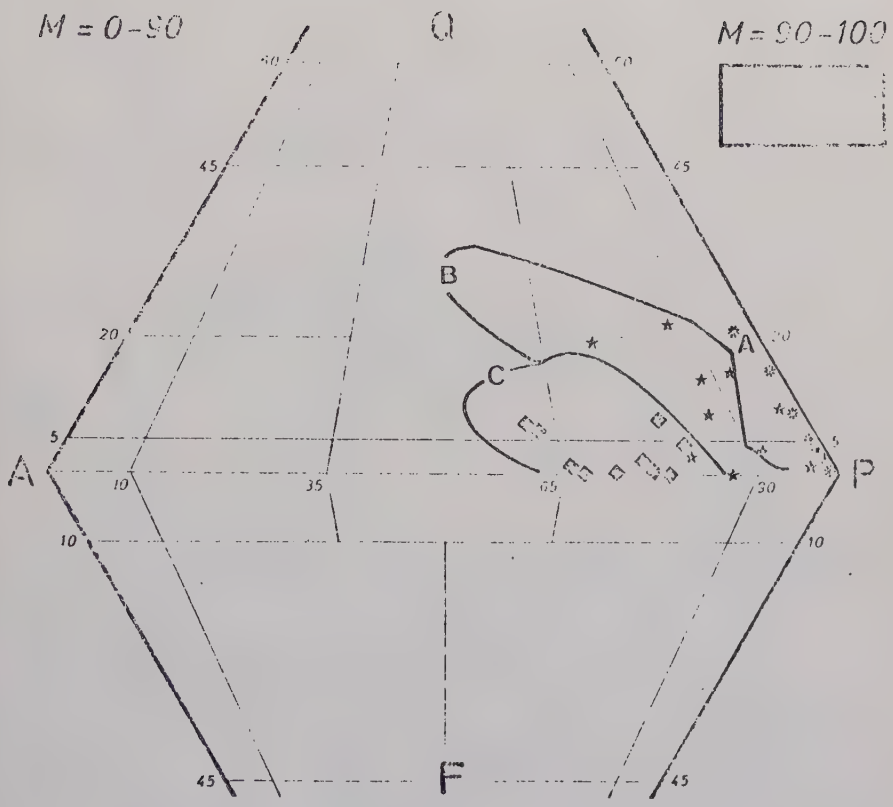

Fig.29. Distribution of Mesozoic lavas of Central Chile in the Q-A-P-F double-triangle diagram. Solid lines represent the fields of series A,B and C of Jurassic lavas,Northern Chile.

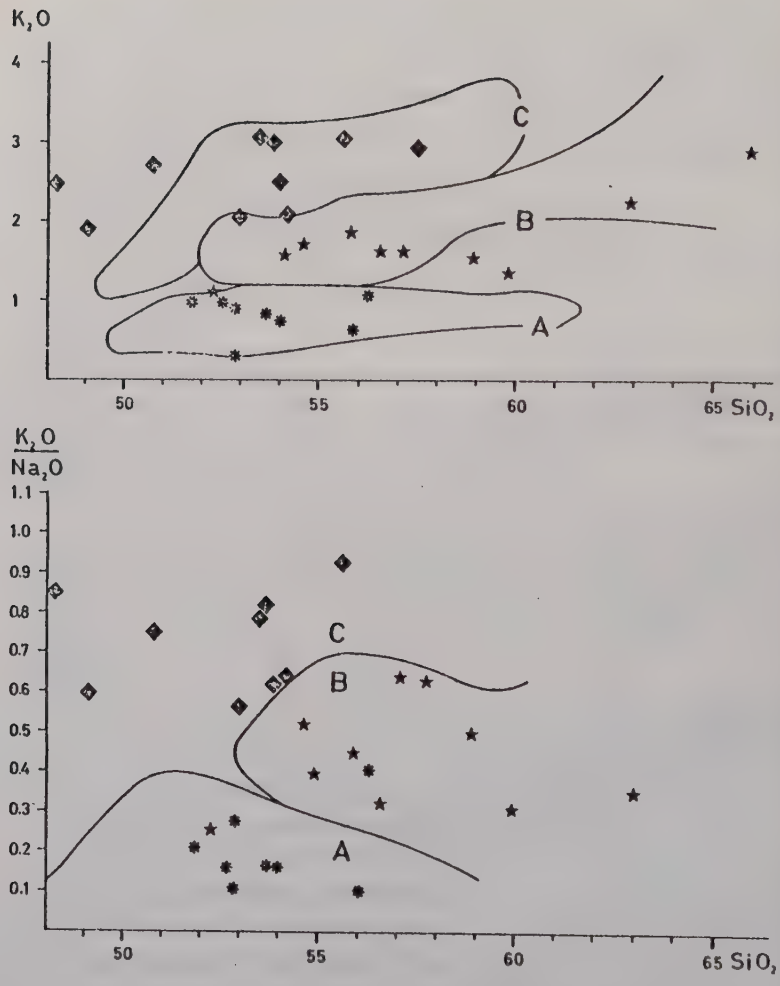

Fig. 30. K_2O (in wt.%) and K_2O/Na_2O versus SiO_2 (in wt.%) for Mesozoic lavas of Central Chile. Solid lines represent the fields of series A, B and C of Jurassic lavas in Northern Chile.

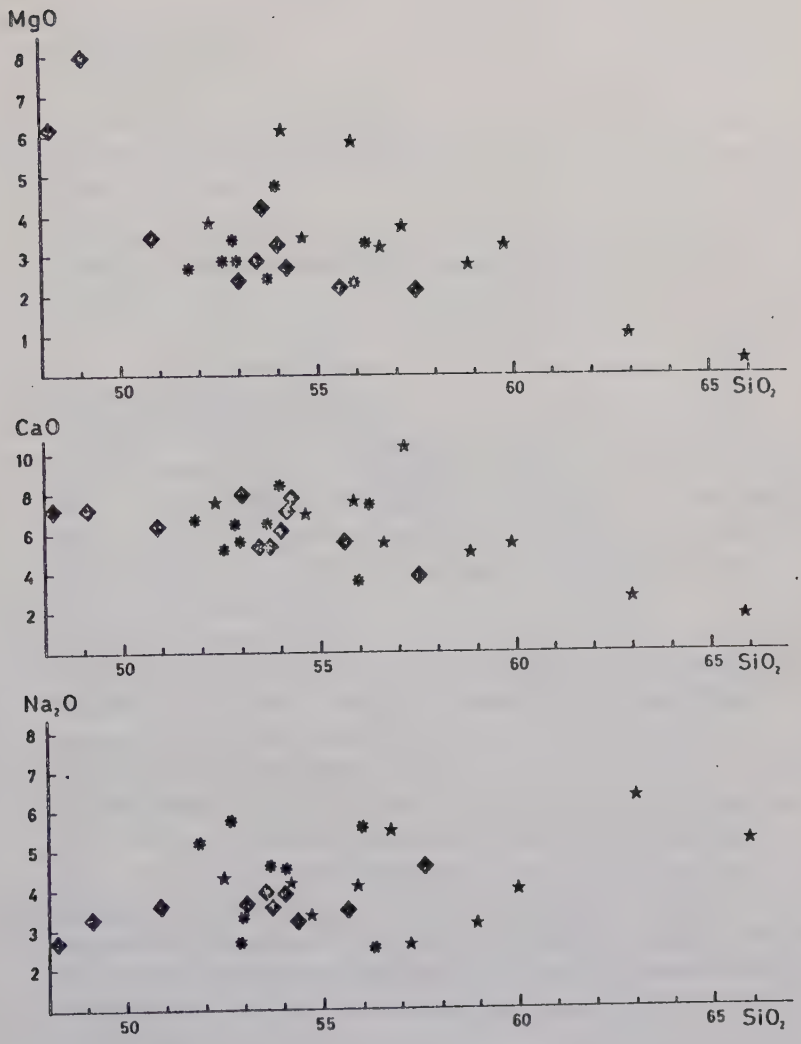

Fig.31. MgO, CaO and Na_2O versus SiO_2 (in wt.%) of the Mesozoic volcanic rocks from Central Chile.

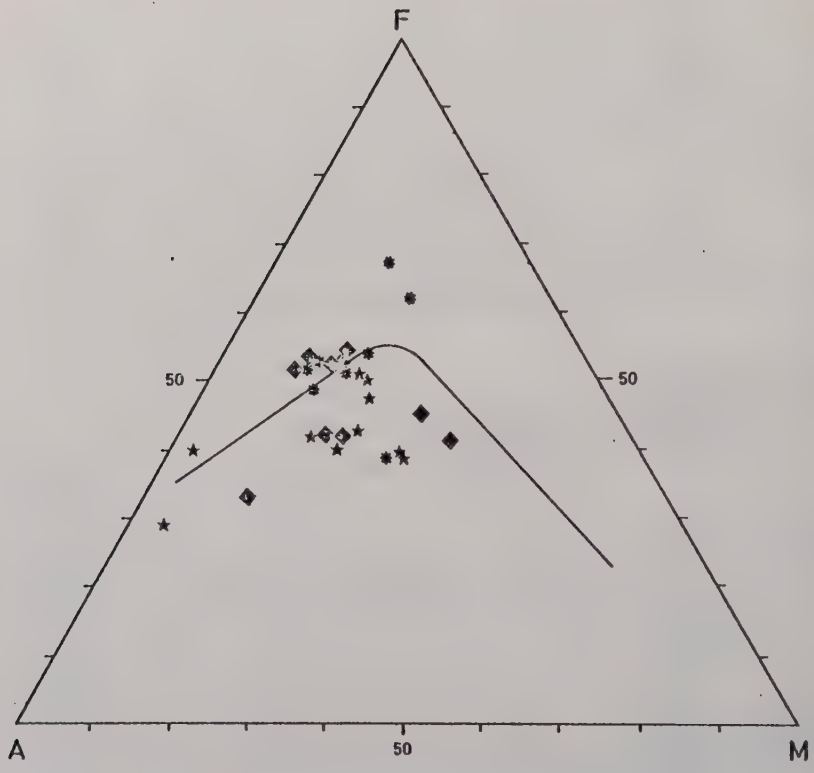

Fig.32. AFM diagram of Mesozoic volcanic rocks from Central Chile.

13. CONCLUDING REMARKS

The following points seem especially important for the understanding of the Jurassic volcanic history in Northern Chile and its tectonic implications:

1) The Jurassic volcanic rocks present mineralogical assemblages that belong to a low-grade regional metamorphism. It is possible to divide the assemblages into four metamorphic zones:
   1. Epidote-prehnite-pumpellyite,
   2. chlorite-calcite,
   3. actinolite-chlorite,
   4. biotite.

   These metamorphic zones are distributed from West to East in parallel belts to the present coast (North-South) and at the inferred Jurassic paleo subduction zone. It is possible to interpret this metamorphism as related to a continental margin tectonic setting during the Mesozoic in Northern Chile.
2) Available petrographical and geochemical data evidence that three different series of igneous activity occur in the Jurassic areas of Northern Chile. Rocks of the first series are tholeiites, the second belong to the calc-alkaline suite and the third series form a group with alkaline affinities.
3) The geochemical differences among the three associations cannot be explained by low-pressure fractionation involving the present phenocrysts phases. These differences probably reflect different source materials.
4) The available geochemical data are insufficient to develope detailed and realistic petrogenetic models for the Jurassic volcanic rocks of Northern Chile, but the few available data suggest the following implications:
   a) The observed REE patterns and the geochemical data of the Jurassic tholeiitic suites (series A) are consequent with moderate degrees (10%) of melting of peridotite. Subsequent fractional crystallization of olivine (Fo_{80}, 9-20%) and clinopyroxene (augite, 2-6%) account for the trace element abundances.

b) The geochemical patterns of the Jurassic series B agree with a derivation by low degrees (3-7%) of partial melting of a garnet-free peridotite mantle, followed by fractional crystallization of olivine (Fo_{80}, 11-12%) and clinopyroxene (augite, 6%).

c) The geochemical patterns of Jurassic series C are consistent with an origin by low degrees (2-5%) of partial melting of a garnet-free peridotite upper mantle, followed by fractional crystallization of olivine (Fo_{80}, 11-25%), clinopyroxene (augite, 2-6%) and plagioclase (An_{60}, 10-30%).

5) The three volcanic series are interlayered in the Jurassic outcrops of Northern Chile and the sequence cannot be correlated with a spatial or temporal zonation. Tholeiitic, calc-alkaline and alkalic volcanism has taken place contemporaneously throughout the Jurassic.

6) Clearly, the Jurassic history in the Southern part of the Central Andes speaks for the formations of an island-arc. If the Jurassic border of the southern South-America continent is analogous with the currently active island-arcs as this discussion has argued, then its coast was probably bordered by an active oceanic trench. This subduction zone was developed in the Western border of the South-America continent, with a Benioff plane dipping eastward.

7) The geochemical relationship suggests a depth of paleoseismic zone beneath the Jurassic volcanoes of about 150 km and the continental crust could have had a thickness between 15 and 27 km.

8) Although the available data are very limited for the Jurassic-Cretaceous volcanic rocks of Central Chile (Southern Andes), the geochemical patterns suggest that these rocks are demonstrably similar with the Jurassic series of Northern Chile (Central Andes).

9) Thus, the paleovolcanism in Northern Chile is of double importance: its igneous rocks offer a well-preserved and rather complete record of evolution and its apparent relationship with an active subduction zone that help for the geological reconstruction of the enigmatic history of the South-East Pacific.

14. ACKNOWLEDGMENTS

Financial support of the Deutsche Akademische Austauschdienst (DAAD) and of the Departamento de Geociencias de la Universidad del Norte, Chile is deeply acknowledged. I express my thanks especially to Prof. Dr. Hans PICHLER, Tübingen for stimulating discussions and valuable suggestions. I also express my appreciation to the colleagues Dr. Rudolf STENGELIN and Dr. H. H. SCHOCK, Tübingen, Germany; Prof. Dr. Leopoldo LOPEZ, Santiago, Prof. Dr. Jorge OYARZUN, Concepción, Dr. Nelson GUERRA and Dr. Patricio CAMPANO, Antofagasta, Chile, for discussions, critically reading the manuscript and help for the chemical analysis. Finally I wish to thank Isolde FREY for her technical help.

15. REFERENCES

ALFARO, G., 1974. Alteración hidrotermal y elementos en trazas en prospección de yacimientos de cobre en andesitas en la zona de Tocopilla. Coloquio de Alteración y metamorfismo en rocas volcánicas e intrusivas. Publ. Depto. Geol. Univ. Chile, Santiago, 41, 87-95.

ARTH, J. G., 1976. Behavior of trace elements during magmatic processes - a summary of theoretical models and their applications. J. Res. U. S. Geol. Surv. 4, 41-47.

BAEZA, L., 1976. Geología de Cerritos Bayos y areas adyacentes entre los 22°30´- 22°45´ Latitud Sur y los 68°55´ - 69°25´ Longitud Oeste. Antofagasta, Chile. - Unpubl. Thesis. Univ. de Norte, Chile, 182 pp.

BAKER, P. E., 1968. Comparative volcanology and petrology of the Atlantic island-arcs. - Bull. Volcanol. 32, 189-206.

BARRON, B. I., 1976. Recognition of the original volcanic suite in altered mafic volcanic rocks at Sofala, New Youth Wales. - Am. Jour. Sci. 276, 604-636.

BROGGEN, J. M., 1950. Fundamentos de la Geología de Chile.. - Inst. Geograf. Militar, Santiago de Chile, 380 pp.

CANN, J. R., 1969. Spilites from the Carlsberg Ridge, Indian Ocean. - J. Petrol. 10, 1-19.

COLEMAN, R. G., LEE, D. E., BEATTY, L. B. and BRANNOCK, W. W., 1965. Eclogites and eclogites. Their differences and similarities. - Bull. Geol. Soc. Am. 76, 483-508.

CORVALAN, J., 1967. Geología, in: Geología Económica de Chile, Corp. Fomento Prod. 3, 35-82.

CHAYES, F. and YODER, H. S., 1971. Some anomalies in the norms of extremely undersaturated lavas. - Carnegie Inst. Year Book, 70, 205-206.

CHURCH, S. E., 1973. Limits of sediment involvement in the genesis of orogenic volcanic rocks. - Contrib. Mineral. Petrol. 39, 17-32.

DARAPSKY, L., 1900. Das Departamento Taltal. Berlin. 230 pp.

DARWIN, Ch., 1838. Journal of Research. - Royal Geol. Soc. London. 448 pp.

DeLONG, S. E., 1974. Distribution of Rb, Sr and Ni in igneous rocks. Central and Western Aleutian Islands, Alaska. - Geochim. Cosmochim. Acta, 38, 245-266.

DICKINSON, W. R., 1970. Relations of andesites, granites, and derivative sandstones to arch-trench tectonics. - Geophys. Space Phys. Rev. 8, 813-860.

DICKINSON, W. R., 1975. Potash-Depth (K-h) relations in continental margin and intra-oceanic magmatic arcs. - Geology, 3, 53-56.

DICKINSON, W. R. and HATHERTON, T., 1967. Andesitic volcanism and seismicity around the Pacific. - Science, 157, 801-803.

DOSTAL, J., ZENTILLI, M., CAELLES, J. C., and CLARK, A. H., 1977. Geochemistry and origin of volcanic rocks of the Andes (26° - 28°S). - Contrib. Mineral. Petrol. 63, 113-128.

DRAKE, M. J., 1975. The oxidation state of europium as an indicator of oxygen fugacity. - Geochim. Cosmochim. Acta 39, 55-64.

DRORY, A., and ULMER, G. C., 1974. Oxygen fugacity determination for Cascadian andesites. EOS 55, 487.

ERNST, W. G., 1973. Blueschist metamorphism and P-T regimes in active subduction zones. - Tectonophysics, 17, 255-272.

EWART, A. and TAYLOR, S. R., 1969. Trace element geochemistry of the rhyolitic volcanic rocks, Central North Island, New Zealand. - Contrib. Mineral. Petrol. 22, 127-145.

FLOYD, P. A., and WINCHESTER, J. A., 1978. Identification and discrimination of altered and metamorphosed volcanic rocks using inmobile elements. - Chem. Geol. 21, 291-306.

FREY, F. A., HASKIN, M. A., POETZ, J. and HASKIN, L. A., 1968. Rare earth abundances in some basic rocks. J. Geophys. Res. 173, 6085-6098.

FREY, F. A., GREEN, D. H., ROY, S. D., 1978. Integrated models of basalt petrogenesis: A study of olivine tholeiites to olivine melilitites from Southeastern Australia utilizing geochemical and experimental petrological data. J. Petrol., in press.

FRUTOS, J. and TOBAR, A., 1973. Evolution of the Southwestern continental margin of South America. III Int. Gondwana Symposium. Canberra, Australia, 38, 565-578.

FRUTOS, J., 1977. Evolution de la marge continentale des Andes du Nord du Chili. Le volcanisme et la Metallogenese. Unpubl. These. Universite de Paris. Sud. Orsay. 160 pp.

FUDALI, R. F., 1965. Oxygen fugacities of basaltic and andesitic magmas. Geochim. Cosmochim. Acta. 29, 1063-1075.

GAST, P. W., 1965. Terrestrial ratio of potassium to rubidium, and the composition of the Earth's Mantle. - Science 147, 858-860.

GAST, P. W., 1968. Trace element fractionation and the origin of tholeiitic and calc-alkaline magma types. - Geochim. Cosmochim. Acta, 329, 1057-1086.

GERTH, H., 1939. Jüngere orogenetische Zonen. Band 3. Abschnitt IV 6: Die Kordilleren von Südamerika. Leipzig. 61 pp.

GERTH, H., 1935. La estructura geológica de la Cordillera Argentina entre río Grande y río Diamante en el sur de la Provincia de Mendoza. Actas Ac. Nac. de Ciencias, Argentina. 23 pp.

GILL, J. B., 1970. Geochemistry of Viti Levu, Fiji, and its evolution as an island arc. Contrib. Mineral. Petrol. 27, 179-203.

GILL, J. B., 1974. Role of underthrust oceanic crust in the genesis of a Fijian calc-alkaline suite. - Contrib. Mineral. Petrol. 43, 29-45.

GORDILLO, C. and LENCINAS, A., 1967. El basalto nefelínico del Pungo. Córdova. Bol. Acad. Nac. Ciencias. Tomo XLVI, 109-115.

GORDILLO, C. and LENCINAS, A., 1969. Perfil geológico de la Sierra Chica de Córdova en la zona del río los Molinos, con especial referencia a los dikes traquibasálticos que la atraviesan. Bol. Acad. Nac. Ciencias. Tomo XLVII, 27-50.

GREEN, T. H., and RINGWOOD, A. E., 1968. Genesis of the calc-alkaline igneous rock suite. Contrib. Mineral. Petrol. 18, 105-162.

HALL, A., 1967. The variation of some trace elements in the Rosses granite complex, Donegal. - Geol. Mag., 104, 99-109.

HALPERN, M., 1978. Geological significance of Rb-Sr isotopic data of Northern Chile crystalline rocks of the Andean orogen between latitudes 23° and 27° South. - Geol. Soc. Am. Bull. 89, 522-532.

HARRINGTON, H., 1961. Geology of parts of Antofagasta and Atacama Provinces, Northern Chile. - Am. Assoc. Petroleum Geol. Bull. 45, 167-197.

HASHIMOTO, M., 1966. On the prehnite-pumpellyite metagrywacke facies. - Geol. Soc. Japan, 72, 253-265.

HATHERTON, T. and DICKINSON, W. R., 1968. Andesitic volcanism and seismicity in New Zealand. - J. Geophys. Res. 73, 4615-4619.

HATHERTON, T. and DICKINSON, W. R., 1969. The relationship between andesitic volcanism and seismicity in Indonesia, the Lesser Antilles and other island arcs. - J. Geophys. Res., 74, 5301-5310.

HILL, R. E., and BOETTCHER, A. L., 1970. Water in the earth's Mentle: Melting curves of basalt-water and basalt-water-carbon dioxide. - Science, 197, 980-981.

HINRICHSEN, T. and SCHOAMANN, K., 1969. Untersuchungen zur Stabilität von Pumpellyit. - Neves J. Miner., 10, 441-445.

HUTCHINSON, C. S., 1976. Indonesian active volcanic arc: K, Sr and Rb variation with depth to the Benioff zone. - Geology, 4, 407-408.

IRVINE, T. N. and BARAGAR, W. R. A., 1971. A guide to the chemical classification of the common volcanic rocks. - Canadian J. Earth Sci. 8, 532-548.

JAKES, P. and SMITH, I. E., 1970. High potassium calc-alkaline rocks from Cape Nelson, Eastern Papua. - Contrib. Mineral. Petrol. 28, 259-271.

JAKES, P. and WHITE, A. J. R., 1972. Major and trace element abundances in volcanic rocks of orogenic areas. - Geol. Soc. Am. Bull. 83, 29-4

JAMES, D. E., 1971. Plate tectonic model for the evolution of the Central Andes. - Geol. Soc. Am. Bull. 82, 3325-3346.

JAMES, D. E., BROOKS, C. and CUYUBAMBA, A., 1975. Early evolution of the Central Andean volcanic arc. - Carnegie Inst. Wash. Year Book, 74, 247-250.

JENSEN, B. B., 1973. Patterns of trace element partitioning. - Geochim. Cosmochim. Acta. 37, 2227-2242.

JOLLY, W. T. and SMITH, R. E., 1972. Degradation and metamorphic differentiation of the Keweenawan tholeiitic lavas of Northern Michigan. - J. Petrol. 13, 273-309.

JURGAN, H., 1977. Strukturelle und lithofazielle Entwicklung des andinen Unterkreide-Beckens im Norden Chiles. (Provinz Atacama). - Geotekt. Forsch. 52, 138 pp.

KLERKX, J., DEUTSCH, S., PICHLER, H. and ZEIL, W., 1977. Strontium isotopic composition and trace element data bearing on the origin of Cenozoic volcanic rocks of the Central and Southern Andes. - J. Volcanol. Geotherm. Res., 2, 49-71.

KOLBE, P. and TAYLOR, R., 1966. Major and trace element relationships in granodiorites and granites from Australia and South Africa. - Contrib. Mineral. Petrol. 12, 202-222.

KUSHIRO, I., SHIMAZU, N., NAKAMURA, Y. and AKIMOTO, S., 1972. Composition of coexisting liquid and solid phases formed upon melting of natural garnet and spinel lherzolites at high pressures: a preliminary report. - Earth Planet. Sci. Lett. 14, 19-25.

LAMBERT, R., HOLLAND, J. and OWEN, P., 1974. Chemical petrology of a suite of lavas from Mount Ararat. Turkey. - J. Geology, 82, 419-438.

LePICHON, X., 1968. Sea-floor spreading and continental drift. - J. Geophys. Res. 73, 3661-3697.

LEVI, B., 1969. Burial metamorphism of Cretaceous volcanic sequence. West from Santiago, Chile. - Contrib. Mineral. Petrol. 24, 30-40.

LEVI, B., 1970. Burial metamorphic episodes in Andean geosyncline. Central Chile. - Geol. Rundschau, 59, 994-1013.

LEVI, B. and CORVALAN, J., 1964. Metamorfismo regional de las rocas volcánicas del geosinclinal Andino. Santiago. - Rev. Minerales, 101, 13-15.

LIPMAN, P. W., PROSTKA, H. J. and CHRISTIANSEN, R. L., 1971. Evolving subduction zones in the Western United States, as interpreted from igneous rocks. - Science, 174, 821-825.

LOPEZ-ESCOBAR, L., FREY, F. A. and VERGARA, M., 1977. Andesites and High-Alumina basalts from the Central-South Chile High Andes: geochemical evidence bearing on their petrogenesis. - Contrib. Mineral. Petrol. 63, 199-228.

LOSERT, J., 1974. Alterations and associated copper mineralizations in the Jurassic volcanic rocks of the Buena Esperanza mining area. Antofagasta Province, Northern Chile. Publ. Depto. Geol. Univ. Chile. 41, 51-85.

MAPA GEOLOGICO DE CHILE, 1968. At scale 1:1 000 000. Inst. Inv. Geol. Santiago, Chile.

McNUTT, R. H., CROKET, J. H., CLARK, A. H., CAELLES, J. C. FARRAR, E., HAYNES, S. J. and ZENTILLI, M., 1975. Initial Sr87/Sr86 ratios of plutonic and volcanic rocks of the Central Andes between Latitudes 26° and 29° South. - Earth Planet. Sci. Lett. 27, 305-313.

MIYASHIRO, A., 1961. Evolution of metamorphic belts. - J. Petrol. 2, 277-311.

MIYASHIRO, A., 1974. Volcanic rock series in Island arcs and active continental margins. - Am. J. Science, 274, 321-355.

MONTANO, M., 1976. Geologia de la zona de Caracoles y áreas adyacentes. Prov. Antofagasta. Chile. Unpubl. Thesis, Depto. Geol. Univ. Chile. Santiago. 153 pp.

MUNOZ CRISTI, J., 1968. Evolución geológica del territorio chileno. Santiago. Bol. Acad. Ciencias, 1, 18-26.

MYSEN, B. O., KUSHIRO, I., NICHOLLS, I.A. and RINGWOOD, A. E., 1974. A possible mantle origin for andesitic magmas. - Earth Planet. Sci. Lett. 21, 221-229.

MYSEN, B. O. and BOETTCHER, A. L., 1975. Melting of a hydrous mantle: II Geochemistry of crystals and liquids formed by anatexis of mantle peridotite at high pressures and high temperatures as a function of controlled activities of water, hydrogen, carbon dioxide - J. Petrol. 16, 543-593.

NICHOLLS, I. A., 1974. Liquids in equilibrium with peridotitic mineral assemblages at high water pressures. - Contrib. Mineral. Petrol. 45, 289-316.

NICHOLLS, I. A. and RINGWOOD, A. E., 1972. Production of silica-satured tholeiitic magmas in island arcs. - Earth Planet. Sci. Lett. 17, 243-246.

NICHOLLS, I. A. and RINGWOOD, A. E., 1973. Effect of water on olivine stability in tholeiites and the production of silica-satured magmas in the island arc environment. J. Geol. 81, 285-300.

NISTERENKO, G. and CHAVEZ, L., 1971. Génesis de yacimientos de cobre tipo manto en Chile. Santiago, Depto. Geol. Univ. Chile Unpubl. report, 32 pp.

NITSCH, K. H., 1971. Stabilitätsbeziehungen von Prehnit und Pumpellyithaltigen Paragenesen. - Contrib. Mineral. Petrol. 30, 240-260.

OCOLA, L. C., MEYER, R. P. and ALDRICH, L. T., 1971. Gross crustal structure under Peru-Bolivia altiplano. - Earthquake Notes, 42 33-48.

ORTIZ, F., CORVALAN, J., SEGERSTROM, K. and GARCIA, F., 1960. Geología y estratigrafía del área Chanaral-Taltal. Inst. Inv. Geol. Unpubl. report. 23 pp.

OXBURG, E. R. and TURCOTTE, D. L., 1970. The thermal structure of island arcs. - Geol. Soc. Am. Bull. 81, 1665-1688.

OYARZUN, J. and VILLALOBOS, J., 1969. Recopilación de analisis químicos de rocas chilenas. - Publ. Depto. Geol. Univ. Chile. 33, 1-47.

PALACIOS, C., 1974 a. Geología y metalogenesis de la formación volcánica La Negra y las rocas graníticas en el area Tocopilla, Prov. Antofagasta. - Publ. Dept. Geol. Univ. Chile. 43, 1-48.

PALACIOS, C., 1974 b. Notes about the Jurassic paleovolcanism in Northern Chile. - Proc. of Symposium on Andean and Antarctic Volcanology Problems, IAVCEI., 238-249.

PALACIOS, C., 1975. Desarrollo del volcanismo temprano del Sistema Andino en el Norte de Chile. VI Geol. Congr.: Geol. Soc. of Argentina. In press.

PALACIOS, C., 1977. Metamorfismo regional en rocas volcânicas Jurâsicas en el Norte de Chile. - Est. Geol. 33, 11-16.

PEARCE, J. A. and CANN, J. R., 1973. Tectonic setting of basic volcanic rocks determined using trace element analyses. - Earth Planet. Sci. Lett. 19, 290-300.

PICHLER, H. and STENGELIN, R., 1973. Application of the Rittmann norm method to petrological problems. In: Rittmann, 1973. Stable Mineral Assemblages of igneous rocks, 225-248.

REED, J. C. and MORGAN, B. A., 1971. Chemical alteration and spilitization of the Catoctin Greenstone, Shenandoah National Park, Virginia. - J. Geol. 79, 226-248.

RHODES, J. M., 1969. The geochemistry of a granite-gabbro association at Hartley, New South Wales. Unpubl. Thesis, Canberra, Australian National Univ., 403 pp.

RINGWOOD, A. E., 1974. The petrological evolution of island arc systems. - J. Geol. Soc. London, 130, 183-204.

RITTMANN, A., 1973. Stable mineral assemblages of igneous rocks. Berlin, 262 pp.

SEKI, Y., 1969. Facies series in low-grade metamorphism. J. Geol. Soc. Japan, 75, 255-266.

SHAW, D. M., 1970. Trace element fractionation during anatexis. Geochim. Cosmochim. Acta, 34, 237-243.

SLEMMONS, D. B., 1962. Determination of volcanic and plutonic plagioclases using a three-or-four axis universal stage: Revision of Turner method. - Geol. Soc. Am. Spec. Paper, 69, 64 pp.

SLEMMONS, D. B., 1962 a. A method of evaluating order-disorder, in: Observation on order-disorder relations of natural plagioclase. Copenhagen, Norsk. Geol. Tidsskr., 42, 533-554.

SMITH, R. E., 1968. Redistribution of major elements in the alteration of some basic lavas during burial metamorphism. J. Petrol. 9, 191-219.

SMITHERINGALE, W. G., 1972. Low-poash Lush's Bight tholeiites: Ancient oceanic crust in Newfoundland? Canadian J. Earth Sci., 9, 574-588.

STEINMANN, G., 1923. Umfang, Beziehungen und Besonderheiten der andinen Geosynklinale, 14, 69-82.

STEINMANN, G., 1929. Geologie von Peru. Heidelberg, 453 pp.

STRECKEISEN, A., 1967. Classification and Nomenclature of igneous rocks. - N. Jb. Mineral. Abh., 107, 144-240.

STRENS, R., 1968. Reconnaissance of the prehnite stability field. Mineral. Mag., 36, 864-867.

TAYLOR, S. R., 1969. Trace element chemistry of andesites and assiciated calc-alkaline rocks. In: Proc. Andesite Conf. (A. R. McBirney ed.), Dept. Geol. Min. Res. Oregon Bull., 65, 43-64.

VALLANCE, T. G., 1960. Concerning spilites: Linnean Soc. New South Wales, Proc., 85, 8-52.

VALLANCE, T. G., 1965. On the chemistry of pillow lavas and the origin of spilites. - Mineral. Mag., 34, 471-481.

VALLANCE, T. G., 1974. Spilitic degradation of a tholeiitic basalt. J. Petrol., 15, 79-96.

VERGARA, M., 1965. Perfil geológico entre Bucalemu y Bancos del Flaco. - Int. Geol. Univ. Chile. Unpubl. report, 21 pp.

VERGARA, M., 1969. Rocas volcánicas y sedimentario-volcánicas, Mesozoicas y Cenozoicas en la Latitud 34°30´S, Chile, Publ. Depto. Geol. Univ. Chile, 32, 1-36.

VERGARA, M., 1972. Note on the paleovolcanism in the Andean Geosyncline from the central part of Chile. 24th. Int. Geol. Congress, Canada, 2, 222-230.

WEILL, D. F. and DRAKE, M. J., 1973. Europium anomaly in plagioclase feldspar: experimental results and semiquantitative model. Science, 180, 1059-1060.

WETZEL, W., 1929. Beiträge zur Erdgeschichte der Mittleren Atacama. - N. Jb. Min. Geol. Pal. Beil. Bd. B. Stuttgart, 505-578.

WOOD, D. A., GIBSON, I. L. and THOMPSON, R. N., 1976. Elemental mobility during Zeolite Facies. Metamorphism of the Tertiary basalts of Eastern Iceland. - Contrib. Mineral. Petrol., 55, 241-254.

YAJIMA, T., HIGUCHI, H. and NAGASAWA, H., 1972. Variation of rare earth concentrations in pigeonitic and hypersthenic rock series from Izu-Hakone region. - Contrib. Mineral. Petrol., 35, 235-244.

16. ANNEX: PHOTOGRAPHY OF SOME THIN-SECTIONS

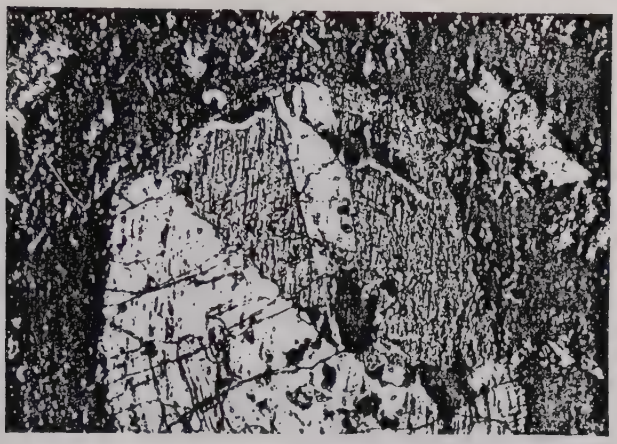

Quartz-tholeiite hawaiite (sample E-5,Series A) with phenocryst of augite in dense microcrystalline groundmass. Polarised light.

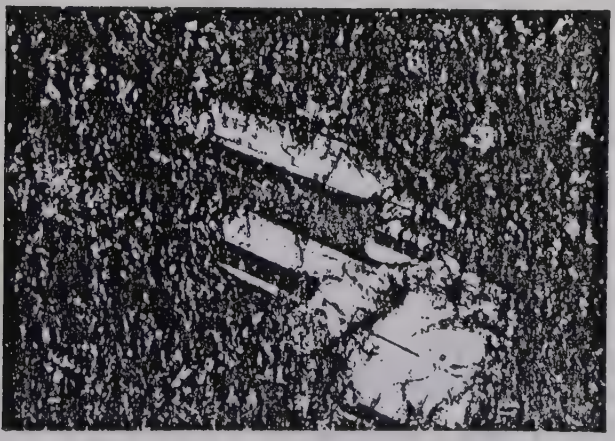

Quartz-latiandesite (sample E-12,Series B) rich in plagioclase phenocrysts. Crossed nicols.

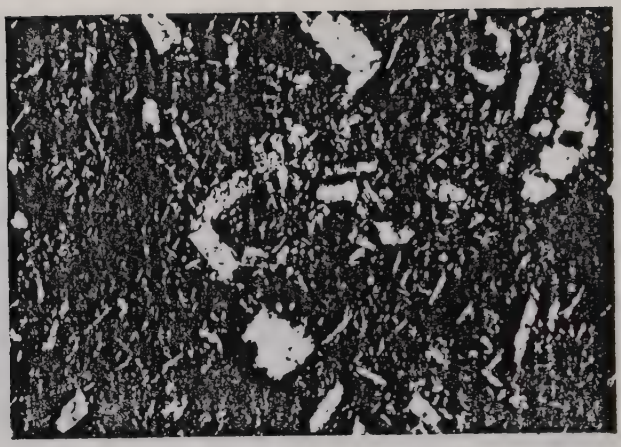

Quartz-latiandesite (sample M-10,Series C) showing dense groundmass of plagioclase and ore minerals. Polarised light.

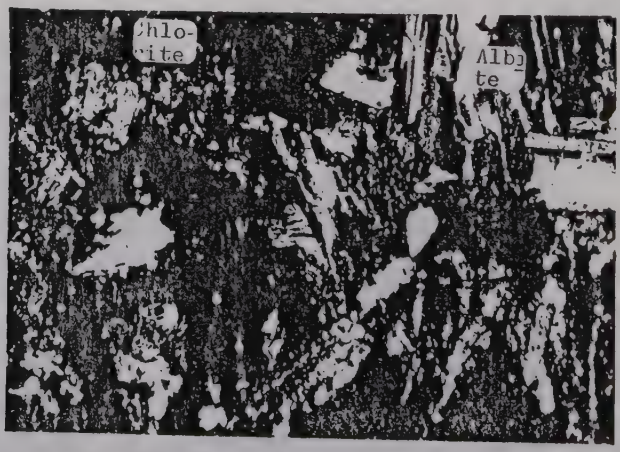

Metamorphic andesite of the Chlorite-Calcite zone. Crossed nicols.

LEBENSLAUF

Name:	Palacios-Monasterio Carlos
Geburtsdatum:	27.1.1950 in Santiago, Chile
Eltern:	Palacios-Palma Carlos, Lehrer Palacios Rosa
Familienstand:	Verheiratet, zwei Kinder
Studium:	
März 1968	Beginn des Studiums der Geologie an der Universität von Chile in Santiago
Februar 1973	Staatsexamen mit dem Titel: "La zona de contacto del intrusivo granîtico de Tocopilla con la Formaciôn volcánica La Negra y su influencia en la mineralizaciôn del área", unter der Anleitung von Prof. ERIK KLOHN
ab März 1974	Geologe und Assistent-Professor beim Departamento de Geociencias de la Universidad del Norte, Antofagasta, Chile.
WS 1977	Immatrikulation an der Universität Tübingen und Beginn der Dissertation mit dem vorliegenden Thema bei Prof. Dr. H. PICHLER am Mineralogisch-Petrographischen Institut.
WS 1978	Abschluß der Dissertation.

Meine akademischen Lehrer waren die Herren Professoren und Dozenten:

In Santiago:	AGUIRRE, CECIONI, CORVALAN, CHARRIER, DIAZ, HERVE, KLOHN, LEVI, LOSERT, MARTINEZ, OYARZUN, PEREZ, REUTTER, ROSSENMANN, TOBAR, VERGARA, VICENTE.
In Tübingen:	MÖLLENSTEDT, PICHLER.